Wireless Transmission Methods for Ultra-dense Cellular Networks and Machine-type Communications

Thomsen, Henning

DOI (link to publication from Publisher):
10.5278/vbn.phd.engsci.00079

Publication date:
2016

Document Version
Publisher's PDF, also known as Version of record

WIRELESS TRANSMISSION METHODS FOR ULTRA-DENSE CELLULAR NETWORKS AND MACHINE-TYPE COMMUNICATIONS

BY
HENNING THOMSEN

DISSERTATION SUBMITTED 2016

AALBORG UNIVERSITY
DENMARK

Wireless Transmission Methods for Ultra-dense Cellular Networks and Machine-type Communications

Ph.D. Dissertation

Henning Thomsen

Dissertation submitted March 9, 2016

Dissertation submitted: March 9, 2016

PhD supervisor: Prof. Petar Popovski
Aalborg University, Denmark

Assistant PhD supervisor: Assoc. Prof. Elisabeth de Carvalho
Aalborg University, Denmark

PhD committee: Associate Professor Tatiana K. Madsen (chairman)
Aalborg University

Associate Professor Kimmo Kansanen
Norwegian University of Science and Technology

Senior Researcher Jesus A. Zarate
Centre Tecnologic Telecomunications de Catalunya

PhD Series: Faculty of Engineering and Science, Aalborg University

ISSN (online): 2246-1248
ISBN (online): 978-87-7112-528-3

Published by:
Aalborg University Press
Skjernvej 4A, 2nd floor
DK – 9220 Aalborg Ø
Phone: +45 99407140
aauf@forlag.aau.dk
forlag.aau.dk

Printed in Denmark by Rosendahls, 2016

Abstract

The emergence of the next generation of cellular communications has requirements spanning several dimensions. Traditional human-centric communications is increasing in number of devices and volume of data. This, as well as an explosive increase in node density, a characteristic of Ultra-dense Networks (UDNs), brings new challenges in satisfying those requirements. Other forms of communication not directly involving humans, including Machine-to-Machine (M2M) communications, also called Machine-type Communications (MTC), are also increasing, and motivate design of transmission protocols taking such forms of communication into account. This Ph.D. thesis is a contribution to the design and analysis of transmission protocols for M2M communications, and a two-fold contribution in UDNs, transmission schemes for two-way traffic in cellular networks using wireless backhauling and emulation of Full Duplex (FD) transmissions using Half Duplex (HD) devices.

There is increased interest in M2M communications in cellular networks such as Long-Term Evolution (LTE), particularly from smart metering applications and the Internet-of-Things. Since LTE is not designed with such traffic in mind, M2M traffic can cause congestion in the random access part of it. Motivated by this, we develop a mathematical model for obtaining the success probability of random access in LTE, for M2M devices. This model also features a limitation in the data phase of the protocol, and is compared with numerical simulations, where we observe a perfect match. Furthermore, the model is general enough to be used in other networks.

In order to accommodate M2M devices in LTE networks, we also consider a reservation scheme for M2M, which we call Code Expanded Radio Access Protocol. The idea of this scheme is to expand the contention space in LTE, so that a large number of M2M devices can be accommodated into the network. The performance and operation of the scheme is analyzed using Markov Chains, and is verified by simulations. Importantly, the scheme allows for an exponential increase in the number of accessing devices, compared to the linear increase in the baseline scheme, for a linear increase in system resources.

Our contributions in the latter part of the thesis are within UDNs, where we make a two-fold contribution: Design and analysis of transmission schemes for cellular networks using wireless backhauling, and FD emulation by HD devices, where we consider both uplink (UL) and downlink (DL) traffic in our analysis.

We study a wireless backhauling scheme for serving two users bidirectional traffic via small cell Base Stations (BSs), while minimizing the power required to satisfy their rate requirements. Using a similar scenario, we then define a transmission scheme termed Wireless Emulated Wire (WEW). This scheme takes advantage of the relationship between the wireless channels of the backhaul, and draws inspiration from the separation of messages into a public and private part, as was done in the Han-Kobayashi scheme of information theory. It is shown that this scheme brings benefits for the nodes in terms of lower power usage compared to using Zero Forcing or a common beamformer.

We also present a scheme, termed CoMPflex: CoMP for In-band Wireless Full Duplex. In this scheme, motivated by the densification trend of cellular communications, we propose and analyze emulation of FD operation by spatially separating HD BSs, for serving UL and DL users. The scheme is shown to have advantages over using a FD BS, in terms of achievable rate and energy efficiency. Importantly, since the BSs are HD, the scheme is backwards compatible with already existing devices. We also analyze the CoMPflex scheme in a two-dimensional setting using stochastic geometry, where we see benefits in terms of success probability, compared to FD BSs. In both cases, this means that we can get performance better than FD, but without the added cost of complexity in signal processing and self-interference reduction at the FD nodes.

Resumé

Fremkomsten af den næste generation af mobilkommunikation har flere krav. Traditionel mobilkommunikation stiger i form af antallet af enheder og datamængde. Desuden er der en eksplosiv stigning i antal enheder i et givent område, et kendetegn ved Ultra-dense Networks (UDN), og dette giver udfordringer med at opfylde kommunikationskravene. Andre typer kommunikation, som ikke direkte involverer mennesker, inklusive Machine-to-Machine (M2M) kommunikation, også kalder Machine-type Communications (MTC), er også stigende, og dette motiverer design og analyse af protokoller som tager højde for denne type kommunikation. Denne Ph.D. afhandling er et bidrag til design og analyse af kommunikationsprotokoller for M2M kommunikation, og et todelt bidrag til UDN: Transmissionsmetoder til tovejs kommunikation i mobilnetværk vha. trådløse backhaul forbindelser, og emulering af fuld dupleks transmissioner vha. halv dupleks enheder.

Der er stigende interesse for M2M kommunikation i mobilnetværk så som LTE, specielt fra anvendelser så som smarte måleenheder og Internet-of-Things. Da LTE ikke er designet med en sådan trafik for øje, kan M2M trafik forårsage overbelastning i enhedernes adgang til LTE netværket. Motiveret af dette udvikler vi en matematisk model til at beregne sandsynligheden for succesfuld adgang til LTE, for M2M enheder. Denne model inkluderer en begrænsning i data delen af protokollen, og bliver desuden sammenlignet med numeriske simuleringer, hvor vi ser en perfekt overensstemmelse. Desuden er denne model generel nok til at kunne anvendes i andre typer netværk.

For at muliggøre adgang for M2M-enheder i LTE netværk betragter vi en metode, kaldet Code Expanded Radio Access Protocol. Idéen i denne metode er at øge ressourcerne i LTE, således at et stort antal M2M-enheder kan få adgang til netværket. Ydeevnen og virkemåden af metoden bliver analyseret vha. Markovkæder, og bliver verificeret med simulationer. Denne metode muliggør en eksponentiel stigning i antallet af enheder som tilgår netværket sammenliget med den lineære stigning i basis metoden, når systemressourcerne stiger lineært.

Vores bidrag i den anden del af afhandlingen er indenfor UDN, hvori vi giver to bidrag: Design og analyse af transmissionsmetoder for mobilnetværk

som bruger trådløse backhaulforbindelser, of fuld dupleks emulering af halv dupleks enheder, hvor vi betragter tovejs trafik i analysen.

Vi studerer en metode hvor trådløs backhaul bliver brugt til at betjene to brugere tovejs trafik via småcelle base stationer. Ud fra samme scenarie definerer vi en transmissionsmetode, kaldet Wireless Emulated Wire (WEW). Denne metode drager nytte af forholdet mellem de trådløse kanaler i backhaulet, og er inspireret af delingen af en besked i en offentlig og privat del, som blev gjort i Han-Kobayashi metoden i informationsteori. Det vises at denne metode bringer fordele for enhederne i form af en reducering i effektforbrug sammenlignet med kun at bruge Zero Forcing eller en fælles beamformer.

Vi præsenterer også en metode, kaldet CoMPflex: CoMP for In-band Wireless Full Duplex. I denne metode, som er motiveret af stigningen i antallet af enheder i mobilnetværk, emuleres fuld dupleks virkemåden. Dette gøres ved at separere halv dupleks basestationer for at betjene brugerne med mobiltrafik. Denne metode har fordele i kommunikationshastighed og energieffektivitet fremfor at bruge en fuld dupleks basestation. Vi undersøger også CoMPflex metoden i en todimensional opsætning vha. stokastisk geometri, hvor vi observerer forbedringer i sandsynligheden for succesfuld transmission sammenlignet med fuld dupleks. I begge tilfælde får vi en ydeevne som er bedre end fuld dupleks, men uden kompleksiteten i signalbehandling og reducering af selv-interferens i fuld dupleks enhederne.

Acknowledgements

This Ph.D. project has been an interesting, enriching and rewarding experience. Many people have influenced and supported me on this journey. First and foremost, I would like to take the opportunity to thank my supervisor, Prof. Petar Popovski, for his patience and guidance during the course of this Ph.D. project. I would also like to thank my co-supervisor, Assoc. Prof. Elisabeth de Carvalho, for her help and assistance. My colleague Nuno Pratas deserves a thank you for discussions and assistance on various aspects of research. It has been a privilege to be a part of the Mass-M2M research group, which has provided me with plenty of interesting discussions on all sorts of research. Thanks to the members of the group, Čeda, Dong Min, Germán, Kasper, Rasmus, Jesper and Jimmy. I would also like to thank Fan Sun for many stimulating discussions on relaying and cellular communications, and to thank my colleagues at the AP-Net section, and Section administrator Charlotte K. Madsen for her help and assistance with various administrative tasks. My family has always been there for me, and for that I thank my father, mother and sister, Katrina.

Contents

Thesis Details

Thesis Title:	Wireless Transmission Methods for Ultra-dense Cellular Networks and Machine-type Communications
Ph.D. Student:	Henning Thomsen
Supervisors:	Prof. Petar Popovski, Aalborg University Assoc. Prof. Elisabeth de Carvalho, Aalborg University

The main body of this thesis consists of the following papers.

[A] Henning Thomsen, Nuno K. Pratas, Čedomir Stefanović, and Petar Popovski, "Analysis of the LTE Access Reservation Protocol," *IEEE Communications Letters*, vol. 17, no. 8, pp. 1616–1619, 2013.

[B] Henning Thomsen, Nuno K. Pratas, Čedomir Stefanović, and Petar Popovski, "Code-expanded radio access protocol for machine-to-machine communications," *Transactions on Emerging Telecommunications Technologies*, vol. 24, no. 4, pp. 355–365, 2013.

[C] Henning Thomsen, Elisabeth de Carvalho and Petar Popovski, "Emulating Wired Backhaul with Wireless Network Coding," *General Assembly and Scientific Symposium (URSI GASS), 2014 XXXIth URSI*, pp. 1–4, 2014.

[D] Henning Thomsen, Elisabeth de Carvalho and Petar Popovski, "Using Wireless Network Coding to Replace a Wired with Wireless Backhaul," *IEEE Wireless Communication Letters*, vol. 4, no. 2, pp. 141–144, 2015.

[E] Henning Thomsen, Petar Popovski, Elisabeth de Carvalho, Nuno K. Pratas, Dong Min Kim and Federico Boccardi, "CoMPflex: CoMP for In-Band Wireless Full Duplex," *IEEE Wireless Communication Letters*, 2015.

[F] Henning Thomsen, Dong Min Kim, Petar Popovski, Nuno K. Pratas and Elisabeth de Carvalho, "Full Duplex Emulation via Spatial Separation of Half Duplex Nodes in a Planar Cellular Network," *Signal Processing Advances in Wireless Communications (SPAWC), 2016 IEEE 17th Workshop on (submitted)*, 2016.

In addition to the main papers, the following publications have also been made.

[1] Nuno K. Pratas, Henning Thomsen, Čedomir Stefanović, and Petar Popovski, "Code-expanded random access for machine-type communications," *IEEE Global Communications Conference 2012 (GLOBECOM)*, pp. 1681–1686, 2012.

[2] Huaping Liu, Fan Sun, Elisabeth de Carvalho, Petar Popovski, Henning Thomsen, Yuping Zhao, "MIMO Four-Way Relaying," *Signal Processing Ad vances in Wireless Communications (SPAWC), 2013 IEEE 14th Workshop on*, pp. 46–50, 2013.

[3] Nuno K. Pratas, Henning Thomsen, and Petar Popovski, "Random access procedures and radio access network (RAN) overload control in standard and advanced long-term evolution (LTE and LTE-A) networks," *Machine-to-machine (M2M) Communications, Ed. by Carles Anton-Haro and Mischa Dohler, Cambridge, United Kingdom: Woodhead Publishing, 2015.*, 2015.

This thesis has been submitted for assessment in partial fulfillment of the PhD degree. The thesis is based on the submitted or published scientific papers which are listed above. Parts of the papers are used directly or indirectly in the extended summary of the thesis. As part of the assessment, co-author statements have been made available to the assessment committee and are also available at the Faculty. The thesis is not in its present form acceptable for open publication but only in limited and closed circulation as copyright may not be ensured.

Preface

This thesis was written under the supervision of Professor Petar Popovski and Associate Professor Elisabeth de Carvalho, and was supported in part by the Danish Council for Independent Research (Det Frie Forskningsråd) within the Sapere Aude Research Leader program, Grant No. 11-105159 "Dependable Wireless bits for Machine-to-Machine (M2M) Communications", and in part by the European Union FP7 project ICT-317669 METIS.

The thesis is comprised by five publications plus one submitted conference publication (i.e. six contributions in total), where two are on protocol design for M2M communications in LTE, two are on the design and analysis of transmission schemes for wireless backhauling in cellular networks, and two are on the design and analysis of a transmission scheme for emulating full duplex operation using half duplex devices.

Henning Thomsen
Aalborg University, March 9, 2016

Part I

Introduction

Chapter 1

Introduction

In both industry and academia, there has been an increased focus on the shape of fifth generation (5G) cellular networks [8], which are envisioned to be more than just an incremental advance over the fourth generation (4G) networks currently deployed and operating [5, 37]. This evolution is driven partially by an increase in the number of use cases [57], as well as the data and connectivity requirements of users. Those requirements have been increasing dramatically in recent years [12], and are expected to increase further in the future.

In addition to the increasing requirements of users, there is also an emerging trend where devices communicate with each other without human intervention. This type of communication, so-called Machine-to-Machine (M2M) communications or Machine-type Communications (MTC), has requirements different from the more traditional human-centric communication [36]. This being due to mainly two things: Firstly, the number of devices, which can be orders of magnitude higher than that of a traditional cellular network. Secondly, the traffic itself has different characteristics: Because M2M-type traffic typically consists of many small packets, this traffic has a higher signaling overhead, compared to traditional cellular traffic. Also, the high number of M2M devices can put a severe stress on the network, in terms of an increase in access requests and signaling.

It is envisioned that in future cellular networks, the number of Base Stations (BSs) will become comparable to the number of users. This, combined with the increase in number of M2M and human-type users means that cellular networks will become much denser than today [5, 37], a characteristic of Ultra-dense Networks (UDNs). The trend of UDNs implies increased requirements on the cellular infrastructure, including the backhaul networks [7].

The backhaul network should be flexible, reliable, and with sufficient capacity to address these challenges. The previous research in this area has

mostly focused on fiber-optical and coaxial links, as well as wireless solutions such as high frequency microwaves [13] and cellular technology [17]. However, the interference in such a scenario is non-negligibile, which can have dramatic impact on network performance. Coordination of transmission and design of protocols are then important to deal with such challenges.

In this thesis we provide contributions to the design and analysis of protocols for M2M traffic in cellular networks, as well as two aspects of UDNs: Wireless backhauling and Full Duplex (FD) emulation for uplink (UL) and downlink (DL) traffic in cellular networks using half duplex (HD) nodes.

1 State-of-the-Art

The research challenges in 5G networks are expected to be significant and focus not only on data rate but also latency, reliability, accommodating an enormous number of devices and energy efficiency [37]. These changes include, but are not limited to the following trends:

Increasing Traffic: The next generation cellular networks have target data rates which are 100-1000 times larger compared to 4G networks, [8, 12]. This increase can come from a variety of sources including real-time video requirements [37], video streaming and on-line multiplayer gaming.

Heterogeneous Networks: In addition, the number of device types is growing. This comes from the fact that the number of use cases for cellular communications is increasing, and there are new traffic type requirements such as M2M and Internet-of-Things [8]. This implies that the cellular networks are becoming more heterogeneous, and can have several tiers, with femto- and pico-cells as examples. Combinations of cellular and WiFi [15] technologies are also being researched, including offloading cellular traffic onto WiFi [49], to deal with the increase in traffic. The Radio Access Network (RAN) itself is also becoming more heterogeneous, where instead of each having processing at each BS, the network instead features a cloud-like architecture, Cloud RAN (C-RAN) [1]. In C-RAN, a BS is attached to several Remote Radio Heads (RRHs), and the processing occurs centrally at the BS.

Ultra Dense Networks: The number of devices in future networks is projected to be several orders of magnitude larger than today [5]. This is a result of a combination of the two previous points: an increase in rates and an increasing diversity of cellular networks. However, this puts requirements on signaling and interference management, as well as the backhaul [51].

Machine-to-Machine Communications: M2M traffic is also increasing, from the proliferation of applications such as smart metering. Such traffic is more intensive in the signaling and access parts, and trends have also been observed where the volume in signaling traffic is increasing at a higher pace than data traffic [2]. This motivates optimization of the signaling and the random access of cellular networks.

Ultra Reliable Communications: The next generation of wireless networks will include stringent device requirements on delay and availability. A target in ultra reliable communications can be defined as having a reliability of at least 99% [39]. Such a requirement is significantly higher than current systems. Examples of types of traffic with such requirements includes M2M traffic and traffic with very low latency requirements [46].

1.1 Massive Machine-to-Machine Communications

The application of M2M type traffic is being considered in legacy cellular networks such as LTE and GSM [34]. Such networks were not designed with this type of traffic to begin with, and several solutions have been researched to solve this issue.

The performance and impact of M2M-type traffic can be analyzed using various metrics, and the success probability of contending M2M devices in LTE is a metric that is often used. In [11], authors give the success probability in the contention phase, assuming Poisson arrivals. Another reference on the success probability and an approximation on it was given in [61], using a combinatorial model. Our paper [56] gives a mathematical analysis of the success probability in the LTE random access protocol is considered. In this work, a possible limitation of the data phase (following the access granting phase) is also taken into consideration. Another relevant metric, from the perspective of battery life, is energy efficiency [58]. A study of the limitations of the random access in LTE was given in [26], where the authors show the effect of the number of accessing devices on the delay and energy consumption.

An access reservation protocol specifies how devices should access and communicate with the receiver on a given network. In contention-based random access, the accessing devices compete for resources, and collisions can occur. The contention-based random access in LTE is shown in Fig. 1.1. The procedure itself consists of four steps, which are detailed below.

1: Preamble Transmission: The user has generated traffic, and wants to communicate with the core network. It transmits one preamble (which can be thought of as a token or signature), chosen uniformly at random from a

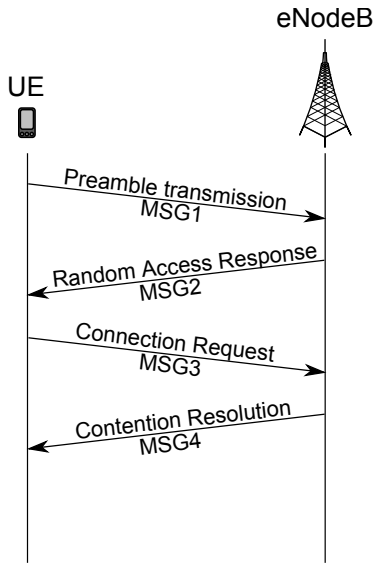

Fig. 1.1: The Random Access Procedure in LTE.

set of preambles, to the BS. The network has defined which preambles are available in the cell that the user is in [3]. This transmission takes place in the first RAO (Random Access Opportunity).

2: Random Access Response: The BS receives the preamble transmissions from contending users, and proceeds to decode them. Upon successful decoding, the BS (also referred to as evolved NodeB, eNodeB) responds with a Random Access Response (RAR) in MSG2 with information about the matching preamble and uplink resources to be used.

3: Connection Request: In this step, each user that received MSG2 in the previous step will transmit information about the device and reasons for initiating in the connection. There is a possibility that two or more users will collide because they chose the same preamble in the first step. If such a collision is undetected, all colliding users get the same RAR, and so will transmit on the same resource. Then, the data of the users will collide, and each user will back off for a random time before attempting a retransmission [25].

4: Contention Resolution: When successfully receiving a connection request in step 3, the BS transmits an acknowledgement message. If a transmitting device does not receive a response, it considers the transmission unsuccessful, and repeats the procedure starting with the first step. When it has

done so a certain number of times, the network is considered unavailable.

In each of these four steps, there might be a chance of failure, e.g. due to resource unavailability or a collision. There are two phases to approach this issue. The first is to identify bottlenecks, and the second to design transmission schemes which take those bottlenecks into account. Then, the schemes are analyzed using e.g. mathematical tools and computer simulations.

1.2 Random Access Protocols for M2M Traffic

In the literature, protocols have been designed with the purpose of serving M2M traffic in LTE-type networks, and they accomplish this in different ways. One of the goals is to deal with the consequence of the possible overload resulting from M2M devices accessing the network. We list the most used methods below, and then comment on the approach used in this thesis in proposing a model for the success probability in the access protocol and a scheme for accommodating a large number of devices.

Access Class Barring (ACB)

In Access Class Barring (ACB) [29], the main idea is to define various *classes* (which can be thought of as groups). This includes classes for high-priority devices such as alarms. In case the network is congested, the accessing devices belonging to some classes can be denied (barred) access. There are several extensions and enhancements of ACB. The classes can be given various priority levels [10]. An example is Extended Access Class Barring (EAB), which is part of the LTE standard, which bars network access to delay tolerant devices.

Backoff-based Mechanisms

Cellular networks can require accessing M2M devices to postpone their retransmissions via a (random) backoff. This implies that those devices will access the network later. The paper [62] analyzes optimal backoff mechanisms in LTE, in terms of throughput and dropout probability. Backoff is also proposed for M2M traffic [45], as a way of dealing with a large number of arrivals. The work [30] uses a dynamic backoff scheme to reduce the contention in the random access, by adjusting the backoff window based on the number of random access attempts.

Allocation of Resources

The resources of cellular networks are typically divided orthogonally. This means that they are divided in e.g. time, frequency or code. Since these re-

sources are orthogonal, they do not interfere with each other. In random access for M2M traffic in LTE, this translates into having specific (i.e. *dedicated*) resources for the M2M traffic. Since LTE should accommodate human-type traffic also, one way of doing this is to divide the resources into M2M and other types of traffic [28].

The allocation of resources for M2M traffic can be done dynamically, i.e. based on the load [33]. Such methods require some form of knowledge of the load, which can be obtained from load estimation methods. Simulation results of this method have been reported in [4]. Dynamic Allocation can be categorized among methods that divide the resources among M2M and other types of traffic (and so is a more general case than having orthogonal resources). In [24], a resource allocation method is studied which takes the spatial locations of devices into account. This is done by allocating identical preambles to devices which are far apart, and it is shown that this method reduces the collision rate. There are other ways to allocate resources, based on metrics such as e.g. required reliability. In the paper [35], the authors study a method for dividing the resources into a pre-allocated pool and a common pool, based on the required reliability of the devices.

Virtual Resources

Instead of considering the actual, physical resources (which are limited) as done using orthogonal resources, an alternative method is to have virtual resources for M2M. In the paper [42], a method termed *Code-Expanded Random Access* was presented. This method defines a set of virtual codewords, on top of the actual, physical LTE resources. The resources which can be available for M2M using this method scale exponentially with the number of LTE resources. We analyze this scheme using a Markov Chain model in [B]. This model has been used and extended in [14] for serving energy-constrained M2M devices.

1.3 Transmission Schemes for Cellular Communications

Traditional cellular networks are largely being designed with Uplink (UL) and Downlink (DL) traffic separated [40]. However, there has recently been increased interest in alternative traffic patterns and protocols. These include coordination of UL and DL traffic, decoupling of UL and DL, using relaying and network coding, and Full Duplex (FD) operation. One recurring trend in these is the focus of serving bidirectional traffic jointly instead of separately. These approaches are detailed in the following subsections.

Coordinated Transmissions for Two-way Traffic

In cellular communications, several transmission schemes have been proposed, with the aim to optimizing performance metrics such as sum-rate, minimum rate, outage probability and energy efficiency. These schemes consider coordination of UL and DL traffic, both separately and jointly, and include the usage of network coding at some of the nodes.

The Coordinated Direct and Relay (CDR) schemes [54] are transmission schemes that define how UL and DL users should be served (i.e. either directly from a BS or through a relay). This and other works such as [53] study which schemes maximize the sum-rate, and also consider design of beamformers [52] to accomplish this. In [55], the authors devise a composite scheme which uses time-sharing between the basic CDR schemes of [54], along with Two-way Relaying (TWR), in order to enlarge the achievable rate region of the users. In TWR, a user is served bidirectional traffic via a relay [41, 55], which utilizes network coding. An extension to TWR is the Four-way relaying [31] and its multiple antenna extension [32], where two users having bidirectional traffic are served simultaneously.

Uplink-Downlink Decoupling

Traditionally, users are served both UL and DL traffic through the same BS. However, recently, there has been interest in *decoupled* UL and DL traffic, which means that a given user receives DL data from one BS, and transmits UL data to another BS [9]. The reason for decoupling the traffic is to get gains in rate performance and lower the power usage [9], since in terms of received power, the optimal UL and DL BSs might not be the same. Decoupling of UL and DL traffic was analyzed in [50] in terms of association probability, using a stochastic geometry framework. In that work, it was shown that users get DL traffic from a Macro BS, while transmitting UL to a Femto BS, in order to maximize received power, and that a large fraction of users choose decoupled access, as the density of Femto BSs increases compared to the density of Macro BSs.

Full Duplex Transmission

Transmissions can be done using half duplex (HD) or full duplex (FD). A device operating in HD can either transmit or receive, but not do both simultaneously using the same time or frequency resource. A device capable of In-band FD can transmit and receive at the same time, on the same frequency. This is different from Time Division Duplex (TDD) and Frequency Division Duplex (FDD), where devices in TDD can transmit and receive at the same time, but on different frequency bands, and in FDD where devices

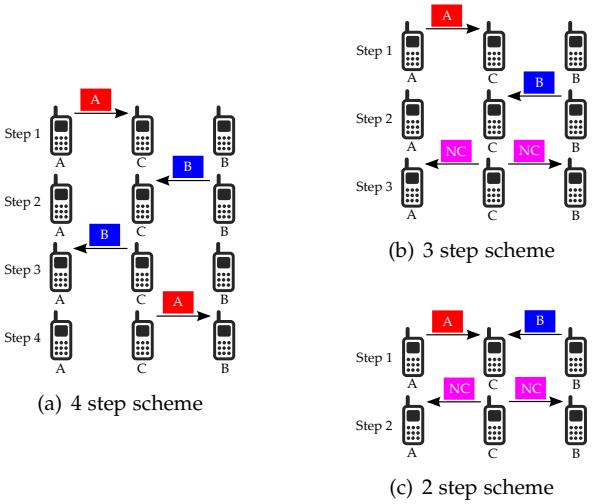

(a) 4 step scheme

(b) 3 step scheme

(c) 2 step scheme

Fig. 1.2: Here, B wants the red packet, while A wants the blue one. Device C can mix these using network coding, and transmit the purple packet labeled NC, a mixture of the red and blue ones.

can transmit and receive on the same frequency band, but not at the same time.

In-band FD is seen as a candidate for increasing the throughput in cellular networks [44], and is shown to double the system capacity of cellular networks [19]. However, the design of in-band FD devices is more complicated, in particular because of the presence of self-interference at the nodes [43]. In Virtual FD, the operation of FD is achieved through alternative methods. These include using buffer-aided relaying [23], having the transmission of nodes partially overlap in time [20], and in [6], the authors define an α-duplexing scheme where the UL and DL channels have a partial overlap in frequency.

Backhauling for Wireless Networks

The increase in number of BSs (including small cells) and users can lead to an increase in transmissions. This puts requirements on the backhaul connectivity, both in terms of cost (deployment and energy usage) [17] as well as flexibility.

Wireless backhaul has clear advantages over its wired counterpart, since it enables rapid and flexible deployment of small cells, which may be placed temporarily, for example in connection with music festivals and concerts [38]. Wireless backhauling transmissions can take place in licensed bands such as

LTE, high frequency bands such as microwave and millimeter-waves, satellite bands and TV-white spaces [48]. Each of these have benefits and drawbacks in interference, propagation characteristics, and licensing costs.

Several wireless backhauling solutions have been given. Some of these consider two-tier networks, where small cells are connected to the macro BSs via wireless connections. This setup is considered in [21], wherein optimal placement of aggregator nodes which gather data to be sent to macro BSs, is studied. Wireless backhauling using FD small cells is considered in [48], and compared with HD in terms of distance between the small cell and macro BS.

Wireless backhauling architectures have been proposed in papers such as [47], where a relay is used to carry the traffic from a small cell to a macro BS, and the optimal position of this relay is analyzed in terms of backhauling capacity. Optimization of Radio Resource Management (RRM) optimization of the Radio Access Network (RAN) is also considered an important part of backhauling in 5G networks [60].

Wireless Network Coding

Network coding is a method in which several information streams can be combined in a network, resulting in traffic flows containing data from or to several different nodes. Network Coding can be done at several layers in the protocol stack, for example at the application layer, network layer or physical layer. At the physical layer, Physical Layer Network Coding (PLNC) takes advantage of collisions of data from several nodes [41, 63].

Consider for example two nodes transmitting simultaneously to a third node C, as shown in Fig. 1.2. Traditionally, the two nodes A and B would not transmit at the same time, but taking turns, as in Fig. 1.2(a). The third node then transmits the decoded data to each sender in a time-sharing fashion. This implies that four transmission slots would be required. However, the receiver could decode the two transmitted signals, and then re-encode them before transmitting back to the senders, as in Fig. 1.2(b). The senders know which information they sent, i.e. they have side-information, and can thus decode the received information in order to obtain the desired signal. The duration of such a method would be three transmission slots.

By intentionally letting the two nodes transmit simultaneously, as is shown in Fig. 1.2(c), we would create a collision at the third node. This node could then transmit this collided signal, and have the two nodes decode the signal. In this latter case, the total transmission time is two slots (see Fig. 1.2(c)).

Coordinated Multipoint Transmission

Interference is an important consideration in wireless and cellular networks. In a cellular context, Coordinated Multi-Point (CoMP) is a method for coordinating BSs, so that they can serve cell-edge users more efficiently [27].

One can distinguish between two types of CoMP schemes for DL: One type where a set of BSs jointly schedule their transmissions, and another type where a subset of the BSs processes the signal jointly before transmitting it to the desired receiver [16]. Such processing can be linear (using Zero Forcing or Minimum Mean Square Error (MMSE)) or nonlinear (using superposition coding or dirty-paper coding) [22]. CoMP is also known as Network MIMO, that is, distributed over several transmitting BSs [18]. CoMP can also be used in UL, where receiving BSs coordinate their reception via beamforming [59].

2 Thesis Objectives

The main research goals of this thesis are listed and commented below:

Design and analysis of protocols for M2M traffic in LTE-type networks

The first part motivates design of protocols for enabling a massive number of accessing devices into cellular networks, where we focus on LTE. We analyze such a protocol, termed Code-Expanded Radio Access in [B]. This scheme permits a high number of devices contention access to the network.

We also want to understand effect of M2M traffic in LTE type networks, where in [A] we present an analysis of the success probability and efficiency of the contending devices in such a network. In this analysis, tools from probability theory and combinatorics are used.

Study the performance of two-way traffic to address the challenge of data rate requirements

Motivated the data rate challenge for 5G cellular networks, we define and study transmission schemes for use in small cell and relay enhanced scenarios. The main drive is the inclusion of small cells connected to the core network via a wireless backhaul connection. These small cells serve users using two-way traffic with the aid of wireless network coding. We put forth and analyze the Wireless Emulated Wire scheme in [D], and investigate a wireless backhauling scheme in [C].

FD and coordination of interference via CoMP are methods which show promising results. However, both methods come with drawbacks in form of increased complexity at the devices involved. In [E], we analyze a scheme for enabling FD emulation using HD devices, termed CoMPflex, in a one-dimensional setting. We show that by spatially separating HD-BSs, we can obtain performance better than having the two users being served by an FD-BS. That is, we get the gains of FD, without the associated complexity. We study the CoMPflex scheme analytically and show numerical results using simulations with realistic parameters. Also, we get what one could regard as

an emulation of CoMP, but without the added cost of the distributed signal processing involved at the BSs as traditional CoMP requires. This is extended to a two-dimensional network model in [F], where we compare CoMPflex against FD in terms of success probability in UL and DL. We analyze the scheme using stochastic geometry, and derive analytical results using reasonable simplifications. It is shown that the analytical results match well with the simulations.

3 Structure of the Thesis

This thesis consists of two parts, a main part and an appendix. The main part consists of an introduction and overview of the state of the art of the topics dealt with in the thesis. Further, the main part provides summaries of each scientific contribution, a discussion of the outcomes of the research and an outlook for future work, as well as a chapter which concludes the thesis.

The second part is an appendix, consisting of the scientific contributions making up the present thesis. These contributions consist of articles which have appeared or are submitted to scientific journals and conferences. The layout of these articles has been revised for readability.

Chapter 2

Contributions in This Thesis

This chapter contains summaries of each of the contributions put forth in this thesis. The contributions are in three sections. In Section 1, the work on random access protocols for M2M communications in cellular networks is given. Section 2 presents the contributions on the transmission schemes for wireless backhauling in cellular networks. Finally, Section 3 details a scheme for FD emulation by spatial separation of HD devices in a cellular network, featuring both one- and two-dimensional scenarios.

1 Machine to Machine Communications

Paper A

Analysis of the LTE Access Reservation Protocol
Henning Thomsen, Nuno K. Pratas, Čedomir Stefanović, and Petar Popovski.
Published in IEEE Communications Letters, Volume 17, Number 8, August 2013, pages: 1616 - 1619

Motivation

In cellular networks, access reservation protocols are important for enabling devices of the network to successfully establish a connection. Such a protocol typically consists of a contention phase and a data phase, where in the first phase, the mobile devices contend for access to the network, while in the second phase, the devices successful in the first phase are allocated resources. In existing analysis of the access protocol used in LTE, it is assumed that there are a sufficient number of resources in the data phase, while this may not be the case due to e.g. varying load of the network and devices with different

traffic patterns than the usual ones. This latter event can happen for M2M-type of traffic.

Paper Content

In this work, we provide an analysis of the features of the LTE access reservation protocol. The analysis uses probability theory and combinatorics, and takes into account the possibility of a limitation in the data phase of the access protocol, i.e. the data phase consisting of a finite number of slots that are available for the devices after contending. Furthermore, in the analysis, we allow for the possibility of a limitation in the number of data slots, which is more realistic. Also, we do not assume that the receiver (i.e. the BS) is able to detect whether a contention token was activated by one or several devices.

Main Results

We derive an expression for the success probability of a finite number of users contending using the LTE access reservation protocol. This analysis is verified by numerical simulations, where we observe a perfect match between the obtained theoretical model and the simulations. Further, we analyze the success rate and energy efficiency (EE) of the contending devices, for a varying number of slots in the data phase, and where we also take the limitation of the detection of contention tokens into account. We analyze the success probability and EE dependent on the number of data slots, and the results can be used for finding the number of data slots giving the optimal EE performance.

Paper B

Code-expanded radio access protocol for machine-to-machine communications

Henning Thomsen, Nuno K. Pratas, Čedomir Stefanović, and Petar Popovski.
Published in Transactions on Emerging Telecommunications Technologies (Special issue on M2M communications), Volume 24, Number 4, June 2013, pages: 355 - 365

Motivation

Cellular networks such as LTE are designed for human centric traffic and as such, they do not initially support other traffic types in an adequate manner. This is especially apparent in the context of M2M types of traffic, where the limitations of current cellular network architectures become apparent. However, as more and more traffic is different from regular cellular traffic, an improvement of the LTE random access scheme is desirable.

Paper Content

Control of the load on cellular networks such as LTE is an approach undertaken by the 3GPP and other standardization bodies. In M2M, Extended Access Class Barring (EAB) is used as a method for the network to control the usage of its resources. We propose an access reservation scheme, Code-Expanded Radio Access, that defines the concept of an access codeword. In each contention round, devices that contend select an access codeword randomly and independently. At the BS side, the BS receives a combination of these codewords, and then proceeds to decode them.

Main Results

We consider two flavors of the Code-Expanded Radio Access scheme. The first is when the entire codebook is at the disposal of the devices, which means that all codewords are available for contention. Second, we consider an adaptive scheme, where the BS defines a subset of the full codebook. The size of the restricted codebook should be such that it matches the user load. It is shown that in contrast to the standard LTE access reservation, the expected efficiency of the Code-Expanded Radio Access scheme has a superior performance in high load conditions. Further, by adapting the codebook to the load, we are able to maintain an efficiency of about 37% for loads up to 1200 devices, which is significantly higher than the LTE reference scheme. This shows that the code expanded scheme is well suited for dealing with M2M traffic on LTE networks.

2 Wireless Backhauling for Cellular Communications

Paper C

Emulating Wired Backhaul with Wireless Network Coding
Henning Thomsen, Elisabeth de Carvalho, and Petar Popovski.
Published in General Assembly and Scientific Symposium (URSI GASS), August 2014.

Motivation

Owing to the need of the increasing requirement of data rate from users, the trend in cellular communications goes in the direction of increasing the number of small cells, while their coverage area is decreased. The deployment of small cells thus requires flexible, power efficient and low-cost backhauling solutions.

Contribution

In this paper, we propose a two-phase transmission scheme for serving two users with two-way traffic using network coding, each of which being attached to and served by different small cell BSs. These users have rate requirements for UL and DL given a-priori. Given these requirements, we solve the problem for how much the transmission power at the BS should be, in order to satisfy the given rates of the users. In addition, we formulate and solve the given problem of finding the transmission power at the BS, when two small cells are considered. The solution being proposed uses theory from the Multiple Access Channel, since at the small cell BS, there are two message streams, one from the user and one from the BS. We also show the feasibility of the second phase. The scheme proposed is transparent to the end user, and can serve those users as if they were served by a small BS with a wired backhaul connection to the cellular infrastructure.

Main Results

We show that the transmission power required is increasing as the DL rate increases. This is under the assumption of Rayleigh fading, and with the BS using Zero Forcing. Also, when the number of antennas at the BS is increased from 2 to 3, the required minimal transmission power decreases by approximately 10 dB over the entire rate range under investigation. This is from the fact that the BS has more degrees of freedom in performing the Zero Forcing. We study the behavior under three different UL rate requirements, and we see the same pattern in each of these three cases.

Paper D

Using Wireless Network Coding to Replace a Wired with Wireless Backhaul

Henning Thomsen, Elisabeth de Carvalho, and Petar Popovski.

Published in IEEE Wireless Communications Letters, Volume 4, Number 2, December 2014, Pages: 141 - 144

Motivation

Future cellular networks are envisioned to be designed with densification in mind, i.e. the number of BSs is increasing, while the coverage area is decreasing, resulting in so-called small cells. One problem is in the connection between these small cells and the core network, especially in the case of low-powered and mobile or non-permanently placed devices. From this, we consider a transmission scheme which uses wireless backhaul to connect to the core network.

Contribution

We design a transmission scheme, termed Wireless Emulated Wire (WEW) for use in a cellular scenario consisting of two small cells. Both of these small cells are connected to a BS by a wireless backhaul connection, and both small cells serve one user. Both devices have a pre-specified Uplink (UL) and Downlink (DL) rate requirements, which must be fulfilled. Given these rate requirements, we formulate and solve the optimization problem of minimizing the transmission power of the BS, given these rate requirements. Inspired by the Han-Kobayashi scheme of information theory, our scheme features the possibility of the BS splitting the DL message for each device into two parts, one common part which is decoded by both small cells, and one private part, which is only to be decoded by the respective small cell. The decoding at both small cells is modeled using the multiple access channel with two users. The rate constraints take into account the presence of the UL message of the respective device. Further, the optimization problem is converted and relaxed using semi-definite programming (SDP), in order to find the optimal splitting factors, transmission powers of the private messages, and the beamformer of the common message and its transmission power.

Main Results

We compare the results of the WEW scheme, with three other schemes. One of these is when the BS uses only Zero Forcing, the second one is when only the common beam former is being used, and the third one is when selecting the splitting factors uniformly at random. We observe that the transmission power at the BS is lowest when the WEW scheme is used, as it adapts to the channel conditions. This is valid for DL rates in the range of 1 to 10 bps, for a fixed UL rate of 1 bps. For the first phase, we see that WEW enables a power reduction of at least 10%. We also show the transmission power required in the second phase of the scheme. In both phases, the transmission power required is increasing with the rate, which is to be expected. Also, from the relaxation, the resulting matrix has rank 1, so a beam forming vector can be extracted directly from the solution obtained via SDP.

3 Full Duplex Emulation with Half Duplex Devices

Paper E

CoMPflex: CoMP for In-Band Wireless Full Duplex.
Henning Thomsen, Petar Popovski, Elisabeth de Carvalho, Nuno K Pratas, Dong Min Kim, and Federico Boccardi.
Accepted in IEEE Wireless Communications Letters, December 2015.

Motivation

Coordination of Base Stations (BSs) in the context of Coordinated Multi-Point (CoMP), along with multi-antenna techniques such as Multiple-Input Multiple-Output (MIMO), is seen as a method to cope with the increasing requirements of future cellular users via managing the interference. In-band Full Duplex (FD) is seen as a important part for increasing the performance in cellular communications. Even though FD enables simultaneous transmission and reception at a device, it comes at a price, namely device complexity and self-interference. In terms of complexity, FD is feasible primarily at the cellular network infrastructure side, while the consumer devices are mainly Half Duplex (HD) for economic and technical reasons.

Contribution

This work considers a cellular scenario consisting of two HD-BSs, one of which serves a Mobile Station (MS) in the DL, the other one in the UL. The BSs are connected by a sufficiently high-capacity connection. We devise a scheme for having two BSs serving one MS each, termed CoMPflex (CoMP for In-band Wireless Full Duplex). An important part of the scheme is the emulation of FD by spatially separating HD devices. The scheme is analyzed both in terms of sum-rate and energy efficiency (EE). For analytical simplicity, and to obtain initial performance indications, the scheme is analyzed in a one-dimensional setting. The model can be seen as an extension of the classical one-dimensional Wyner model for cellular networks. The design parameter to be optimized is the distance between the HD-BSs.

Assuming that the MSs are placed uniformly at random, one in each half of the (one-dimensional) cell, we also introduce a power-adjustment capability, since the adjustment of the splitting brings the BSs closer to the MSs they are serving on the average. Regarding the inter-cell interference, we consider two interference models. The first model is when we assume that nodes in neighboring cells are placed in the same manner as the center cell. The second model is assuming that the nodes are placed in such a way so they cause

maximal interference to the center cell. This latter model is a worst-case interference model. We show analytically that there is a benefit for the sum-rate, when splitting the BSs.

Main Results

We analyze CoMPflex both in terms of sum-rate (i.e. UL and DL rate), as well as the EE. In both cases, all nodes adjust their transmission power, which depends on the BS-BS distance. In both interference models, we observe significant gains in both sum-rate and EE. This stems from the fact that the adjustment of the BS-BS splitting distance brings the nodes closer together on the average. In terms of sum-rate, we see a gain of a factor of two, compared to the sum-rate when the BSs are co-located. This also confirms the analytical derivations.

Focusing on the EE, we consider three different path loss exponents. We see that in all three of these cases, the EE increases as the splitting increases, which can be explained from the definition of power adjustment as well as the increase in sum-rate. We observe gains in EE between 15 and 45 times. Also, in all three cases, the transmission power decreases as the BS-BS splitting increases, which is evident from the power adjustment. This is because as the distance between the BS and the MS it is serving decreases, less transmission power is required to maintain a given rate requirement.

Paper F

Full Duplex Emulation via Spatial Separation of Half Duplex Nodes in a Planar Cellular Network.
Henning Thomsen, Dong Min Kim, Petar Popovski, Nuno K. Pratas and Elisabeth de Carvalho.
Submitted to the 17th IEEE International workshop on Signal Processing Advances in Wireless Communications (SPAWC), 2016.

Motivation

The densification trend of next generation of cellular networks bring challenges in terms of managing the generated interference. Methods such as CoMP and clustering of BSs have been proposed to coordinate BS transmissions, in order to deal with the interference. Other methods are FD transmissions, in order to improve performance. From the study of spatially separating HD-BSs to emulate FD operation in the CoMPflex scheme, using a Wyner model scenario, we study the performance of this scheme in a two-dimensional setting using stochastic geometry, to investigate the performance gains.

Contribution

We study a scheme wherein two connected HD-BSs, one UL and one DL, each serve one user, where the interference between the BSs is cancelled. As a baseline scheme, we consider one where one FD-BS serves two users, one in UL and one in DL. We approximate the positions of the MSs as a two-dimensional Poisson Point Process, and provide analytical expressions of the success probability for UL and DL transmission. A mathematical proof of the UL success probability is provided, and a similar approach can be used for the DL success probability.

We also show the results of the scheme using numerical simulations, and observe a close match between the analytical derivations and the numerical simulations. This implies that our analytical model can be used to approximate the performance of the scheme. We also study the effect of our scheme on the distances of the signal and interference links by analyzing the Cumulative Distribution Functions (CDFs) of the distances.

Main Results

Using both simulations and analytical results, and comparing with a FD baseline scheme, we show that having two connected BSs serving one user in UL and another in DL brings improvements in success probability in terms of SINR thresholds, for both UL and DL. The improvements are approximately a doubling of the success probability, which can be attributed to the effects of our scheme in decreasing the signal distances while increasing the interference distances. This implies that we obtain a better performance than FD, while using only HD devices. Therefore, the scheme can support the ongoing densification trend. The increase in success probability can bring benefits for the users, such as increase in rate, and is otherwise transparent to the users.

Chapter 3

Discussion

In this thesis, we have studied and made contributions to two trends in the evolution of cellular networking, massive M2M communication and two-way traffic schemes for communications in dense cellular networks via wireless backhauling and FD emulation. This chapter contains a discussion of the outcomes of the research, and an outlook to future work.

1 Interpretation of the Results

In our analysis of the applicability of LTE as a M2M network, we assumed that there were not enough resources in the data phase to accommodate the large number of M2M devices. Even though the results were in the context of LTE as a M2M-type network, they are not restricted to such networks.

In light of the suitability of LTE as an M2M-type network, we then devised and studied a random access protocol termed Code-Expanded Radio Access. It was observed that this protocol made an exponential increase in the number of devices possible. This fact is important from the projections of increased traffic, and should be contrasted to the linear increase in LTE-type networks with added system resources. In the Code-Expanded Radio Access protocol, this also means that no changes in the physical layer of the devices involved is necessary, and only a minimal change in the MAC-layer. Therefore, the scheme is backwards compatible with already deployed networks, which is useful since LTE already enjoys a wide deployment, and thus the initial stages would not require changes to the network. Extra system resources would make LTE with its standard random access protocol more suitable. However, it would also make the Code-Expanded Radio Access *even more* suitable for M2M-type communications, due to the exponential versus linear increase of capacity with increased system resources.

A two-way small-cell transmission scheme using wireless backhaul was

analyzed. We used Zero Forcing at the BS, and solved the problem of serving the users in UL and DL with their respective rates, while at the same time minimizing the power required to do so. We saw that increasing the number of antennas made possible a decrease in the required power. In the WEW scheme, we defined a partitioning of the message intended for the users into a public and a private part. Further, we looked at the power consumption of the nodes, since this metric is important in a scenario with wireless backhaul connections, since the nodes could be battery-powered and/or located in difficult to reach places. We saw that by using WEW implied a decrease in total transmission power, compared to using only ZF or a common beamformer.

We devised a scheme, termed CoMPflex, where we investigated FD emulation by using HD BSs. This was done for two reasons: First, there are complexities in FD, particularly in terms of self-interference, and second, the usage of HD BSs means that CoMPflex permits backwards compatibility. It was observed that there was an optimal distance between the UL- and DL-BSs, and from that, optimal placement of BSs to maximize the sum rate of the users. This is useful in order to address the increasing rate requirements of the users. Further, the CoMPflex scheme is transparent to the users, which implies that the changes required at the users' terminals can be minimized.

We then analyzed the CoMPflex scheme in a two-dimensional setting, where we saw that serving users in the network jointly with UL and DL traffic, as well as having the UL-BSs and DL-BSs adjacent, gave a benefit in success probability. This is because in CoMPflex, the interference between UL and its paired DL-BS is cancelled, and the UL and DL users are, on average, farther away from each other than in the baseline FD scheme.

2 Limitations of the Results

As we looked at the suitability of LTE and a M2M-type network, some simplifying assumptions were made to ease the analysis. We assumed that the BS had a-priori knowledge about the number of users contending (i.e. the load). Such knowledge could be obtained by using e.g. a user load estimation method.

When studying the WEW scheme and CoMPflex, we made some simplifying assumptions. These assumptions were mainly in the channel modelling, where we assumed Rayleigh fading. Such an assumption is often made, and it was made in our work because we were mainly interested in obtaining performance indications of the two schemes. We also assumed that the communication (i.e. handshaking) between the nodes had already been established, and thus the focus was on the exchange of data. Indeed, some sort of signaling would have to be made in a real life situation when the nodes would set up their connection. This, however, was outside the scope of the analy-

sis. When analyzing CoMPflex, we began by assuming that the nodes (BSs and MSs) were placed on a line. More specifically, we assumed a Wyner-type one-dimensional deployment model. This first assumption was made to get a first look at the performance of CoMPflex. In the two-dimensional extension, we approximated the placement of the users by a Poisson Point Process, even though each user was restricted to the Voronoi cell of its BS. This was done for analytical simplicity, but it gave a good indication of the performance.

3 Potential for Extending the Research and Future Work

The results obtained in our analysis of the LTE protocol show that LTE type networks can be made to accommodate M2M type communications. The analysis itself is also has enough generality to be able to be used in other types of networks, such as the next generation 5G networks. As was seen in the analysis of the Code-Expanded Radio Access protocol, it would theoretically be possible to enable LTE as an M2M type network. The Code-Expanded Radio Access protocol could also be used in conjunction with the reference method employed. From that, one could design a scheme that divided the resources between M2M-type and human-type traffic. How much should be used for each of these could be decided from a-priori knowledge of the traffic or by estimation. The Code-Expanded Radio Access protocol scales the possible resources exponentially, and one could also take advantage of this when dividing the resources between two (or more) types of traffic. As we saw, the adaptive Code-Expanded Radio Access protocol could also be used, to minimize the probability of wasted resources, and in situations with varying user load.

Furthermore, one could consider analyzing the Code-Expanded Radio Access protocol in situations where the number of users is not known a-priori. This would imply either designing a load estimation algorithm, or using an existing one. In both cases, one would need to know the performance of such a method, in order to assess its performance. The Code-Expanded Radio Access protocol could also be used in scenarios such as smart metering. However, in this case, one would need to take the arrival type of the traffic into account, since bursty arrivals could be possible.

We considered the WEW scheme, where we analyzed its performance in terms of rate. One could go a step further, and consider other metrics such as outage and energy efficiency. Such metrics are very relevant in 5G networks, in particular in green communications. Another path, inspired by the interest in deployment modes for cellular networks beyond the classical hexagonal model, would be taking the positions of the nodes to follow a more general model, for example using stochastic geometry.

The placement of BSs, as well as the FD-emulation by spatially separating HD-devices was the main idea of the CoMPflex scheme. It could also be used in other communication methods, for example Vehicle-to-Vehicle and Device-to-Device communications. For example, the intra-cell interference between the UL and DL users is an issue, and interference mitigation methods would be interesting to study, for further performance improvements.

The two-dimensional extension of CoMPflex opens many interesting paths to take. For instance, it would be interesting to analyze more general clustering schemes with two-way traffic, where more than two BSs would cooperate, to leverage on the interference cancellation. Further, the CoMPflex scheme is more flexible in that we can choose which BSs are to be paired. Like in the one-dimensional Wyner model, the two-dimensional case also suffers from intra-cell interference between the users. It would also be interesting to take user scheduling into consideration, and to analyze a model which serves several users in each cell. A hybrid scheme, consisting of both FD BSs as well as CoMPflex HD BSs would also be interesting to study, in terms of optimal trade-offs. Further, since the CoMPflex BSs are connected by a backhaul connection, one could study the influence of the reliability of the backhaul connection, and taking examples such as wireless backhaul into this study.

Chapter 4

Conclusion

The focus of this thesis has been on communication protocols for enabling a massive number of M2M devices into cellular networks. Also, we have designed and analyzed transmission schemes for dense cellular networks, focusing on wireless backhauling and FD emulation.

The analysis included looking at the suitability of LTE for M2M communications. More specifically, the success probability of the LTE random access schemes was derived under the assumption of a finite population of accessing devices. This analysis was performed using tools from probability theory and combinatorics, and the possibility and limitations of the LTE random access procedure was shown. We devised a protocol, Code-Expanded Radio Access, to deal with the problem of massive random access by M2M devices in LTE-type (and other) networks. It was analyzed by numerical simulations and analytically via a Markov Chain model, and we observed that it is superior to the standard LTE random access in terms of efficiency in high load conditions.

We have also defined transmission schemes for use in dense cellular networks. Herein, the main themes were wireless backhaul and FD emulation. Motivated by the increasing importance of wireless backhaul, we studied a two-way transmission scheme using small cells connected wirelessly to a macro BS. We derived the power required to satisfy the users' rates, for scenarios consisting of one and two small cells. We designed and analyzed the Wireless Emulated Wire (WEW) scheme. In this scheme, private and common messages are transmitted from a BS to users via relays. It was observed that the WEW scheme brings improvements over either broadcasting the desired information using separate beamformers or jointly via a common beamformer. It was also seen that the common beamforming vector could be extracted directly from the solution of the optimization problem.

The emulation of FD transmissions using HD BSs was put forth in the

CoMPflex scheme. Therein, we analyzed via a one-dimensional Wyner-type model the performance of the scheme in terms of sum rate and energy efficiency. The analysis was done under two settings, in the first when the nodes held their transmission power constant, and in the second when the nodes varied their transmission power. We observed that an optimal BS placement, averaged over the MS placement, implied an significant increase in the considered metrics, even under worst-case conditions. In the work, we showed that a gain in sum-rate was also possible via analytical derivations.

The CoMPflex scheme was then analyzed in a two-dimensional setting, where the tools from stochastic geometry were used to facilitate the analysis. It was observed that using CoMPflex, and serving the users with two-way traffic, had clear advantages over using FD-BSs.

References

[1] "C-RAN: The Road Towards Green RAN," *China Mobile White Paper*, vol. 2, 2011.

[2] "Signalling is growing 50 % faster than data traffic," *Nokia Siemens Networks White paper*, 2012.

[3] *Radio Resource Control (RRC); Protocol specification*, 3GPP TS 36.331.

[4] *MTC simulation results with specific solutions*, 3GPP TSG RAN WG2 71 R2-104662, August 2010.

[5] P. Agyapong, M. Iwamura, D. Staehle, W. Kiess, and A. Benjebbour, "Design considerations for a 5G network architecture," *Communications Magazine, IEEE*, vol. 52, no. 11, pp. 65–75, 2014.

[6] A. AlAmmouri, H. ElSawy, O. Amin, and M.-S. Alouini, "In-Band α-Duplex Scheme for Cellular Networks: A Stochastic Geometry Approach," *arXiv preprint arXiv:1509.00976*, 2015.

[7] J. G. Andrews, "Seven ways that HetNets are a cellular paradigm shift," *Communications Magazine, IEEE*, vol. 51, no. 3, pp. 136–144, 2013.

[8] J. G. Andrews, S. Buzzi, W. Choi, S. V. Hanly, A. Lozano, A. C. Soong, and J. C. Zhang, "What Will 5G Be?" *Selected Areas in Communications, IEEE Journal on*, vol. 32, no. 6, pp. 1065–1082, 2014.

[9] F. Boccardi, J. Andrews, H. Elshaer, M. Dohler, S. Parkvall, P. Popovski, and S. Singh, "Why to Decouple the Uplink and Downlink in Cellular Networks and How To Do It," *arXiv preprint*, vol. abs/1503.06746, 2015. [Online]. Available: http://arxiv.org/abs/1503.06746

[10] J.-P. Cheng, C.-h. Lee, and T.-M. Lin, "Prioritized Random Access with dynamic access barring for RAN overload in 3GPP LTE-A networks," in *GLOBECOM Workshops (GC Wkshps), 2011 IEEE*. IEEE, 2011, pp. 368–372.

[11] R.-G. Cheng, C.-H. Wei, S.-L. Tsao, and F.-C. Ren, "Rach Collision Probability for Machine-type Communications," in *IEEE Veh. Tech. Conf., Spring 2012*. IEEE, 2012, pp. 1–5.

[12] Cisco, "Cisco Visual Networking Index: Global Mobile Data Traffic Forecast Update, 2013–2018," *White Paper*, 2014.

[13] M. Coldrey, J.-E. Berg, L. Manholm, C. Larsson, and J. Hansryd, "Non-line-of-sight small cell backhauling using microwave technology," *Communications Magazine, IEEE*, vol. 51, no. 9, pp. 78–84, 2013.

[14] M. Condoluci, G. Araniti, M. Dohler, A. Iera, and A. Molinaro, "Virtual code resource allocation for energy-aware MTC access over 5G systems," *Ad Hoc Networks*, 2016.

[15] O. Galinina, A. Pyattaev, S. Andreev, M. Dohler, and Y. Koucheryavy, "5G Multi-RAT LTE-WiFi Ultra-Dense Small Cells: Performance Dynamics, Architecture, and Trends," *Selected Areas in Communications, IEEE Journal on*, vol. 33, no. 6, pp. 1224–1240, 2015.

[16] V. Garcia, Y. Zhou, and J. Shi, "Coordinated Multipoint Transmission in Dense Cellular Networks With User-Centric Adaptive Clustering," *Wireless Communications, IEEE Transactions on*, vol. 13, no. 8, pp. 4297–4308, 2014.

[17] X. Ge, H. Cheng, M. Guizani, and T. Han, "5G wireless backhaul networks: challenges and research advances," *Network, IEEE*, vol. 28, no. 6, pp. 6–11, 2014.

[18] D. Gesbert, S. Hanly, H. Huang, S. S. Shitz, O. Simeone, and W. Yu, "Multi-Cell MIMO Cooperative Networks: A New Look at Interference," *Selected Areas in Communications, IEEE Journal on*, vol. 28, no. 9, pp. 1380–1408, 2010.

[19] S. Goyal, P. Liu, S. Hua, and S. Panwar, "Analyzing a full-duplex cellular system," in *Proc. of the IEEE Conference on Information Sciences and Systems (CISS 2013)*, Mar. 2013.

[20] D. Guo and L. Zhang, "Virtual full-duplex wireless communication via rapid on-off-division duplex," in *Communication, Control, and Computing (Allerton), 2010 48th Annual Allerton Conference on*. IEEE, 2010, pp. 412–419.

[21] M. N. Islam, A. Sampath, A. Maharshi, O. Koymen, and N. B. Mandayam, "Wireless backhaul node placement for small cell networks," in *Information Sciences and Systems (CISS), 2014 48th Annual Conference on*. IEEE, 2014, pp. 1–6.

[22] S. Jing, D. N. Tse, J. B. Soriaga, J. Hou, J. E. Smee, and R. Padovani, "Multicell Downlink Capacity with Coordinated Processing," *EURASIP Journal on Wireless Communications and Networking*, vol. 2008, p. 18, 2008.

[23] S. M. Kim and M. Bengtsson, "Virtual full-duplex buffer-aided relaying—relay selection and beamforming," in *Personal Indoor and Mobile Radio Communications (PIMRC), 2013 IEEE 24th International Symposium on*. IEEE, 2013, pp. 1748–1752.

[24] T. Kim, H. S. Jang, and D. K. Sung, "An Enhanced Random Access Scheme With Spatial Group Based Reusable Preamble Allocation in Cellular M2M Networks," *Communications Letters, IEEE*, vol. 19, no. 10, pp. 1714–1717, 2015.

[25] A. Laya, L. Alonso, and J. Alonso-Zarate, "Is the Random Access Channel of LTE and LTE-A Suitable for M2M Communications? A Survey of Alternatives," *Communications Surveys & Tutorials, IEEE*, vol. 16, no. 1, pp. 4–16, 2014.

[26] A. Laya, L. Alonso, P. Chatzimisios, and J. Alonso-Zarate, "Massive access in the Random Access Channel of LTE for M2M communications: An energy perspective," in *Communication Workshop (ICCW), 2015 IEEE International Conference on*. IEEE, 2015, pp. 1452–1457.

[27] D. Lee, H. Seo, B. Clerckx, E. Hardouin, D. Mazzarese, S. Nagata, and K. Sayana, "Coordinated multipoint transmission and reception in LTE-advanced: deployment scenarios and operational challenges," *Communications Magazine, IEEE*, vol. 50, no. 2, pp. 148–155, 2012.

[28] K.-D. Lee, S. Kim, and B. Yi, "Throughput comparison of random access methods for M2M service over LTE networks," in *GLOBECOM Workshops (GC Wkshps), 2011 IEEE*. IEEE, 2011, pp. 373–377.

[29] S.-Y. Lien, T.-H. Liau, C.-Y. Kao, and K.-C. Chen, "Cooperative Access Class Barring for Machine-to-Machine Communications," *Wireless Communications, IEEE Transactions on*, vol. 11, no. 1, pp. 27–32, 2012.

[30] G.-Y. Lin, S.-R. Chang, and H.-Y. Wei, "Estimation and Adaptation for Bursty LTE Random Access," *Transactions on Vehicular Technology, IEEE*, vol. PP, no. 99, 2015.

[31] H. Liu, P. Popovski, E. de Carvalho, Y. Zhao, and F. Sun, "Four-way Relaying in Wireless Cellular Systems," *Wireless Communications Letters, IEEE*, vol. 2, no. 4, pp. 403–406, 2013.

[32] H. Liu, F. Sun, E. de Carvalho, P. Popovski, H. Thomsen, and Y. Zhao, "MIMO four-way relaying," in *Signal Processing Advances in Wireless Communications (SPAWC), 2013 IEEE 14th Workshop on*. IEEE, 2013, pp. 46–50.

[33] A. Lo, Y. W. Law, M. Jacobsson, and M. Kucharzak, "Enhanced LTE-Advanced Random-Access Mechanism for Massive Machine-to-Machine (M2M) Communications," in *27th World Wireless Research Forum (WWRF) Meeting*, 2011, pp. 1–5.

[34] G. C. Madueno, Č. Stefanović, and P. Popovski, "Efficient LTE Access with Collision Resolution for Massive M2M Communications," in *Globecom Workshops (GC Wkshps), 2014*. IEEE, 2014, pp. 1433–1438.

[35] ——, "Reliable Reporting for Massive M2M Communications With Periodic Resource Pooling," *Wireless Communications Letters, IEEE*, vol. 3, no. 4, pp. 429–432, 2014.

[36] Y. Mehmood, C. Görg, M. Muehleisen, and A. Timm-Giel, "Mobile M2M communication architectures, upcoming challenges, applications, and future directions," *EURASIP Journal on Wireless Communications and Networking*, vol. 2015, no. 1, pp. 1–37, 2015.

[37] A. Osseiran, F. Boccardi, V. Braun, K. Kusume, P. Marsch, M. Maternia, O. Queseth, M. Schellmann, H. Schotten, H. Taoka *et al.*, "Scenarios for 5G mobile and wireless communications: the vision of the METIS project," *Communications Magazine, IEEE*, vol. 52, no. 5, pp. 26–35, 2014.

[38] P. Popovski, V. Braun, H. Mayer, P. Fertl, D.-S. Z. Ren, E. Ström, T. Svensson, H. Taoka, P. Agyapong, A. Benjebbour *et al.*, "ICT-317669-METIS/D1. 1 Scenarios, requirements and KPIs for 5G mobile and wireless system," *EU-Project METIS (ICT-317669), Deliverable*, 2013.

[39] P. Popovski, "Ultra-reliable communication in 5G wireless systems," in *5G for Ubiquitous Connectivity (5GU), 2014 1st International Conference on*. IEEE, 2014, pp. 146–151.

[40] P. Popovski and E. de Carvalho, "5G Architectures for Small Cells with Wireless Backhaul and Two-Way Communication," 2013.

[41] P. Popovski and H. Yomo, "Physical Network Coding in Two-Way Wireless Relay Channels," in *Communications, 2007. ICC'07. IEEE International Conference on*. IEEE, 2007, pp. 707–712.

[42] N. Pratas, H. Thomsen, Č. Stefanović, and P. Popovski, "Code-Expanded Random Access for Machine-Type Communications," in *IEEE Global Communications Conference 2012 (GLOBECOM) - Second International Workshop on Machine-to-Machine Communications 'Key' to the Future Internet of Things*, 2012.

[43] C. Psomas and I. Krikidis, "Outage Analysis of Full-Duplex Architectures in Cellular Networks networks," in *Vehicular Technology Conference (VTC Spring), 2015 IEEE 81st*. IEEE, 2015, pp. 1–5.

[44] A. Sabharwal, P. Schniter, D. Guo, D. W. Bliss, S. Rangarajan, and R. Wichman, "In-Band Full-Duplex Wireless: Challenges and Opportunities," *Selected Areas in Communications, IEEE Journal on*, vol. 32, no. 9, pp. 1637–1652, 2014.

[45] M. Z. Shafiq, L. Ji, A. X. Liu, J. Pang, and J. Wang, "Large-Scale Measurement and Characterization of Cellular Machine-to-Machine Traffic," *Networking, IEEE/ACM Transactions on*, vol. 21, no. 6, pp. 1960–1973, 2013.

[46] H. Shariatmadari, S. Iraji, and R. Jantti, "Analysis of transmission methods for ultra-reliable communications," in *Personal, Indoor, and Mobile Radio Communications (PIMRC), 2015 IEEE 26th Annual International Symposium on*. IEEE, 2015, pp. 2303–2308.

[47] Y. Shi, M. Li, X. Xiong, and G. Han, "A flexible wireless backhaul solution for emerging small cells networks," in *Signal Processing, Communications and Computing (ICSPCC), 2014 IEEE International Conference on*. IEEE, 2014, pp. 591–596.

[48] U. Siddique, H. Tabassum, E. Hossain, and D. I. Kim, "Wireless backhauling of 5G small cells: challenges and solution approaches," *Wireless Communications, IEEE*, vol. 22, no. 5, pp. 22–31, 2015.

[49] S. Singh, H. S. Dhillon, and J. G. Andrews, "Offloading in Heterogeneous Networks: Modeling, Analysis, and Design Insights," *Wireless Communications, IEEE Transactions on*, vol. 12, no. 5, pp. 2484–2497, 2013.

[50] K. Smiljkovikj, P. Popovski, and L. Gavrilovska, "Analysis of the decoupled access for downlink and uplink in wireless heterogeneous networks," *Wireless Communications Letters, IEEE*, vol. 4, no. 2, pp. 173–176, 2015.

[51] B. Soret, K. I. Pedersen, N. T. Jørgensen, and V. Fernández-López, "Interference coordination for dense wireless networks," *Communications Magazine, IEEE*, vol. 53, no. 1, pp. 102–109, 2015.

[52] F. Sun, E. de Carvalho, P. Popovski, and C. D. T. Thai, "Coordinated direct and relay transmission with linear non-regenerative relay beamforming," *Signal Processing Letters, IEEE*, vol. 19, no. 10, pp. 680–683, 2012.

[53] F. Sun, P. Popovski, C. D. T. Thai, and E. de Carvalho, "Sum-rate maximization of coordinated direct and relay systems," in *European Wireless, 2012. EW. 18th European Wireless Conference*. VDE, 2012, pp. 1–7.

[54] C. Thai, P. Popovski, M. Kaneko, and E. de Carvalho, "Coordinated transmissions to direct and relayed users in wireless cellular systems," in *IEEE ICC 2011*, june 2011, pp. 1 –5.

[55] C. D. T. Thai, P. Popovski, M. Kaneko, and E. de Carvalho, "Multi-Flow Scheduling for Coordinated Direct and Relayed Users in Cellular Systems," *IEEE Trans. Commun.*, vol. 61, no. 2, pp. 669–678, Feb. 2013.

[56] H. Thomsen, N. Pratas, Č. Stefanović, and P. Popovski, "Analysis of the LTE Access Reservation Protocol," *IEEE Communications Letters*, vol. 17, no. 8, pp. 1616–1619, Aug 2013.

[57] H. Tullberg, P. Popovski, D. Gozalvez-Serrano, P. Fertl, Z. Li, A. Höglund, M. A. Uusitalo, H. Droste, Ö. Bulakci, J. Eichinger *et al.*, "METIS System Concept: The Shape of 5G to Come."

[58] F. Vázquez-Gallego, J. Alonso-Zarate, L. Alonso, and M. Dohler, "Analysis of energy efficient distributed neighbour discovery mechanisms for machine-to-machine networks," *Ad hoc networks*, vol. 18, pp. 40–54, 2014.

[59] S. Venkatesan, "Coordinating Base Stations for Greater Uplink Spectral Efficiency in a Cellular Network," in *Personal, Indoor and Mobile Radio Communications, 2007. PIMRC 2007. IEEE 18th International Symposium on*. IEEE, 2007, pp. 1–5.

[60] N. Wang, E. Hossain, and V. K. Bhargava, "Backhauling 5G small cells: A radio resource management perspective," *Wireless Communications, IEEE*, vol. 22, no. 5, pp. 41–49, 2015.

[61] C.-H. Wei, R.-G. Cheng, and S.-L. Tsao, "Modeling and Estimation of One-Shot Random Access for Finite-User Multichannel Slotted ALOHA Systems," *Communications Letters, IEEE*, vol. 16, no. 8, pp. 1196–1199, 2012.

[62] X. Yang, A. O. Fapojuwo, and E. E. Egbogah, "Performance Analysis and Parameter Optimization of Random Access Backoff Algorithm in LTE," in *Vehicular Technology Conference (VTC Fall), 2012 IEEE*. IEEE, 2012, pp. 1–5.

[63] S. Zhang, S. C. Liew, and P. P. Lam, "Hot topic: physical-layer network coding," in *Proceedings of the 12th annual international conference on Mobile computing and networking*. ACM, 2006, pp. 358–365.

Part II

Papers

Paper A

Analysis of the LTE Access Reservation Protocol for Real-Time Traffic

Henning Thomsen, Nuno K. Pratas, Čedomir Stefanović and Petar Popovski

The paper has been published in the
IEEE Communications Letters Vol. 17(8), pp. 1616–1619, 2013.

The layout has been revised.

Abstract

*LTE is increasingly seen as a system for serving real-time Machine-to-Machine (M2M) communication needs. The asynchronous M2M user access in LTE is obtained through a two-phase access reservation protocol (*contention *and* data *phase). Existing analysis related to these protocols is based on the following assumptions: (1) there are sufficient resources in the* data phase *for all detected contention tokens, and (2) the base station is able to detect collisions, i.e., tokens activated by multiple users. These assumptions are not always applicable to LTE - specifically, (1) due to the variable amount of available data resources caused by variable load, and (2) detection of collisions in contention phase may not be possible. All of this affects transmission of real-time M2M traffic, where data packets have to be sent within a deadline and may have only one contention opportunity. We analyze the features of the two-phase LTE reservation protocol and asses its performance, when assumptions (1) and (2) do not hold.*

1 Introduction

An access reservation protocol is instrumental in any multi-user communication system in order to enable users to connect asynchronously or transmit intermittently [1]. The Long Term Evolution (LTE) system [2] uses an access protocol consisting of two phases: a *contention phase*, where each user contends by activating a particular reservation token chosen from the set of available tokens; and a *data phase*, where the reservation tokens (i.e., token holders) detected by the base station (BS) get assigned resources for the data transfer. The asynchronous access in LTE gains importance as the needs to support traffic related to Machine-to-Machine (M2M) communications gets increasingly important. In many cases, M2M traffic is a real-time traffic, where data packets become obsolete after a deadline and thus may undergo only a single contention and data phases, i.e., unsuccessful transmissions cannot be postponed for later contention or scheduled to a later data phase.

The available analysis of the two-phase access reservation protocols typically assumes that: (1) there are sufficient resources in the data phase to serve all detected reservation tokens; (2) the BS is able to discern between reservation tokens activated by one or more than one users, i.e., the contention phase has a ternary output (idle, single or collision). However, assumption (1) does not hold in cellular networks such as LTE, where the data phase has limited number of resources, while the network load is variable; this implies that there is a possibility that the users with real-time traffic that contended successfully may not be assigned a data transmission slot at all [2]. Assumption (2), by default does not hold in LTE, as the BS may not able to discern if a token was activated by one or multiple users [3, Sec. 17.5.2.3]. In other words,

there are practical setups in which the BS can "see" that a preamble has been activated, but it does not know how many users activated it. This implies that in the contention phase, collisions "over" tokens are treated as singles, i.e., the output of the contention phase is binary (idle or active) instead of the commonly assumed ternary output (idle, single or collision).

In LTE, a reservation token is activated by transmitting a specific preamble in the random access sub-frame [4]. The preambles are chosen from the orthogonal set of preambles obtained from Zadoff-Chu sequences [5]. Due to orthogonality of the preambles, the LTE contention phase can be modeled as a framed slotted ALOHA scheme, where "slots" represent preambles over which the users contend.

Asynchronous M2M communications based on LTE are considered in several works found in the literature. In [6], the authors propose a preamble retransmission method, subject to optimization of the transmission rate. In [7], a packet aggregation method is proposed. Here, M2M devices do not necessarily transmit their packets immediately, but buffer them until a certain threshold. A closed form expression of the collision probability of M2M traffic at the LTE contention phase is provided in [8]. A recent work using a combinatorial model to study the random access in LTE is given in [9]. Different from [9], we also consider the data phase in our analysis.

An early study of the ALOHA protocol in a reservation framework was done in [10], and [11] consideres two reservation methods based on framed ALOHA. Access reservation protocols with several parallel data channels have been studied in [12]. Herein, the authors find the optimal ratio of control to data channels, and the optimal number of data channels, in terms of throughput. Note that in contrast to [12], in this letter, we consider collisions in the contention phase to be non-destructive. Finally, we point out a recent analysis of random access protocols in the context of RFID systems given in [13]; the results presented therein are directly applicable to the contention phase of the access reservation protocol and are used as a starting point for the analysis presented in the paper.

In this letter, we derive the exact probability mass function (pmf) that a number of reservation tokens activated by a single user are assigned resources in the data phase, when assumptions (1) and (2) do not hold. Based on the obtained results, we calculate the corresponding one-shot success rate and efficiency of the LTE access reservation scheme. The presented analysis and derived results are directly applicable to the LTE access reservation scheme for the increasingly important case of asynchronously served users with real-time constraints.

The remainder of this paper is organized as follows. In Section 2, we present the system model. Section 3 elaborates the method to obtain the exact pmf of the number of reservation tokens that are activated by a single user and that are assigned resources in the data phase, following by the derivation

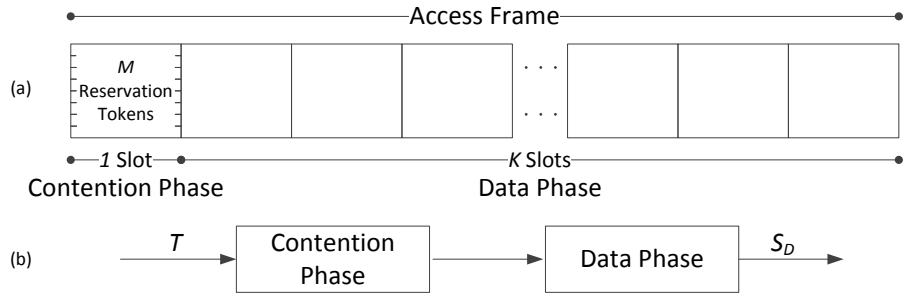

Fig. A.1: (a) Access Frame and (b) System Model.

of the success rate and efficiency. Examples demonstrating derived results are given in Section 4, while the letter is concluded in Section 5.

2 System Model

Fig. A.1(a) shows a simplified version of the LTE access reservation protocol that captures the details essential for the presented analysis [4]. The access reservation is composed of a contention phase and data phase. The contention phase lasts a single slot and is modeled as a variant of a framed slotted ALOHA, where users contend over a set of of available tokens[1]; we assume that in this slot, there are available M reservation tokens for contention. The data phase is a actually a Time Division Multiplexing (TDM) scheme and we assume that there are available K resource slots (i.e., K TDM slots). The combination of the two phases is denoted as an access frame, consisting of $K+1$ slots in total. Finally, we assume that there are T users contending for the available resource slots.

The access reservation protocol operates as follows:

1. Each of T users activates randomly and independently one of the M available tokens. A token can be activated by more than one user.

2. Base Station (BS) detects all activated tokens, irrespective whether they have been activated by one or several users [3, Sec. 17.5.2.3]. The BS chooses uniformly randomly K tokens from the set of detected tokens.

3. The selected tokens are assigned a resource slot each and the corresponding users, i.e., token holders, are informed about the respectively assigned slots through the feedback channel.

[1]In contrast to standard ALOHA, in the considered model there are no collisions, as elaborated in the letter.

Variable	Description
M	No. of reservation tokens
K	No. of TDM slots
T	No. of accessing users
S_D	No. of users succeeding in the data phase
s	No. of reservation tokens selected by one user
c	No. of reservation tokens selected by more than one user
k	$\min\{s+c, K\}$
m	$\min\{M, T\}$
σ	Success Rate
ρ	Efficiency

Table A.1: Definition of used variables.

4. The selected token holders transmit their data packets in the assigned resource slots. If two or more holders activated the same token and thus were assigned the same resource slot, their transmissions collide and are considered as lost.

The assumption that the BS is unable to detect collision in contention phase holds in small cells [3, Sec. 17.5.2.3], and refers to the worst case scenario where the detected preamble does not reveal anything about the number of users that transmitted it[2]. Obviously, if the BS knows that there are two or more users using a certain preamble, then a straightforward way to operate is not to assign any resource slot to the preamble, thus preventing collisions and the respective resource waste in the data phase.

3 Analysis

3.1 Derivation of the pmf

The conditional probability of having assigned $S_D = d$ contention tokens used exactly by one user each from the contention phase of size M to the data phase of size K when $T = t$, denoted by $P(S_D = d \mid T = t, K, M)$, is derived in this section. The parameters used in the derivation are listed in Table A.1.

[2]Note that, in practical LTE systems, if the cell size is more than twice the distance corresponding to the maximum delay spread, the BS may, in some circumstances, be able to differentiate the transmission of the same preamble by two or more users, provided that the users are separable in terms of the Power Delay Profile [3]. However, the analysis of such operation is straightforward and therefore not of interest in this letter.

$$P(S_D = d \mid T = t, K, M)$$
$$= \sum_{0 \le s \le m} \sum_{0 \le c \le m-s} \frac{\binom{M}{s} T \cdot (T-1) \cdots (T-s+1) \binom{M-s}{c} S_2(T-s, c) c!}{M^T} \frac{\binom{s}{d}\binom{c}{k-d}}{\binom{s+c}{k}} \tag{A.1}$$

Suppose that out of the M available tokens, s are used by exactly one user each (singles), and c are used by two or more users (collisions), where $0 \le s + c \le M$. From the M available tokens, s single tokens can be selected in $\binom{M}{s}$ ways.[3] Further, as the tokens are distinguishable, the number of ways in which s of the T users can be selected is $T \cdot (T-1) \cdots (T-s+1)$ ways.

From the remaining $M - s$ tokens, we choose c for the colliding users, which can be done in $\binom{M-s}{c}$ ways. As the tokens are distinguishable, we need to count all permutations of them, which equals $c!$. Further, the number of ways in which $T - s$ users can be distributed among c tokens such that there are at least two users selecting each token is given by the 2-associated Stirling number of the second kind $S_2(T-s, c)$ [14, pp.221-222], which can be computed using the recurrence relation (A.7) exposed in the Appendix.

The total number of ways in which T users can select among M tokens without restriction is M^T. Therefore, the probability of the T users selecting among M tokens such that there are s tokens used by exactly one user each, and c tokens used by two or more users each, equals

$$\frac{\binom{M}{s} T \cdot (T-1) \cdots (T-s+1) \binom{M-s}{c} S_2(T-s, c) c!}{M^T}, \tag{A.2}$$

as similarly derived in [13], although in a different context.

In the data phase, the $s + c$ used tokens are mapped randomly to the K resource slots. Here we distinguish between two cases, $s + c \le K$ and $s + c > K$. In the first case, all used tokens are assigned to data slots. In the second case, K out of the $s + c$ tokens are randomly selected and assigned to the data slots. We then have that the probability of selecting d slots out of the K, such that the selected slots are used by one user each, is given by the hypergeometric distribution

$$\frac{\binom{s}{d}\binom{c}{k-d}}{\binom{s+c}{k}}. \tag{A.3}$$

where $k = \min\{s + c, K\}$. Note that when $k = s + c$, then Eq. (A.3) equals 1 when $s = d$, and 0 otherwise.

The probability of selecting d slots containing one user each, given that $T = t$ users transmit, is obtained by summing over all cases of s and c such

[3] We define $\binom{n}{k} = 0$ when $n < k$.

that $0 \leq s + c \leq M$, which yields the complete expression of $P(S_D = d \mid T = t, K, M)$ presented in Eq. (A.1), where $m = \min\{M, T\}$ and $k = \min\{s + c, K\}$.

We conclude by noting that (A.1) holds when $M > K$ and also when $M \leq K$.

3.2 Success Rate and Efficiency

We use the pmf derived in the previous subsection in obtaining an expression for the success rate, defined as the expected value of S_D given a number of transmitting users T

$$\sigma = \frac{E\left[S_D | T = t, K, M\right]}{t} = \frac{1}{t} \sum_{s=0}^{\min\{K,M\}} s \cdot P(S_D = s | T = t). \tag{A.4}$$

As defined, the success rate takes into account both phases of the LTE access reservation scheme and measures the expected fraction of successfully accessing users.

In order to assess how well the slots of the access frame (see Fig. A.1(a)) are utilized, we define the efficiency, given $T = t$, K and M, as

$$\rho = \frac{E\left[S_D | T = t, K, M\right]}{K + 1} \tag{A.5}$$

where the denominator corresponds to the length of the access frame in slots.

4 Results

In this section, we give examples of the pmf in Eq.(A.1), the success rate in Eq.(A.4) and efficiency in Eq.(A.5), both for the cases when $M > K$ and $M \leq K$.

4.1 pmf Evaluation

We first describe the method to obtain the pmf from the simulation. The method can be summarized in the following three steps.

1. Let the T users select their tokens randomly and independently. For every token, count the number of times this token is selected by the users.

2. To simulate a limited data phase, select a random subset of size K from the set of tokens. Count the number of successful tokens in this subset, i.e. tokens used by one user. Call this number S.

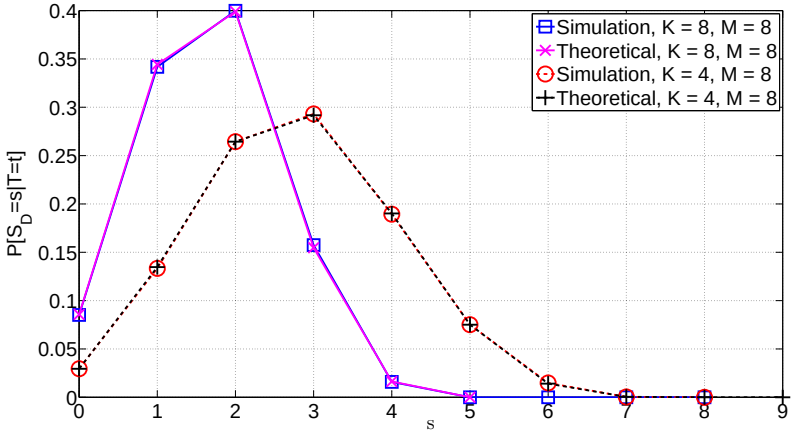

Fig. A.2: Comparison of theoretical and simulated pmfs for $M > K$ and $M \leq K$.

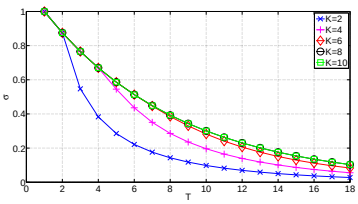

Fig. A.3: Comparison of success rate σ, for $M = 8$, varying user load T, and different sizes of the data phase K.

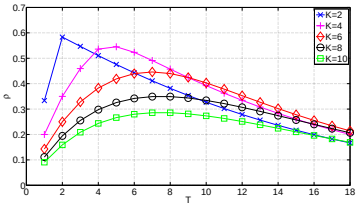

Fig. A.4: Comparison of efficiency ρ, for $M = 8$, varying user load T, and different sizes of the data phase K.

3. Let $S^{(n)}$ be the value of S obtained in iteration $1 \leq n \leq N$, where N is the total number of iterations. The simulated pmf is then

$$\widehat{P}(S_D = s \mid T = t) = \frac{\sum_{n=1}^{N} \mathbb{I}(S^{(n)})}{N}, \tag{A.6}$$

where $\mathbb{I}(\cdot)$ is an indicator function, giving $\mathbb{I}(S^{(n)}) = s$ if $S^{(n)} = s$, and 0 otherwise.

Fig. A.2 compares the analytical and simulated pmfs for $T = 12$ accessing users, when number of tokens is set to $M = 8$ and the number of resource slots is $K = 4$ and $K = 8$. The analytical pmf is obtained from Eq. (A.1), while the simulated one is obtained from running $N = 100000$ simulation iterations. We observe a correlation between the analytical and simulated pmfs, validating the presented analysis.

4.2 Success Rate and Efficiency Evaluation

Fig. A.3 and Fig. A.4 show respectively the success rate σ, Eq. (A.4), and the efficiency ρ, Eq. (A.5) as functions of number of users T, for $M = 8$ and varying K.

From Fig. A.3 it can be observed that success rate decreases as the number of users T increase; this is due to increasing probability of multiple users selecting the same tokens and, consequently, increasing number of collisions happening in the data phase. On the other hand, increasing the number of available resource slots K increases the success rate at first, until K reaches the number of available tokens M. Afterwards, there is no benefit in increasing K, as no more than M users can be successfully detected and admitted in the system and $K - M$ resource slots will always be left unassigned.

From Fig. A.4 it is clear that the higher efficiency is achieved when is K considerably lower than M, which is not a straightforward conclusion. Again, this is because of multiple users selecting the same preambles, which results both in *collision* and *idle* slots in the data phase; the chances for the latter increase with the number of available resource slots K. We end this section by noting that, by using the framework presented in paper, the optimal number of resource slots K that maximizes the efficiency can be calculated, for fixed number of tokens M and number of users T.

5 Conclusion

In this letter we studied a LTE based access reservation protocol and provided a method to obtain the exact pmf describing the number of reservation tokens activated by a single user that gets assigned resources in the data phase. The obtained results are applicable to the case where there are not enough resources in the data phase to serve all detected reservation tokens, and when the base station is not able to discern between reservation tokens selected by one or more than one user; both assumptions may occur in practice, affecting the operation of the access reservation protocol.

Further, based on the presented method we derived the one-shot success rate and efficiency of the scheme, which can be used as performance measures of the constrained access reservation systems, such as LTE, in the emerging scenarios with real-time M2M communication, when there is a limited time to carry out the contention and the data transmissions. Finally, it was observed that although the success rate is maximized when there are the same number of contention and data resources, there is a non-negligible efficiency tradeoff for doing so.

6 Appendix

Here, a method to compute the 2-associated Stirling numbers of the second kind is presented, based on [14]. By definition, $S_2(n,k)$ is the number of ways in which k objects can be put into n boxes, such that each box contains at least 2 objects. The values of $S_2(n,k)$ can be computed using the recurrence relation

$$S_2(n+1,k) = kS_2(n,k) + nS_2(n-1,k-1), \tag{A.7}$$

with initial condition $S_2(2,1) = 1$. If $k > \lfloor \frac{n}{2} \rfloor$, $n \leq 0$ or $k \leq 0$, then $S_2(n,k) = 0$.

References

[1] D. P. Bertsekas and R. G. Gallager, *Data Networks*. Prentice-Hall, 1987.

[2] *LTE physical layer; General description*, 3GPP TS 36.201.

[3] S. Sesia, I. Toufik, and M. Baker, *LTE-The UMTS Long Term Evolution: From Theory to Practice*. Wiley, 2011.

[4] *Medium Access Control (MAC) protocol specification*, 3GPP TS 36.321.

[5] *Physical layer procedures*, 3GPP TS 36.213.

[6] Z. Jiang and X. Zhong, "Fast Retrial and Dynamic Access Control Algorithm for LTE-Advanced Based M2M Network," in *AICT 2012, The Eighth Adv. Internat. Conf. on Telecommun.*, 2012, pp. 24–28.

[7] K. Zhou and N. Nikaein, "Packet Aggregation for Machine Type Communications in LTE with Random Access Channel," in *IEEE Wirel. Commun. Netw. Conf., Apr. 7-10, 2013, Shanghai, China*, 04 2013. [Online]. Available: http://www.eurecom.fr/publication/3938

[8] R.-G. Cheng, C.-H. Wei, S.-L. Tsao, and F.-C. Ren, "Rach Collision Probability for Machine-type Communications," in *IEEE Veh. Tech. Conf., Spring 2012*. IEEE, 2012, pp. 1–5.

[9] C.-H. Wei, R.-G. Cheng, and S.-L. Tsao, "Modeling and Estimation of One-Shot Random Access for Finite-User Multichannel Slotted ALOHA Systems," *IEEE Commun. Lett.*, vol. 16, no. 8, pp. 1196 –1199, Aug. 2012.

[10] W. Crowther, R. Rettberg, D. Walden, S. Ornstein, and F. Heart, "A System for Broadcast Communication: Reservation-ALOHA," *Proc. 6th Hawaii Int. Conf. Syst. Sci*, pp. 596–603, 1973.

[11] W. Szpankowski, "Analysis and Stability Considerations in a Reservation Multiaccess System," *IEEE Trans. Commun.*, vol. 31, no. 5, pp. 684–692, May 1983.

[12] Y. S. Han, J. Deng, and Z. J. Haas, "Analyzing Multi-Channel Medium Access Control Schemes with ALOHA reservation," *IEEE Trans. Wirel. Commun.*, vol. 5, no. 8, pp. 2143–2152, 2006.

[13] J. Alcaraz, J. Vales-Alonso, E. Egea-López, and J. Garcia-Haro, "A Stochastic Shortest Path Model to Minimize the Reading Time in DFSA-Based RFID Systems," *IEEE Commun. Lett.*, vol. 17, no. 2, pp. 341–344, 2013.

[14] L. Comtet, *Advanced Combinatorics. The Art of Finite and Infinite Expansions, Revised and Enlarged edition*. Riedel Publishing Co., Dordrecht, 1974.

Paper B

Code-expanded radio access protocol for machine-to-machine communications

Henning Thomsen, Nuno K. Pratas, Čedomir Stefanović, and Petar Popovski

The paper has been published in the
Transactions on Emerging Telecommunications Technologies Vol. 24(4),
pp. 355–365, 2013.

The layout has been revised.

Abstract

The random access methods used for support of Machine-to-Machine (M2M), also referred to as Machine-Type Communications (MTC), in current cellular standards are derivatives of traditional framed slotted ALOHA and therefore do not support high user loads efficiently. We propose an approach that is motivated by the random access method employed in LTE, which significantly increases the amount of contention resources without increasing the system resources, such as contention sub-frames and preambles. This is accomplished by a logical, rather than physical, extension of the access method in which the available system resources are interpreted in a novel manner. Specifically, in the proposed scheme, users perform random access by transmitting orthogonal preambles in multiple random access sub-frames, in this way creating access codewords that are used for contention. We show that, for the same number of random access sub-frames and orthogonal preambles, the amount of available contention resources is drastically increased, enabling the massive support of MTC users that is beyond the reach of current systems.

1 Introduction

In the past few years there has been an increase in the number of networked machines on current networks designed for human-centric communications. This has led to a shift in the conventional perception on human-centric communications towards device-centric communications, which are independent of human interaction [1, 2]. While the common requirements of traditional human-centric communications are high bit-rates and lower latency, in device-centric communications, one of the main requirements is the massive transmission of simultaneous low data rate messages.

Within 3GPP, there is an ongoing study on the adaptation of the 3GPP cellular networks to handle Machine-Type Communications (MTC) traffic [3, 4], through the inclusion of enhanced load control mechanisms in the Radio Access Network (RAN). This is paramount, because due to the expected large number of deployed MTC devices, the cellular networks are expected to withstand traffic bursts [5]. In such situations, radio and signalling network congestions may occur due to mass concurrent transmissions [6], which can lead to large delays, packet loss and, in the extreme case, service unavailability.

1.1 3GPP Load Control Approach

In 3GPP there have been proposed several solutions for managing the Random Access Channel (RACH) load [3], which are here listed briefly:

- **Access Class Barring** - where the network controls the load by restricting the access of devices based on their class. In case of overload due to

MTC traffic, the network can restrict the access of those same devices, while allowing other devices to continue normal network access [7, 8];

- **Orthogonal Resources** - where the network provides separated RACH resources for MTC devices and traditional devices. In LTE this can be accomplished by dividing the random access slots and the preamble sequences, i.e. in the time and preamble domain [9];
- **Dynamic Resources Allocation** - where the network allocates dynamically additional RACH resources based on the RACH load condition and overall traffic load [2]. The scheme proposed in this paper is of this type, although it is accomplished through a non-traditional approach, which will be exposed later in the paper;
- **Backoff** - where the network in case of overload enacts a backoff request making the connecting devices retry the random access at a later stage. This scheme is less effective upon massive batch arrivals, as expected from MTC traffic [5];
- **Slotted access** - where the network assigns specific random access slots to a MTC device or a group of MTC devices and where each MTC device is only allowed to access on its dedicated access slot;
- **Pull-based** - where an entity within the core network triggers the eNodeB to page the intended MTC terminals. Upon receiving the paging signal, the MTC devices initiate the random access. Here the eNodeB only proceeds with the paging when the traffic load is favourable.

Among these, the 3GPP decided to extend the Access Class Barring method to handle the MTC traffic. In this method, denoted as Extended Access Barring (EAB), the network is able to selectively control the access attempts from multiple MTC User Equipment (M-UE) configured for EAB [3]. This approach, according to 3GPP [3], allows to control the access network load without the need to introduce new access classes.

1.2 Proposed Scheme

In contrast with the current 3GPP direction, in this paper we propose an extension to the LTE random access method, which is in line with the dynamic resource allocation approach. Here the dynamic resource allocation is not accomplished through traditional means, such as the increase of the number of available preambles and/or random access sub-frames, but instead by introducing the concept of Code-Expanded random access scheme. This scheme is an application of the Protocol Coding approach, first introduced

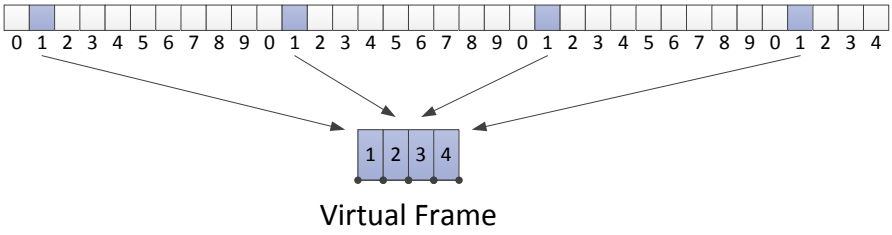

Fig. B.1: Example of PRACH opportunities organized in virtual frames.

in [10], [11], [12], [13]. The motivation behind this proposal is to enable existing systems to sustain a large and bursty random access loads, while preserving the physical layer unchanged and incurring minimal changes in the medium access control layer.

To illustrate what is meant by code-expanded random access, first consider that the random access in LTE occurs only in specific sub-frames, here denoted as contention sub-frames. Further, as depicted in the Fig. B.1, we assume that a group of consecutive contention sub-frames are grouped together in a contention *virtual frame*. Now consider the diagrams in Fig. B.2, where the selection of preambles and sub-frames in the reference and in the proposed code-expanded random access schemes are depicted. In both schemes the sub-frames are grouped in contention virtual frames and the random access is performed always at the virtual frame level.

In the reference scheme, the M-UE performs the random access by selecting one of the available preambles, in this example denoted as A and B, and then selecting one of the virtual frame sub-frames to transmit the chosen preamble, as depicted in Fig. B.2(a). The proposed code-expanded random access scheme is a generalization of the reference scheme, where the M-UE transmits one or none of the available preambles in each of the virtual frame sub-frames, as depicted in Fig. B.2(b). For both schemes, when the M-UE does not transmit any preamble in the sub-frame, we assume that the M-UE actually transmits an *idle* preamble, henceforth denoted as I. Therefore, in both schemes each M-UE contends using an *access codeword* with length equal to the length of the virtual frame.

When multiple M-UEs transmit the same preamble in the same sub-frame the BS is still able to detect that preamble [14], i.e. the collisions are assumed to be non-destructive. Therefore, the Base Station (BS) discerns between M-UEs according to the observed preambles in each random access sub-frame, as shown in Fig. B.2(c) and Fig. B.2(d), i.e., observes a set of access codewords that are then used to discern between M-UEs.

In the reference scheme the codewords are composed of just one preamble sent in one of the sub-frames of the virtual frame, with the remaining

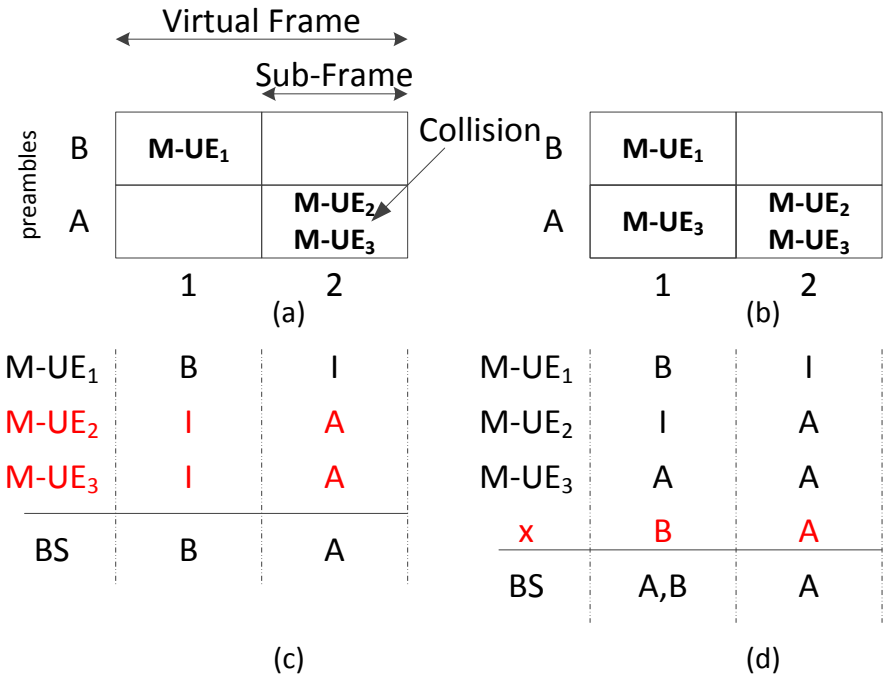

Fig. B.2: (a) Reference random access, (b) Code-expanded random access, (c) Reference random access codewords, with collisions in red, (d) Code-expanded codewords, with phantom codewords in red.

sub-frames at idle. Taking as example the case depicted in Fig. B.2(c), the BS perceives the preamble B in the first sub-frame and the preamble A in the second sub-frame. Therefore, the BS perceives the transmission of the codewords (B, I) and (I, A).

In the proposed scheme, each M-UE selects a codeword consisting of a randomly chosen preamble (including the idle preamble) in every sub-frame of the virtual frame. In this way, the number of contention resources are increased and the amount of collisions is reduced - a collision occurs when two or more M-UEs select the same codeword, as depicted in Fig. B.2(c) where both M-UE$_2$ and M-UE$_3$ choose the codeword (I, A).

While reducing the amount of collisions, the code-expanded generalization introduces a shortcoming not present in the reference scheme. In the reference scheme, the codewords do not introduce ambiguities at the BS in regards to which codewords where transmitted, i.e., based on the observation of the preambles in the virtual frame, the BS can always discern which codewords were actually sent. In the proposed scheme, such ambiguities exist - based on the observation, the BS may conclude that there are more code-

words present in the virtual frame than there were actually sent. Namely, multiple combinations of transmitted codewords can yield the same observation, introducing phantom codewords which were not sent by any of the transmitting M-UEs.

In Fig. B.2(d) is depicted a combination of the three codewords used by M-UEs ((B, I), (I, A) and (A, A)), which misleads the BS to perceive the phantom codeword (B, A). The existence of phantom codewords affects adversely the performance, however, we show that this is significant only when the network is experiencing low user loads. Specifically, we show that the efficiency of the proposed approach (i.e., the fraction of M-UEs that successfully contended for access) for moderate and high loads and for the same number of used preambles and sub-frames in the virtual frame, is substantially higher than the efficiency of the reference scheme, despite the drawbacks caused by phantom codewords. We also show that by choosing the operating random access method according to the user load, it is possible to maintain an efficient random access over a large load region using the same number of preambles and sub-frames.

The work presented in this paper is an extended version of the material first presented in [15]. The extension pertains to the following: a comprehensive explanation of the reference random access mechanism; a generalization of the method used to compute the distribution that models the number of perceived codewords by the BS for any codebook size; and a extension of that method to the case where subsets of the codebook are used.

1.3 Related Work

The Code-Expanded random access scheme belongs to a broader class of novel advanced random access schemes. The recent advancements include the work found in [16] and [17], where the authors propose a random access protocol that takes advantage of the analogies that have been established between use of successive interference cancellation in slotted ALOHA based access schemes and iterative belief-propagation erasure-decoding, enabling application of theory and tools from codes-on-graphs for the design of random access schemes.

There are several works found in the literature that deal with the machine-to-machine (M2M) challenges in different settings and following different approaches than the one considered in this paper. In [18] the authors examine and propose schedule based solutions for dealing with diverse M2M time-controlled traffic profiles within a LTE context. This approach complements the one here presented, since we focus instead on the enhancement of the random access part for the serving of M2M traffic generated by a massive amount of M-UEs.

In [19], a new concept of M2M communicatios infrastructure is intro-

duced, which is accomplished via airliners. This work presents a first study on possible coverage within Europe and North America using airliners. This approach can be used to complement the coverage of M2M communications currently provided mainly by cellular networks.

In [20] the authors discuss how sensor and electronic-health networks can be served by the 3GPP networks (GSM, UMTS, LTE), with the goal of offering quality-of-service to this kind of applications. The proposed code-expanded approach enables to address some of this issues, since it enables random access for a large number of devices.

Finally, in [21] the authors revisit the LTE random access procedure in regards to its application to the synchronization of the user equipment within the network. The authors propose a novel scheme that provides superior performance in comparison with the existing methods, by taking in account the frequency selectivity of the channel. It should be noted that in this paper we do not consider how the proposed code-expanded scheme can be used to enable synchronization within the network. Such extension is left for future work.

1.4 Article Structure

The remainder of this paper is organized as follows. In Section 2 we model and analyse both the reference and the proposed random access scheme. In Section 3 we discuss how the proposed code-expanded scheme can be used to enable a random access mechanism which adapts according to the load in the random access. Finally, Section 4 concludes the paper.

2 System Model

In LTE the random access is performed through the Random Access Channel (RACH), which is mapped in the physical layer to the Physical Random Access Channel (PRACH) [22].

The random access procedure is depicted in Figure B.3, and is composed of the following steps [23–26]:

1. The UE selects one of the preamble sequences available in the cell, [25], and transmits the preamble in one of the sub-frames reserved for the PRACH transmissions;

2. The eNodeB decodes the preamble and responds to the UE by sending a Random Access Response. This response includes the matching preamble information together with the information about the uplink resource that the UE should use for further information exchange as well as the timing advance to be used;

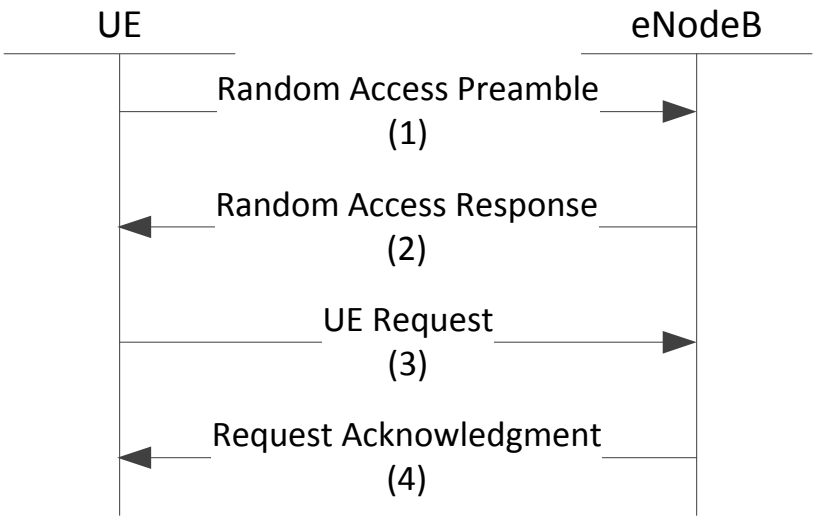

Fig. B.3: LTE Random Access Procedure

3. The UE proceeds with the information exchange on the resources indicated by the PRACH response;

4. Finally. the eNodeB acknowledges the information received from the UE.

The periodicity of the PRACH resources can scale according to the expected RACH load [24]. Therefore, the PRACH resources can occur from once in every sub-frame (1000 RACH sub-frames per second) to once in every two frames (50 RACH sub-frames per second), where a frame consists of 10 sequential sub-frames lasting 1 ms [27].

As previously mentioned, we assume that a group of consecutive sub-frames is organized in a virtual frame reserved for PRACH (i.e., random access), as depicted in the Fig. B.1. We denote the number of sub-frames within a virtual frame by L and the number of available preambles by M.

2.1 Reference Random Access Scheme

The reference scheme considered here is inspired by the LTE random access [23, 24]. We model it as an access reservation scheme [28], as depicted in Figure B.4. We focus on the contention phase, which consists of L sub-frames (contention slots), and these sub-frames constitute a single virtual frame. To ease the analysis, we assume that in the non-contention phase there are always available enough data slots to serve the incoming requests. We assume that there are N contending M-UEs; where each M-UE randomly chooses a

Fig. B.4: Access reservation.

preamble and a sub-frame of the virtual frame in which the chosen preamble is sent.

In the LTE random access scheme, the contention occurs at the sub-frame level, in contrast with the reference scheme presented here, where the contention occurs at the virtual frame level. However, the amount of contention opportunities is the same in both cases, therefore one could argue that for high user loads, the efficiency of the contention phase of the LTE scheme is worse than of the reference scheme, as the number of collisions in the former is higher, due to the M-UEs being able to contend more than once within the virtual frame.

The expected fraction of the M-UEs that succeed in the contention phase is denoted as the expected efficiency of the contention phase S_r, which is given by:

$$S_r = \frac{N_S}{N_P}, \tag{B.1}$$

where N_S is the expected number of codewords used by a single M-UE (singles) and N_P is the expected number of perceived codewords by the BS. [1]

The expected number of perceived codewords, N_P, in the reference random access scheme accounts for all the single and collision codewords is given by:

$$N_P = N_S + N_C \tag{B.2}$$

where N_C is the number of codewords used by multiple M-UEs (collisions), $N_P \leq A_r$, and A_r is the number of codewords available in the reference scheme. As outlined earlier, in a contention phase consisting of L sub-frames, each M-UE sends only one preamble, therefore the number of available codewords, A_r, is given by:

$$A_r = M \cdot L. \tag{B.3}$$

Assuming that the number of M-UEs contending per codeword is modeled by the random variable X, then the probability that in a given contention codeword there are k M-UEs contending is:

$$\Pr[X = k] = \binom{N}{k} \left(\frac{1}{A_r}\right)^k \left(1 - \frac{1}{A_r}\right)^{N-k}. \tag{B.4}$$

[1] We note that the strict definition of the expected efficiency is the expectation of the ratio between N_S and N_P, instead of the ratio of the expectations as here considered. This approximation holds with the increase of the number of contending M-UEs.

The expected number of codewords chosen by a single M-UE, N_S, is given by:

$$\begin{aligned} N_S &= \Pr[X = 1] \cdot A_r \\ &= \binom{N}{1} \left(\frac{1}{A_r}\right)^1 \left(1 - \frac{1}{A_r}\right)^{N-1} \cdot A_r \\ &= N \left(1 - \frac{1}{A_r}\right)^{N-1}, \end{aligned} \tag{B.5}$$

and, similarly, the expected number of codewords chosen by multiple M-UEs, N_C, is:

$$\begin{aligned} N_C &= \Pr[X > 1] \cdot A_r \\ &= (1 - \Pr[X = 0] - \Pr[X = 1]) \cdot A_r \\ &= \left(1 - \left(1 - \frac{1}{A_r}\right)^N - \frac{N}{A_r} \left(1 - \frac{1}{A_r}\right)^{N-1}\right) \cdot A_r. \end{aligned} \tag{B.6}$$

Substituting (B.5) and (B.6) in (B.1), we get the estimate of the efficiency of the contention phase.

2.2 Code-Expanded Random Access

In the code-expanded random access, the outcome of the contention phase is the set of the codewords perceived by the BS, which the BS assumes to belong to the M-UEs that successfully contended for the access. However, the set of perceived codewords actually contains the codewords that are used just by a single M-UE (singles), codewords that are used by multiple M-UEs (collisions) and codewords that are used by none of the M-UEs (phantom codewords, see Fig. B.2). The expected efficiency of the code-expanded random access S_e is:

$$S_e = \frac{N_S}{N_P}. \tag{B.7}$$

where the N_S is the expected number of single codewords, and N_P is the expected number of codewords that the BS perceives, i.e., N_P accounts for all single, collision and phantom codewords. As in the reference case, we note that the strict definition of the expected efficiency is the expectation of the ratio between N_S and N_P, instead of the ratio of the expectations. As shown in Fig. B.8, this approximation holds with the increase of the number of contending M-UEs.

In the code-expanded approach, the M-UEs send in each sub-frame of the virtual frame either one of the M preambles or the idle preamble I, so the total number of available codewords is:

$$A_e = (M + 1)^L - 1, \tag{B.8}$$

Codeword	L	
	1	2
1	I	A
2	I	B
3	A	I
4	A	A
5	A	B
6	B	I
7	B	A
8	B	B

Table B.1: Codebook, $L = 2$, $M = 2$.

where the all-idle codeword is excluded. Furthermore, $N_P \leq A_e$.

The distribution of devices contending per virtual frame is modeled in the same way as in (B.4), with the difference that the number of available codewords is now higher.

The expected number of codewords chosen by a single M-UE, N_S, is given by:

$$\begin{aligned} N_S &= \Pr[X = 1] \cdot A_e \\ &= \binom{N}{1} \left(\frac{1}{A_e}\right)^1 \left(1 - \frac{1}{A_e}\right)^{N-1} \cdot A_e \\ &= N \left(1 - \frac{1}{A_e}\right)^{N-1}. \end{aligned} \tag{B.9}$$

The method to obtain the expected value of N_P is discussed in the next subsection.

2.3 Calculation of N_P

For the calculation of N_P we use a representation based on a Markov Chain (MC) that describes the evolution of the perceived number of codewords by the BS when the number of contending M-UEs increases sequentially from 1 to N. We note that it is assumed that the M-UEs select their codewords independently and uniformly at random from the set of available codewords.

The MC states are determined by the configuration that corresponds to the number of the observed preambles in the sub-frames of the virtual frame, which is created by the actual codewords selected by the M-UEs. The configuration is denoted by $(C_1, C_2, C_3, ..., C_L)$, where C_j is the number of observed preambles by the BS in the j-th subframe. We note here that C_j always includes the idle preamble, i.e., if the number of unique preambles in the j-th sub-frame is C_j, then the number of actually observed preambles is $C_j - 1$.

Each state is characterized by a cardinality, which is the cardinality of the set of codewords perceived by the BS that is created by the given configuration.

We define the vector $\boldsymbol{\alpha}$ as a vector with s entries, where s is the number of states in the MC. Also, if the number L of subframes is given, then we indicate this with a superscript, i.e. $\boldsymbol{\alpha}^{(L)}$. For the i-th state configuration $(C_1^i, C_2^i, C_3^i, ..., C_L^i)$ the corresponding cardinality is the i'th entry in $\boldsymbol{\alpha}$, and it is given by

$$\alpha_i = \prod_{j=1}^{L} C_j^i - 1, \tag{B.10}$$

where, once again, we assumed that the all-idle codeword is not used by any of the M-UEs. Using this model, N_P can be assessed as the average cardinality of the set of the codewords perceived after $N-1$ transitions of the MC, averaged over the probability distribution of the MC states after $N-1$ transitions.

To ease the explanation, we focus on an example case where $L = 2$ and $M = 2$, and therefore $A_e = 8$. The full codebook is shown in Table B.1, while the MC representation including the state configurations, cardinalities and possible state transitions is shown in Table B.2. For example, the state configuration of the state 2 is $(1, 3)$, implying that in the first sub-frame of the virtual frame there is an idle preamble I, and in the second sub-frame there is an idle preamble and both available preambles, A and B. The cardinality of state 2 is then $\alpha_2 = 2$.

Initially, when there is only one M-UE attempting random access, the system can be in the states 1, 3 and 4. The probability of the system being in any of those states is simply the ratio of the number of codewords from the codebook which provides the corresponding state configuration and the total number of available codewords A_e, as depicted in Figure B.5.

For example, for state 1, where the state configuration is $(1, 2)$, from Table B.1 and Figure B.5 it can be seen that there are only two codewords that satisfy the state configuration, which are (I, A) and (I, B). Therefore, the probability of the BS perceiving this state upon the M-UE transmission of one of the available codewords is $\frac{2}{8}$. A similar reasoning is done for the remaining possible initial states, and the following initial state probability vector $\boldsymbol{\pi}^{(1)}$ is:

$$\boldsymbol{\pi}^{(1)} = \frac{1}{8}\begin{bmatrix} 2 & 0 & 2 & 4 & 0 & 0 & 0 & 0 \end{bmatrix} \tag{B.11}$$

where $\pi_i^{(1)}$ is the probability that the system is initially in the i-th state. Therefore, when one M-UE attempts random access, i.e. when $N = 1$, N_P is obtained as:

$$N_P = \sum_{i=1}^{A_e} \alpha_i \cdot \pi_i^{(1)} = 2 \tag{B.12}$$

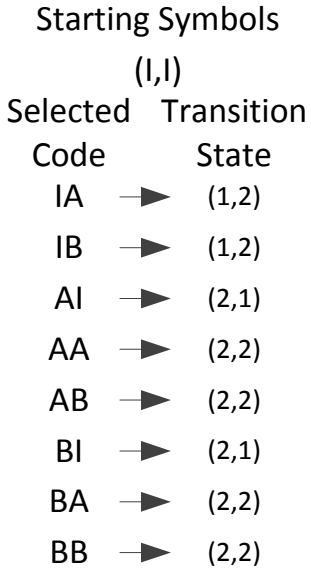

Fig. B.5: Initial state vector selection procedure.

where α_i is the cardinality of the i-th state, obtained from (B.10) and listed in Table B.2.

In the case where there are two M-UEs attempting random access, it is assumed that the selection of the transmitted codewords is sequential and independent. Therefore, the codeword selected by the first M-UE leads the system to be in one of the possible initial states, which are 1, 3 and 4. When the second M-UE selects the codeword, the system can transit to any of the states listed in Table B.2. The transition between each state and the corresponding transition probabilities are depicted in Figure B.6.

The transition probabilities can be obtained following the same reasoning as the one used to obtain $\boldsymbol{\pi}^{(1)}$. Consider that the first M-UE selects a codeword that puts the system in state 1, i.e. the M-UE selected either (I, A) or (I, B). Now, whatever codeword the second M-UE selects, the system can only transit to the states $1, 2, 4, 5$, as depicted in Figure B.7(a). For the system to transit from state 1 to state 5, it means that the second M-UE has to select a codeword that consists of either preamble A or B in the first sub-frame, and the remaining yet unused preamble in the second sub-frame. For the considered example, this is the codeword (A, B) or (B, B) if the initial codeword was (I, A), or the codeword (A, A) or (B, A) if the initial codeword was (I, B), thus making the configuration become $(2, 3)$. From the preceding discussion, we see that no matter which codeword caused the chain to be in state 1, the transition to state 5 can be caused by the second M-UE selecting (one of) two

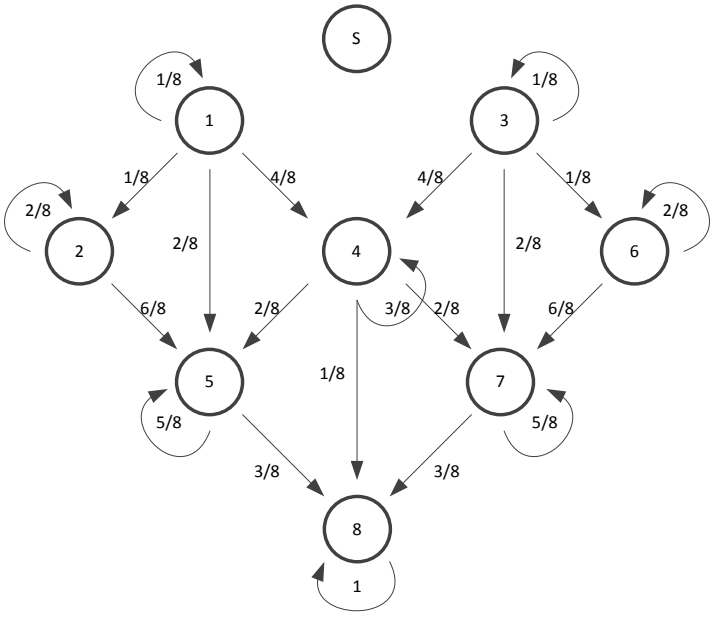

Fig. B.6: Markov Chain Transition Model, $L = 2$, $M = 2$; where S represents the state.

codewords from the set of all codewords. Therefore, this transition probability is equal to $\frac{2}{8}$ and it does not depend on which codeword the first M-UE selected to bring the system to state 1.

To further illustrate the described procedure, consider that the second M-UE puts the system in state 5. From Figure B.7(b), it can be seen what are the possible state transitions based on both the state configuration of the system as well as on the selection of a codeword by a third M-UE.

Using similar reasoning, it can be shown that the transition probabilities do not depend on the choices of codewords that brought the system to a given state and, for every state transition, the transition probability is the ratio of the number of codewords that enable the transition and the total number of available codewords A_e. For the considered example, the transition matrix $\boldsymbol{P}$ is:

$$\boldsymbol{P} = \frac{1}{8}\begin{bmatrix} 1 & 1 & 0 & 4 & 2 & 0 & 0 & 0 \\ 0 & 2 & 0 & 0 & 6 & 0 & 0 & 0 \\ 0 & 0 & 1 & 4 & 0 & 1 & 2 & 0 \\ 0 & 0 & 0 & 3 & 2 & 0 & 2 & 1 \\ 0 & 0 & 0 & 0 & 5 & 0 & 0 & 3 \\ 0 & 0 & 0 & 0 & 0 & 2 & 6 & 0 \\ 0 & 0 & 0 & 0 & 0 & 0 & 5 & 3 \\ 0 & 0 & 0 & 0 & 0 & 0 & 0 & 8 \end{bmatrix}$$

State (i)	C_1^i	C_2^i	α_i	Transitions
1	1	2	1	1,2,4,5
2	1	3	2	2,5
3	2	1	1	3,4,6,7
4	2	2	3	4,5,7,8
5	2	3	5	5,8
6	3	1	2	6,7
7	3	2	5	7,8
8	3	3	8	8

Table B.2: Markov Chain Model, $L = 2$, $M = 2$.

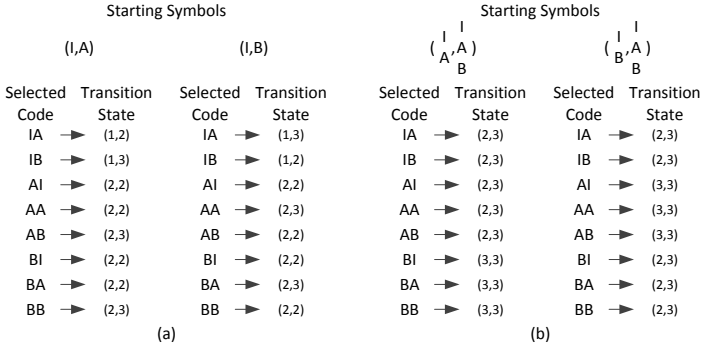

Fig. B.7: Transition matrix element deduction for configuration state (a) (1,2) and (b) (2,3).

where the (i, j)'th entry is the transition probability for going from state i to j.

The expected number of perceived codewords N_P can be obtained as follows:

$$N_P = \sum_{i=1}^{A_e} \alpha_i \cdot \pi_i^{(N)}, \tag{B.13}$$

where $\pi_i^{(N)}$ is the i-th element of the state vector $\boldsymbol{\pi}^{(N)}$, i.e., the probability of the BS perceiving a state configuration given by the i-th state after the N-th M-UE has chosen its codeword. The α_i is the cardinality of the i-th state, given by (B.10). As for any MC, the state probability distribution $\boldsymbol{\pi}^{(N)}$ is:

$$\boldsymbol{\pi}^{(N)} = \boldsymbol{\pi}^{(1)} \cdot \boldsymbol{P}^{(N-1)}. \tag{B.14}$$

Fig. B.8 depicts the comparison of the efficiencies for the reference scheme calculated using (B.1), code-expanded scheme calculated using (B.7) and (B.13), and code-expanded scheme that is obtained using Monte Carlo simulations, for the example case when $L = 2$ and $M = 2$. It is obvious that, as the number

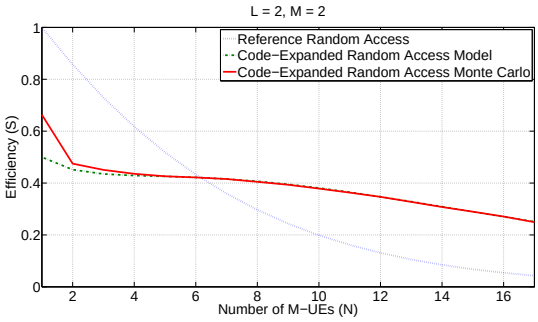

Fig. B.8: Reference random access and code-expanded random access comparison.

of M-UEs grows, the efficiency of the code-expanded method outperforms the reference one. Also, both curves corresponding to the code-expanded method converge, justifying the use of (B.13) when computing the expected efficiency using (B.7).

Finally, we note that the described methodology for modelling N_P can be generalized for arbitrary L and M, as shown in the next sub-section.

2.4 Derivation of N_P for the general case

We now generalize the N_P model to any arbitrary L and M. The generalized model is constructed in a three step approach:

1. Construction of the model for the case where all the possible codewords are considered;
2. Removal of the all idle codeword from the transition matrix;
3. Construction of the initial state vector $\boldsymbol{\pi}^{(1)}$.

The transition matrix is constructed iteratively, with the base case being $L = 1$. The matrix for the base case is:

$$\boldsymbol{P}_1 = \frac{1}{M+1}\begin{bmatrix} 1 & M & & & \\ & 2 & M-1 & & \\ & & \ddots & \ddots & \\ & & & M & 1 \\ & & & & M+1 \end{bmatrix}, \tag{B.15}$$

where the rows and columns are ordered according to how many distinct preambles are used. The first row corresponds to the state 0, i.e. when only the *Idle* preamble is present. If a user selects the codeword 0, then the system stays in this state. Otherwise, as there are M preambles excluding the idle

preamble, there are M possibilities for the system going to the next state. We note that for $L = 1$ the number of codewords and preambles is the same. For the second row, the $(2, 2)$ matrix entry counts the number of ways the second user can select a codeword, given that the first user has selected one. The second user can either select the all-idle codeword or the same codeword as the first user. This accounts for the 2 in the second collumn of the second row of the matrix (B.15). The entry with $M - 1$ counts the number of other codewords that the second user can select. Continuing in this way, the matrix for M preambles and $L = 1$ is as given in (B.15).

Now we consider the case where the codeword is of length $L = 2$. When the second sub-frame is added, we get that this sub-frame can contain $0, 1, 2, \ldots, M$, corresponding to how many distinct preambles were transmitted in that sub-frame. For the case of $L = 2$, the transition matrix is then:

$$\boldsymbol{P}_2 = \frac{1}{M+1} \cdot \begin{bmatrix} \boldsymbol{P}_1 & M\boldsymbol{P}_1 & & \\ & 2\boldsymbol{P}_1 & (M-1)\boldsymbol{P}_1 & \\ & \ddots & \ddots & \\ & & M\boldsymbol{P}_1 & \boldsymbol{P}_1 \\ & & & (M+1)\boldsymbol{P}_1 \end{bmatrix},$$

by a similar counting argument as the case of $L = 1$.

The cardinality state vector, $\boldsymbol{\alpha}^{(1)}$ for the case of $L = 1$ is of the form

$$\boldsymbol{\alpha}^{(1)} = (1, 2, 3, \ldots, M+1), \tag{B.16}$$

where each entry corresponds to the number of distinct preambles transmitted. For the case where $L = 2$, the cardinality state vector is of the form

$$\boldsymbol{\alpha}^{(2)} = (\boldsymbol{\alpha}^{(1)}, 2\boldsymbol{\alpha}^{(1)}, 3\boldsymbol{\alpha}^{(1)}, \ldots, (M+1)\boldsymbol{\alpha}^{(1)}). \tag{B.17}$$

We now explain the meaning of the entries in this vector. Firstly, this vector is composed of $M + 1$ blocks of the form $k\boldsymbol{\alpha}^{(1)}$, where $1 \leq k \leq M + 1$. The k'th block in $\boldsymbol{\alpha}^{(2)}$, $k\boldsymbol{\alpha}^{(1)}$, corresponds to the case where k preambles, including the idle preamble, are used in the second slot.

The transition matrix and $\boldsymbol{\alpha}^{(\boldsymbol{L+1})}$ for the case of $L + 1$ slots can then be constructed from the case of L slots, in the same manner shown. For the case

of $L+1$ slots, the transition matrix is:

$$\boldsymbol{P}_{L+1} = \frac{1}{M+1} \cdot \begin{bmatrix} \boldsymbol{P}_L & M\boldsymbol{P}_L & & \\ & 2\boldsymbol{P}_L & (M-1)\boldsymbol{P}_L & \\ & \ddots & \ddots & \\ & & M\boldsymbol{P}_L & \boldsymbol{P}_L \\ & & & (M+1)\boldsymbol{P}_L \end{bmatrix},$$

and the $\boldsymbol{\alpha}$ is

$$\boldsymbol{\alpha}^{(L+1)} = (\boldsymbol{\alpha}^{(L)}, 2\boldsymbol{\alpha}^{(L)}, 3\boldsymbol{\alpha}^{(L)}, \ldots, (M+1)\boldsymbol{\alpha}^{(L)}). \tag{B.18}$$

Because the way the transition matrix $\boldsymbol{P}_L$ is constructed, we can write it as:

$$\boldsymbol{P}_L = \frac{1}{(M+1)^L}\boldsymbol{Q}, \tag{B.19}$$

where $\boldsymbol{Q}$ is a $(M+1)^L \times (M+1)^L$ matrix.

The next step is to remove the all-idle codeword from the transition matrix and state cardinality vector. This is accomplished through the following four steps:

1. For the transition matrix $\boldsymbol{P}_L$, the first row and first column are deleted;
2. Then all entries on the diagonal of the resulting matrix are decreased by one, since the all-idle codeword is no longer a valid choice;
3. The transition matrix is normalized with $\frac{1}{(M+1)^L-1}$ instead of $\frac{1}{(M+1)^L}$;
4. The first entry of the state cardinality vector, $\boldsymbol{\alpha}$, is removed, and the other entries are decreased by one.

The next step is to determine the initial vector $\boldsymbol{\pi}^{(1)}$. From the case when the idle is a valid codeword, this vector is $(1, 0, \ldots, 0)$. The row that is removed from the matrix, contains in its entries the probability for going from the state configuration $(0, \ldots, 0)$ to another state when selecting a new codeword. Since the all-idle codeword is removed, the starting probabilities of the current case are contained in this row. Therefore, the $\boldsymbol{\pi}^{(1)}$ vector is set equal to the removed row of the transition matrix.

3 Adaptive Code-Expanded Random Access

In the previous subsection we considered using only the codebook consisting of all the available codewords (i.e., the full codebook). In this subsection we

State (i)	C_1^i	C_2^i	α_i	Transitions
1	1	2	1	1,2,5,6
2	1	3	2	2,3,7
3	1	4	3	3,4,8
4	1	5	4	4,9
5	2	1	1	5,6,10,11
6	2	2	3	6,7,11,12
7	2	3	5	7,8,12,13
8	2	4	7	8,9,13,14
9	2	5	9	9,14
10	3	1	2	10,11,15,16
11	3	2	5	11,12,16,17
12	3	3	8	12,13,17,18
13	3	4	11	13,14,18,19
14	3	5	14	14,19
15	4	1	3	15,16,20,21
16	4	2	7	16,17,21,22
17	4	3	11	17,18,22,23
18	4	4	15	18,19,23,24
19	4	5	19	19,24
20	5	1	4	20,21
21	5	2	9	21,22
22	5	3	14	22,23
23	5	4	19	23,24
24	5	5	24	24

Table B.3: Markov Chain Model, $L = 2$, $M = 4$.

consider the case where a subset of the full codebook is selected based on the system input load. A subset is obtained by restricting the number of preambles that could be used in each of the sub-frames of the virtual frame (we note that these restrictions are not necessarily the same for every sub-frame). We note that the strategy used here to define the codebook subsets may not be the optimal one. The efficiency in this case can be computed following the procedure described in the previous subsections.

As an illustrative example consider the case where $L = 2$ and $M = 4$, for which the MC model is given in Table B.3. The possible cardinality values of the states for this MC are then $\{1, 2, 3, 4, 5, 7, 8, 9, 11, 14, 15, 19, 24\}$. This sequence represents all the possible subsets in regards to the number of codes that can be used. For $L = 2$ and $M = 4$ the number of codewords for the reference scheme is $A_r = 8$, so the cardinalities of interest are the ones where $A_e = \{9, 11, 14, 15, 19, 24\}$. In Figure B.9 is depicted the efficiency for

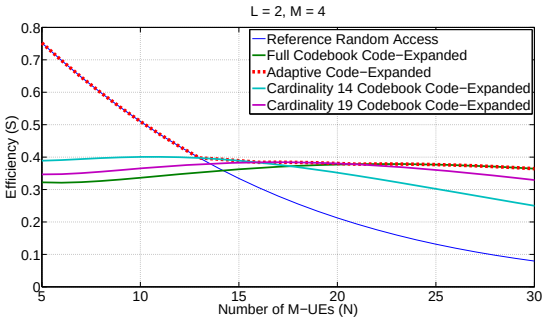

Fig. B.9: Adaptive Random Access example with $L = 2$ and $M = 4$.

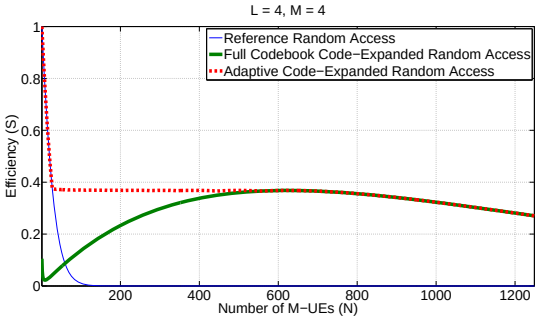

Fig. B.10: Adaptive Random Access example with $L = 4$ and $M = 4$.

the given example, both for the reference scheme and for the code-expanded scheme when cardinalities of interest are used. As it can be observed, there is a set of threshold values in regards to the number of M-UEs, where the system should increase the cardinality of the codebook in use, in order to maintain the efficiency. Overall, it could be concluded that an adaptive approach, where the codebook is selected based on the estimate of the user load is the preferred operating strategy.

In Figure B.10 is depicted the efficiency of the adaptive code-expanded approach for $L = 4$ and $M = 4$. Comparing these results with the results given in Fig. B.9, it can be observed that the region where the gain of the adaptive approach over the case when the full codebook is used is more obvious. Also, the increased M provides for significant expansion of the supported user load region.

In next subsection we give the method to compute N_P for the case where a subset of the codebook is used.

3.1 Derivation of N_P for a subset of the codebook

The method exposed in sub-section 2.4, can be extended to compute the expected value of N_P when only a restricted subset of the codewords available in the codebook are used.

We define the vector $\boldsymbol{v}$ as:

$$\boldsymbol{v} = (v_1, v_2, \ldots, v_L), \tag{B.20}$$

where v_j is the maximum number of distinct preambles that are allowed to be used in sub-frame j. For example, $\boldsymbol{v} = (1, 3, 2)$ means that only the idle preamble is allowed in sub-frame 1, two preambles are allowed in sub-frame 2, and one preamble is allowed in sub-frame 3.

The construction of the transition matrix $\boldsymbol{P}_L$ is then as follows. For the base case:

$$\boldsymbol{P}_1 = \frac{1}{v_1+1}\begin{bmatrix} 1 & v_1 & & & & \\ & 2 & v_1-1 & & & \\ & & \ddots & \ddots & & \\ & & & v_1 & 1 & \\ & & & & v_1+1 \end{bmatrix}, \tag{B.21}$$

and the matrix for the case when the $(j+1)$'th sub-frame is added is

$$\boldsymbol{P}_{j+1} = \frac{1}{v_j+1}\cdot \begin{bmatrix} \boldsymbol{P}_j & v_j\boldsymbol{P}_j & & & \\ & 2\boldsymbol{P}_j & (v_j-1)\boldsymbol{P}_j & & \\ & & \ddots & \ddots & \\ & & & v_j\boldsymbol{P}_j & \boldsymbol{P}_j \\ & & & & (v_j+1)\boldsymbol{P}_j. \end{bmatrix}.$$

The $\boldsymbol{\alpha}$ for the base case is:

$$\boldsymbol{\alpha}^{(1)} = (1, 2, 3, \ldots, v_1), \tag{B.22}$$

and the cardinality state vector $\boldsymbol{\alpha}$ for the $(j+1)^{th}$ step is obtained from the j'th step as:

$$\boldsymbol{\alpha}^{(j+1)} = (\boldsymbol{\alpha}^{(j)}, 2\boldsymbol{\alpha}^{(j)}, \ldots, v_j\boldsymbol{\alpha}^{(j)}). \tag{B.23}$$

The initial vector $\boldsymbol{\pi}^{(1)}$ is obtained as in the non-restricted case, i.e. it is obtained from the first row that is removed from the transition matrix which includes the all idle codeword. Also, the computation of the expected N_P proceeds as in the non-restricted case.

4 Conclusion

In this paper we proposed a code-expanded random access scheme inspired by the LTE random access. The proposed scheme increases the amount of available contention resources, without resorting to the increase of system resources, such as contention sub-frames and preambles. This increase is accomplished by expanding the contention space to the code domain, through the creation of random access codewords.

It was shown that for high user loads the proposed scheme is significantly more efficient than the reference scheme. Also, it was shown that by selecting the appropriate number of random access codewords it is possible to maintain the random access scheme efficiency over a large load region. This suggests the usage of an adaptive random access scheme, i.e., a combination of the reference and the code-expanded random access, which allows to maintain the efficiency both for low and high user load regions.

Finally, we note that for optimal operation of the proposed adaptive random access scheme, it is necessary to obtain the estimates of the user loads. The design of the adaptive random access scheme that implements the estimation of the user load is a topic of ongoing research. Considerations on the energy usage due to the transmission of codewords needs to be investigated in the future.

Acknowledgment

The research presented in this paper was supported by the Danish Council for Independent Research (Det Frie Forskningsråd) within the Sapere Aude Research Leader program, Grant No. 11-105159 "Dependable Wireless Bits for Machine-to-Machine (M2M) Communications".

References

[1] R. Hu, Y. Qian, H.-H. Chen, and A. Jamalipour, "Recent progress in machine-to-machine communications [guest editorial]," *IEEE CM*, vol. 49, no. 4, pp. 24 –26, april 2011.

[2] M. J. Anthony Lo, Yee Wei Law and M. Kucharzak, "Enhanced lte-advanced random-access mechanism for massive machine-to-machine (m2m) communications," in *27th World Wireless Research Forum (WWRF) Meeting*, 2011.

[3] *Study on RAN Improvements for Machine-type Communications*, 3GPP TR 37.868 V11.0, October 2011.

[4] M.-Y. Cheng, G.-Y. Lin, H.-Y. Wei, and A.-C. Hsu, "Overload control for machine-type-communications in lte-advanced system," *IEEE CM*, vol. 50, no. 6, pp. 38 –45, june 2012.

[5] M. Z. Shafiq, L. Ji, A. X. Liu, J. Pang, and J. Wang, "A first look at cellular machine-to-machine traffic - large scale measurement and characterization," in *Proceedings of the International Conference on Measurement and Modeling of Computer Systems (SIGMETRICS)*, London, United Kingdom, June 2012.

[6] *Service requirements for MTC; Stage 1*, 3GPP TS 22.368.

[7] S.-Y. Lien, T.-H. Liau, C.-Y. Kao, and K.-C. Chen, "Cooperative access class barring for machine-to-machine communications," *Wireless Communications, IEEE Transactions on*, vol. 11, no. 1, january 2012.

[8] J.-P. Cheng, C. han Lee, and T.-M. Lin, "Prioritized random access with dynamic access barring for ran overload in 3gpp lte-a networks," in *GLOBECOM Workshops, 2011 IEEE*, dec. 2011, pp. 368 –372.

[9] K.-D. Lee, S. Kim, and B. Yi, "Throughput comparison of random access methods for m2m service over lte networks," in *GLOBECOM Workshops, 2011 IEEE*, dec. 2011, pp. 373 –377.

[10] P. Popovski, Z. Utkovski, and K. F. Trillingsgaard, "Communication schemes with constrained reordering of resources," *IEEE Transactions on Communications*, 2013.

[11] P. Popovski and O. Simeone, "Protocol coding for two-way communications with half-duplex constraints," in *Global Telecommunications Conference (GLOBECOM 2010), 2010 IEEE*. IEEE, 2010, pp. 1–5.

[12] P. Popovski and Z. Utkovski, "On the secondary capacity of the communication protocols," in *Global Telecommunications Conference, 2009. GLOBECOM 2009. IEEE*. IEEE, 2009, pp. 1–7.

[13] Z. Utkovski and P. Popovski, "Protocol coding with reordering of user resources: Capacity results for the z-channel," in *Communication, Control, and Computing (Allerton), 2011 49th Annual Allerton Conference on*. IEEE, 2011, pp. 1678–1685.

[14] S. Sesia, I. Toufik, and M. Baker, *LTE, The UMTS Long Term Evolution: From Theory to Practice*. Wiley Publishing, 2009.

[15] N. K. Pratas, H. Thomsen, Č. Stefanović, and P. Popovski, "Code-Expanded Random Access for Machine-Type Communications," in *Globecom Workshops (GC Wkshps), 2012 IEEE*, 2012, pp. 1681–1686.

[16] Č. Stefanović, P. Popovski, and D. Vukobratovic, "Frameless aloha protocol for wireless networks," *Communications Letters, IEEE*, vol. 16, no. 12, pp. 2087–2090, 2012.

[17] C. Stefanovic, K. F. Trilingsgaard, N. K. Pratas, and P. Popovski, "Joint Estimation and Contention-Resolution Protocol for Wireless Random Access," *Accepted on ICC 2013*, 2013.

[18] A. Gotsis, A. S. Lioumpas, and A. Alexiou, "Analytical modelling and performance evaluation of realistic time-controlled m2m scheduling over lte cellular networks," *Transactions on Emerging Telecommunications Technologies*, pp. n/a–n/a, 2013. [Online]. Available: http://dx.doi.org/10.1002/ett.2629

[19] S. Plass, M. Berioli, R. Hermenier, G. Liva, and A. Munari, "Machine-to-machine communications via airliners," *Transactions on Emerging Telecommunications Technologies*, 2013. [Online]. Available: http://dx.doi.org/10.1002/ett.2615

[20] S. Adibi, A. Mobasher, and T. Tofigh, "Lte networking: extending the reach for sensors in mhealth applications," *Transactions on Emerging Telecommunications Technologies*, pp. n/a–n/a, 2013. [Online]. Available: http://dx.doi.org/10.1002/ett.2598

[21] L. Sanguinetti, M. Morelli, and L. Marchetti, "A random access algorithm for lte systems," *Transactions on Emerging Telecommunications Technologies*, vol. 24, no. 1, pp. 49–58, 2013. [Online]. Available: http://dx.doi.org/10.1002/ett.2575

[22] *Multiplexing and channel coding*, 3GPP TS 36.212.

[23] *Medium Access Control (MAC) protocol specification*, 3GPP TS 36.321.

[24] *Physical layer procedures*, 3GPP TS 36.213.

[25] *Radio Resource Control (RRC); Protocol specification*, 3GPP TS 36.331.

[26] A. T. Harri Holma, Ed., *LTE for UMTS: Evolution to LTE-Advanced, 2nd Edition*. Wiley, 2011.

[27] *Physical Channels and Modulation*, 3GPP TS 36.211.

[28] D. P. Bertsekas and R. G. Gallager, *Data Networks*. Prentice-Hall, 1987.

Paper C

Emulating Wired Backhaul with Wireless Network Coding

Henning Thomsen, Elisabeth de Carvalho and Petar Popovski

The paper has been published in the
General Assembly and Scientific Symposium (URSI GASS), 2014 XXXIth URSI,
pp. 1–4, 2014.

1 Abstract

In this paper we address the need for wireless network densification. We propose a solution wherein the wired backhaul employed in heterogeneous cellular networks is replaced with wireless links, while maintaining the rate requirements of the uplink and downlink traffic of each user. The first component of our solution consists of a two-way, two-phase communication between the macro base station and a user in a small cell through the small cell base station. The second component consists of an optimized adjustment of the transmit power from the macro base station during the multiple access phase of the two-way protocol. The transmit power is set high enough to enable successive decoding at the small cell base station where the downlink data to the user is first decoded and its contribution removed from the received signal followed by the uplink data from the user. The decoding of the second layer, the uplink traffic to the user, remains identical to the one performed in a wired system. In the broadcast phase, the decoding of the downlink traffic can also be guaranteed to remain identical. Hence, our solution claims an emulation of a wired backhaul with wireless network coding with same performance. We provide numerical examples involving a macro base stations serving a single small cell or two small cells.

2 Motivation and Introduction

There is a growing evidence that small cells will play a major role in the upcoming generation of wireless communication systems [1]. This is in line with the trend of wireless network densification [2], which indicates that the bit rate per unit area will grow immensely. The key element in small cell deployments is the *backhaul connection* that connects the small cell Base Stations (SBSs) to the infrastructure. The choice of the backhaul needs to hit the right tradeoff between the connectivity and deployment flexibility/cost, thus putting into consideration a mix of wired and wireless backhaul solutions.

Fig. C.1 shows an example deployment of three small cells within the coverage area of the macrocell. Each Small Base Station (SBS) uses a wired backhaul to connect to the common infrastructure. We consider a Time-Division Duplex (TDD) operation and each Mobile Station (MS) associated with one SBS uses equal periods, each of duration T, to receive the downlink traffic from the SBS and transmit the uplink traffic to the SBS. Specifically, the downlink and uplink data rate of the $k-$th user terminal is denoted by $R_{D,k}$ and $R_{U,k}$, respectively. When there is no danger of causing confusion, we will drop the index k and use simply R_D and R_U. The capacity of the backhaul link is denoted by C_B and it is assumed that:

$$C_B \geq \max\{R_D, R_U\}. \tag{C.1}$$

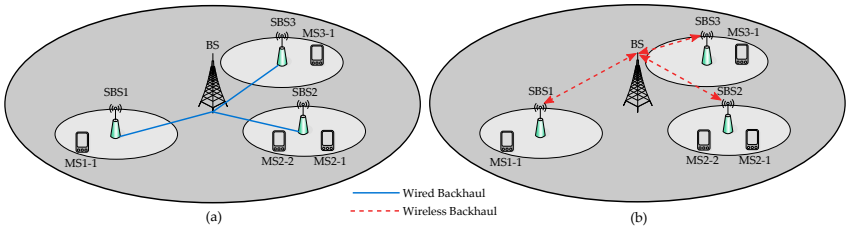

Fig. C.1: (a) Original deployment with wired backhauls (b) Deployment where the wired backhaul is emulated by the wireless backhaul.

Two observations are in order. *First*, even if the wired backhaul is capable of full-duplex transmission, it is essentially used in a TDD manner, as dictated by the TDD regime in the wireless access part, from SBS to the terminal. This means that, at a given instant, the data flow over the wire can be considered to be unidirectional. *Second*, the capacity C_B of the wire does not need to be excessively high. It needs to be just above the uplink/downlink rates that can be supported by the wireless access part, in order for (C.1) to be satisfied. If multiple users are present in the small cells, then R_D and R_U in (C.1) represent the sum-rates of all users.

The central question treated in this paper is the following: *How to remove the wired backhaul and rely on wireless connections between BS and the SBSs, while preserving the same performance of the* ***two-way communication*** *with a Mobile Station connected to the small cell?*

The motivation for doing that is the need for network densification and deployment of SBSs that is rapid, flexible and low cost. We will refer to the solution of the above problem as a *Wireless-Emulated Wire (WEW)*, since we would like to preserve the uplink/downlink rates of the user to be the same as if the wired backhaul is present. The main assumption is that the wireless backhaul BS-SBS link uses the same spectrum as the link SBS-MS, which implies that SBS has the role of a relay. WEW is possible only when two-way traffic is considered from the MS.

The operation of WEW is based on two principles: First, by having both BS and a MS transmitting to each SBS simultaneously, we create a *two-way communication flow* between them. This is enabled by the principle of network coding [3], [4]. Second, each transmitting node *knows* its own signal a priori, and can therefore subtract it from any received signal. Previously, these principles have been applied in [5], [6] in the study of coordinated transmissions in a cellular network. We use these principles in creating a wireless backhaul solution.

3 System Model

We consider a cellular scenario consisting of one BS and several SBSs. Each SBS serves a number of MSs in its small cell. The case of one BS and three SBSs is shown in Figure C.1(b). All MSs are assumed to have two-way, infinitely backlogged traffic to the BS. In our model, every node is assumed to have full Channel State Information (CSI). The uplink rate requirement of MSi-j is R_{Uij} bps, while it has a downlink rate requirement of R_{Dij} bps. All nodes are assumed to operate in half-duplex mode. Without loss of generality, we normalize the bandwidth to 1 Hz. Since we impose that WEW needs to be transparent to the MSs, their transmission power is assumed to be the same as the wired backhaul case, as is the channel between each MS and its SBS. Each SBS has a fixed transmission power identical to the wired backhaul case. In order for that to work, we need to assume that the channel SBS-BS is better than the channel SBS-MS. WIth that, SBS can broadcast XOR-ed data to both BS and MS at the rate of the SBS-MS link, which is identical to the downlink rate in the wired backhaul. Our goal is thus to find the *minimal transmission power* at the BS, such that the rate requirements of the MSs can be fulfilled.

The uplink and downlink transmissions are done over two phases. In the first phase (Multiple Access (MA) phase), the BS and MSi-j transmit simultaneously to SBSi. The Multiple Access Channel (MAC) rate region at each SBSi consists of all uplink and downlink rates that are achievable at this SBSi, and depends on the transmission power at the BS and MS. Since each MS transmits at rate equal to capacity of the link MS-SBS, each SBS is *required to decode all received signals*, such that th uplink signal from the MS is decoded last, in absence of any interference and thus under identical conditions as in the wired case. In the second phase (the Broadcast Channel (BC) phase), the SBS transmits the exclusive-or (XOR) of the decoded signals in the first phase. The BS and each MS then receive this signal, and because each node knows its own transmitted signal (has side information), it can decode the XORed signal to obtain the desired signal.

4 WEW with one SBS and one MS

We first consider the case of one MS, one SBS and one BS. The channel between MS and SBS has capacity $C(\gamma_M) = \log_2(1+\gamma_M)$, where $\gamma_M = \frac{P_M|h_M|^2}{\sigma^2}$ is the SNR between MS and SBS, P_M is the transmit power of the MS, and σ^2 the power of the additive white Gaussian noise. This channel is assumed to be able to support the rates R_D and R_U, i.e. $R_D, R_U \leq C\,(1+\gamma_M)$. For the SBS-BS link, we need to find the P_B that supports the rate R_D. At the SBS, we

have a MAC with rate bounds

$$R_U \leq C(\gamma_M), \tag{C.2}$$
$$R_D \leq C(\gamma_B), \tag{C.3}$$
$$R_U + R_D \leq C(\gamma_M + \gamma_B). \tag{C.4}$$

By assumption, MS transmits at rate equal to capacity, so $R_U = C(\gamma_M)$. Then, we need to solve the third inequality for P_B, to find the condition on the transmission power. We have

$$\log_2(1+\gamma_M) + R_D \leq \log_2(1+\gamma_M+\gamma_D) \Leftrightarrow \tag{C.5}$$
$$\log_2\left(1+\frac{P_M|h_M|^2}{\sigma^2}\right) + R_D \leq \log_2\left(1+\frac{P_M|h_M|^2}{\sigma^2}+\frac{P_B|h_B|^2}{\sigma^2}\right) \Leftrightarrow \tag{C.6}$$
$$\frac{\sigma^2}{|h_B|^2}\left(1+\frac{P_M|h_M|^2}{\sigma^2}\right)\left(2^{R_D}-1\right) \leq P_B, \tag{C.7}$$

which is the condition on the transmission power at the BS, P_B, in order for the SBS-BS link to support the required rates. The feasibility of WEW for the second phase follows from the assumption that the MS-SBS channel is identical to the wired backhaul case, and from Eq (C.1).

5 WEW with two SBSs and two MSs

To illustrate the case of two small cells, we consider a scenario consisting of one BS, two small BSs SBS1 and SBS2, each serving one MS. The channel between SBSi and its MS is $h_{Mi} \in \mathbb{C}$, while the channel between BS and SBSi is $\boldsymbol{h}_{Bi} \in \mathbb{C}^{[2M\times 1]}$, M being the number of antennas at the BS. The BS uses zero forcing to create spatially separated channels [7], and $\boldsymbol{w}_{Bi} \in \mathbb{C}^{[2M\times 1]}$ is the beam forming vector for SBSi. The downlink signal for MSi is $x_{Bi} \in \mathbb{C}$, which is transmitted with power P_{Bi}. The uplink signal is $x_{Mi} \in \mathbb{C}$. The noise at node k is denoted z_k and is assumed to be zero mean complex Gaussian. In the first phase (MA phase), BS transmits the signal

$$\boldsymbol{w}_{B1}\left(P_{B1}\right)^{\frac{1}{2}} x_{B1} + \boldsymbol{w}_{B2}\left(P_{B2}\right)^{\frac{1}{2}} x_{B2}. \tag{C.8}$$

At each SBS, the signal y_{Si} is received, where

$$y_{Si} = \boldsymbol{h}_{Bi}^H \boldsymbol{w}_{Bi}\left(P_{Bi}\right)^{\frac{1}{2}} x_{Bi} + \boldsymbol{h}_{Bi}^H \boldsymbol{w}_{Bj}\left(P_{Bj}\right)^{\frac{1}{2}} x_{Bj} + h_{Mi}\left(P_{Mi}\right)^{\frac{1}{2}} x_{Mi} + z_{Si} \tag{C.9}$$
$$= \boldsymbol{h}_{Bi}^H \boldsymbol{w}_{Bi}\left(P_{Bi}\right)^{\frac{1}{2}} x_{Bi} + h_{Mi}\left(P_{Mi}\right)^{\frac{1}{2}} x_{Mi} + z_{Si}, \tag{C.10}$$

where $i, j = 1, 2, i \neq j$, and where we have used that $\boldsymbol{h}_{Bi}^H \boldsymbol{w}_{Bj} = 0$ from the zero forcing.

The power in the signal from BS to SBSi is $P_{Bi}|\boldsymbol{h}_{Bi}^H \boldsymbol{w}_{Bi}|^2$, and the noise power is σ^2. Because we assume that each MS transmits at rate equal to capacity of its link, the SNR of the link between MSi-i and SBSi is $\gamma_{Mi} = 2^{R_{Ui}} - 1$ The SNR between BS and SBSi is $\gamma_{Bi} = \frac{P_{Bi}|\boldsymbol{h}_{Bi}^H \boldsymbol{w}_{Bi}|^2}{\sigma^2}$. From this, we can determine the rate region at SBSi in the MAC phase:

$$R_{Ui} \leq \log_2 (1 + \gamma_{Mi}), \tag{C.11}$$

$$R_{Di} \leq \log_2 (1 + \gamma_{Bi}), \tag{C.12}$$

$$R_{Ui} + R_{Di} \leq \log_2 (1 + \gamma_{Mi} + \gamma_{Bi}). \tag{C.13}$$

Assuming equality in (C.11), since user transmits at full rate, we substitute (C.11) into (C.13). After some manipulations, we get

$$\frac{\sigma^2 (1 + \gamma_{Mi}) \left(2^{R_{Di}} - 1\right)}{|\boldsymbol{h}_{Bi}^H \boldsymbol{w}_{Bi}|^2} \leq P_{Bi}, \tag{C.14}$$

which is the condition on the transmission power of the BS for SBSi. The conditions for the second phase follow from the same arguments as the single SBS case, and that the BS uses receive zero forcing.

6 Numerical Examples

To evaluate the performance of WEW, we consider the setup of one BS and two SBSs, each of which serving one MS. Two cases are considered, the BS having either 2 or 3 antennas. In both cases, we show three different uplink rate requirements, and for each of these, we vary the downlink rate requirements. Each channel element is assumed to be zero-mean circulary complex symmetric Gaussian. For the case of 2 antennas, which is shown in Fig. C.2, we see that for increasing downlink rates, the required minimum transmission power at the BS increases. For the uplink rates, we see that an increase by a factor of 2 requires an increase in transmission power by approximately 8 dB. For the case of 3 antennas at the BS, shown in Fig. C.3, we see the same behaviour. However, in this case, the BS has 3 antennas, which means that it has 3 degrees of freedom in performing the zero forcing. This translates into a decrease in minimal transmission power of about 10 dB, compared to the 2 antenna case, when considering the same uplink and downlink rate requirements.

7 Conclusion

In this paper, we have investigated solutions for addressing the network densification challenge in next-generation wireless networks. We have proposed

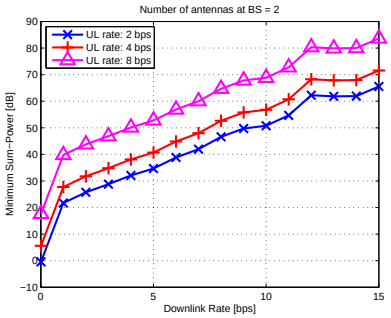

Fig. C.2: Case of 2 antennas at BS.

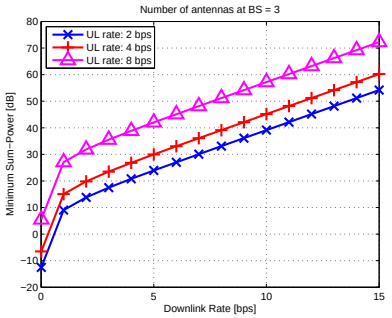

Fig. C.3: Case of 3 antennas at BS.

a wireless backhaul solution and provided conditions under which it can emulate a wired backhaul solution, in a way that is transparent, at the physical layer, for the end user. We have looked at two examples, with a single and two SBSs, respectively. For a single MS we have determined the minimal power required for emulation, while for the case of two small cells, we have used zero forcing at the BS to spatially separate the data streams. Numerical results were provided to show the relative performance in terms of transmission power for several uplink and downlink rates.

8 Acknowledgement

Part of this work has been performed in the framework of the FP7 project ICT-317669 METIS, which is partly funded by the European Union. The authors would like to acknowledge the contributions of their colleagues in METIS, although the views expressed are those of the authors and do not necessarily represent the project.

References

[1] J. G. Andrews, H. Claussen, M. Dohler, S. Rangan, and M. C. Reed, "Femtocells: Past, present, and future," *Selected Areas in Communications, IEEE Journal on*, vol. 30, no. 3, pp. 497–508, 2012.

[2] N. Bhushan, J. Li, D. Malladi, R. Gilmore, D. Brenner, A. Damnjanovic, R. Sukhavasi, C. Patel, and S. Geirhofer, "Network densification: the dominant theme for wireless evolution into 5g," *Communications Magazine, IEEE*, vol. 52, no. 2, pp. 82–89, February 2014.

[3] P. Popovski and H. Yomo, "Bi-directional amplification of throughput in a wireless multi-hop network," in *Vehicular Technology Conference, 2006. VTC 2006-Spring. IEEE 63rd*, vol. 2. IEEE, 2006, pp. 588–593.

[4] ——, "Wireless network coding by amplify-and-forward for bi-directional traffic flows," *Communications Letters, IEEE*, vol. 11, no. 1, pp. 16–18, 2007.

[5] C. Thai and P. Popovski, "Coordinated direct and relay transmission with interference cancelation in wireless systems," *Communications Letters, IEEE*, vol. 15, no. 4, pp. 416–418, 2011.

[6] C. Thai, P. Popovski, M. Kaneko, and E. de Carvalho, "Coordinated Transmissions to Direct and Relayed Users in Wireless Cellular Systems," in *Communications (ICC), 2011 IEEE International Conference on*. IEEE, 2011, pp. 1–5.

[7] T. Brown, E. de Carvalho, and P. Kyritsi, *Practical Guide to MIMO Radio Channel: with MATLAB Examples*. John Wiley & Sons, 2012.

Paper D

Using Wireless Network Coding to Replace a Wired with Wireless Backhaul

Henning Thomsen, Elisabeth de Carvalho and Petar Popovski

The paper has been published in the
IEEE Wireless Communication Letters Vol. 4(2), pp. 141–144, 2015.

Abstract

Cellular networks are evolving towards dense deployment of small cells, which requires flexible and efficient backhauling solutions. A viable solution that reuses the same spectrum is wireless backhaul where the Small Base Station (SBS) acts as a relay. In this paper we consider a reference system that uses wired backhaul and each Mobile Station (MS) in the small cell has its uplink and downlink rates defined. The central question is: if we remove the wired backhaul, how much extra power should the wireless backhaul use in order to support the same uplink/downlink rates? *We introduce the idea of wireless-emulated wire (WEW), based on two-way relaying and network coding. This setup leads to a new type of broadcast problem, with decoding conditions that are specific to the requirement for equivalence to the wired backhaul. We formulate and solve the associated optimization problems. The proposed approach is a convincing argument that wireless backhauling solutions should be designed and optimized for two-way communication.*

1 Introduction

The next leap in increasing the wireless data rates for multiple users is bringing the access point closer to the users and enable spatial reuse over smaller distances. Such a *network densification* [1] is a key feature of the upcoming 5G systems. The trend of densification has already started with the deployment of femtocells (small cells). The proliferation of small cells is conditioned on the existence of a flexible, cost-effective backhaul solution [2] between a Base Station (BS) and a Small-cell Base Station (SBS), which can permit rapid deployment of SBSs. Wired backhaul does not use spectrum, but is not always feasible due to cost or even not possible at all, as it is the case with nomadic cells with SBS on a car [3].

We consider a wireless backhaul link BS-SBS that uses the same spectrum as the link Mobile Station (MS)-SBS, such that SBS acts as an in-band relay. During the last decade, a relay has been seen as an enabler of improved coverage [4], but Wireless Network Coding (WNC) has introduced a fresh potential by exhibiting gains in spectral efficiency for scenarios with two-way relaying [5–7]. Perhaps the most important message of WNC is that the design of two-way communication schemes, rather than decoupling the uplink and downlink traffic, significantly expands the space of communication strategies and the potential gains. This has been shown in [8]. In [9], the authors study cooperative communication strategies which use network coding and beamforming, in a relay-aided two-source two-sink network, and a backhaul between the sources. Rate gains are shown in the schemes using backhaul.

The objective of this letter is to show how wired backhaul can be replaced

by a wireless one without using additional spectrum and by reusing the existing modulation/coding over the wireless air interface. The simplest version of the problem can be explained using Figs. D.1 and D.2. We first ignore SBS2/MS2 and consider only two-way communication between BS and MS1 through SBS1. The system is based on Time Division Duplex (TDD) with a time frame of duration T, such that $\frac{T}{2}$ is allocated to the Downlink (DL) and $\frac{T}{2}$ to the uplink (UL) transmission, respectively. The transmission rates of MS1 on Fig. D.1 are R_{D1}/R_{U1} in DL/UL. These rates are supported by the backhaul. The DL and UL rates averaged over the whole interval T, are $\left(\frac{R_{D1}}{2}, \frac{R_{U1}}{2}\right)$. The central question in this letter is: *Can we remove the wired backhaul and still support the same rate pair* $\left(\frac{R_{D1}}{2}, \frac{R_{U1}}{2}\right)$ *within the interval of length* T*, without requiring any changes in the baseband of MS1?* To show that this is indeed the case, we leverage the idea of two-way relaying with XOR-WNC and devise a two-phase transmission. In Phase 1, BS and MS1 transmit simultaneously. MS1 transmits with the same power and rate R_{U1}, as in Fig. D.1. BS now needs to use power P_B for the wireless transmission at rate R_{D1}. Assuming that R_{U1} is equal to the capacity of the link MS1-SBS1, then we should ensure that SBS1 decodes the "clean" signal of MS1, without any residual interference from the BS. Therefore, the minimal P_B should allow SBS1 to decode the signal of rate R_{D1} from the BS by treating the signal from MS1 as noise, then cancel the signal from the BS and proceed to decode the signal of rate R_{U1} from MS1. In Phase 2, SBS1 XORs the decoded messages and broadcasts them to MS1 and BS, such that at the end of T, the performance is equivalent to the wired backhaul i.e. we have obtained a *wireless-emulated wire (WEW)*.

This letter treats a more advanced version of the problem, where a multi-antenna BS has two simultaneous two-way links to MS1 and MS2 through SBS1 and SBS2, respectively. The first phase gives rise to a broadcast problem with a new type of constraint, since each SBSi needs to remove all the interference from the BS before decoding the signal from MSi. This is different from the conditions in standard broadcast or interference channels and we propose a new transmission technique in order to address the problem. Although the letter treats the case of only $L = 2$ two-way links, the approach can be generalized to an arbitrary number of two-way links.

2 System Model and Scheme Description

The wired scenario is shown in Fig. D.1, and the wireless in Fig. D.2. Here, MSi is connected to SBSi through the channel $h_{Mi} \in \mathbb{C}$, while SBSi is connected to BS by wire. For convenience, we denote the wireless channel from BS to SBSi by $\boldsymbol{h}_i^* \in \mathbb{C}^{[2M\times 1]}$, where $(\cdot)^*$ is complex conjugation. All channels

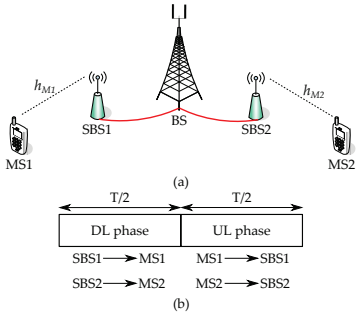

Fig. D.1: (a) A reference system with two small cells. (b) The transmissions in the uplink and downlink; only the wireless transmissions are depicted, the transmissions over the wired backhaul are taking place in parallel.

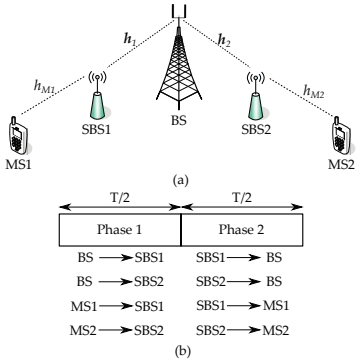

Fig. D.2: System Model used in this paper, where the two SBSs are antipodal, and each of them serve two-way traffic flow of the MS.

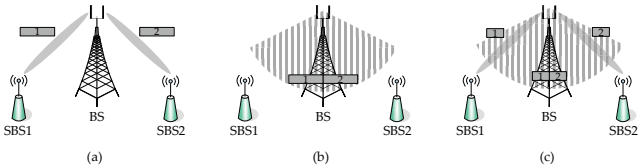

Fig. D.3: The three transmission methods considered in this paper. In (a), the BS transmits to the SBSs using ZF. In (b), the BS broadcasts the concatenated data to both SBSs. The WEW is shown in (c), wherein the BS transmits data using both ZF, and the common beamforming.

are reciprocal and constant through the entire transmission. MSi and SBSi are single-antenna nodes, while BS has $2M$ antennas. BS transmits at power P_B, SBSi at P_{Si}, and MSi at P_{Mi}. All nodes are half-duplex, and full Channel State Information is assumed. The small cells are spatially separated, causing negligible interference to each other.

The bandwidth-normalized capacity of the link is $C(\gamma) = \log_2(1+\gamma)$, where γ is the Signal-to-Noise Ratio (SNR). Denoting the noise power by σ^2, in the wired case we can define the UL and the DL SNR as $\gamma_{Ui} = \frac{P_{Mi}|h_{Mi}|^2}{\sigma^2}$ and $\gamma_{Di} = \frac{P_{Si}|h_{Mi}|^2}{\sigma^2}$, respectively. The uplink and the downlink rates, chosen for the wired backhaul, are equal to the capacity $R_{Ui} = C(\gamma_{Ui})$ and $R_{Di} = C(\gamma_{Di})$, respectively. In order to preserve equivalent rates for the MSi, the parameters from the wired backhaul case that are kept to be identical for the wireless backhaul are h_{Mi}, P_{Mi}, as well as the rates R_{Ui} and R_{Di}.

Our WEW scheme is designed to benefit from two transmission options at the BS. A natural choice is to use Zero Forcing (ZF) beamforming at the BS and send data to the two SBSs through two orthogonal spatial channels. Each SBSi receives only its intended message from the BS. This is shown in Fig. D.3(a), where message 1 is sent to SBS1, and message 2 to SBS2. Because the message sent by ZF is received only by the intended SBS, it is referred to as a *private* message. This terminology is inspired by the Han-Kobayashi scheme in interference channels [10], but the reader should note that our setup is completely different.

ZF beamforming is detrimental when the channel is ill-conditioned, resulting in noise enhancement at low SNR. A viable alternative could be MMSE beamforming; however it cannot be used as it leaves a residual interference at the SBS that cannot be decoded, hence violating our condition that MS should be able to send to SBS over a "clean" channel as with wired backhaul. In the extreme case where the channels $\boldsymbol{h}_1$ and $\boldsymbol{h}_2$ are collinear, a better solution is to send a *common* message that is broadcasted to both receivers, see Fig. D.3(b): the data bits of the two messages are concatenated at the BS into a common message, which is then encoded. Both SBSs must decode this common message in its entirety, and therefore remove its contri-

bution before decoding the UL signal.

In WEW, the BS splits the message for each MS into a private and common part, see Fig. D.3(c). The private part is sent using ZF. The common parts of the messages to both MSs are concatenated and sent using a common beam. SBS1 must decode the private message 1 (gray narrow beams) and the common message (wide patterned beam). SBS2 is treated analogously. The transmission is carried out in two phases.

Phase 1

The BS transmits the downlink message for MSi, to SBSi at rate R_{Di}. The message consists of NR_{D_i} bits, where N is the total number of channel uses in a slot. The message is split into a private data containing $N\alpha_i R_{Di}$ bits and a common data containing $N(1-\alpha_i)R_{Di}$ bits, where $0 \leq \alpha_i \leq 1$, $i = 1,2$ is the splitting factor that is subject to optimization. We define the private rate $R_{Pi} = \alpha_i R_{Di}$ and the common rate $R_{Ci} = (1-\alpha_i)\, R_{Di}$. The common data parts for both users are concatenated in order to obtain a single common message consisting of $N(R_{C1} + R_{C2}) = NR_C$ bits. Each of the three messages, two private and one common, are now encoded separately, using random Gaussian codebooks with appropriate rates, such that the signal sent by the BS is:

$$\boldsymbol{x}_B = \sqrt{P_1}\boldsymbol{w}_1 x_1 + \sqrt{P_2}\boldsymbol{w}_2 x_2 + \boldsymbol{w}_C x_C, \tag{D.1}$$

where x_i is private message for MSi with rate R_{Pi}, and x_C is the common message with rate R_C. The private message is sent using power P_i. The beamformers $\boldsymbol{w}_i \in \mathbb{C}^{[2M\times 1]}$ are defined using the ZF condition, i.e. they must satisfy $\boldsymbol{h}_i^H \boldsymbol{w}_j = 0, i, j = 1,2, i \neq j$. For the two-stream case, $\boldsymbol{w}_i = (I_{2M} - (\boldsymbol{h}_j^* \boldsymbol{h}_j^H)/|\boldsymbol{h}_j|^2)\boldsymbol{h}_i^*$, for $i, j = 1,2$, $i \neq j$ [11]. Here I_{2M} is the $2M \times 2M$ identity matrix and $(\cdot)^H$ is Hermitian transpose. For analytical convenience, $\boldsymbol{w}_i$ is normalized. The beamformer $\boldsymbol{w}_C \in \mathbb{C}^{[2M\times 1]}$ is used for the common message, sent at power $P_C = \|\boldsymbol{w}_C\|^2$, and is found in Sec. 3.

Simultaneously, MSi transmits x_{Mi}. SBSi then receives

$$\begin{aligned} y_{Si} =& \boldsymbol{h}_i^H \boldsymbol{x}_B + h_{Mi} x_{Mi} + z_{Si} \\ =& \boldsymbol{h}_i^H \sqrt{P_i}\boldsymbol{w}_i x_i + \boldsymbol{h}_i^H \boldsymbol{w}_C x_C + h_{Mi} x_{Mi} + z_{Si}, \end{aligned} \tag{D.2}$$

where we use the ZF condition and z_{Si} is the AWGN at SBSi.

Phase 2

After SBSi has decoded the private and the common message, it recreates the original message for MSi, computes the XOR of that message and the message decoded from the MSi and broadcasts the result. BS, MS1 and MS2 decode the signal sent by their respective SBSi and apply XOR to recover the desired message from the broadcasted message.

3 Optimization Problems

We first look at the minimization of the the transmit power at the BS, subject to the given UL/DL rate constraints. The variables are the powers P_i for the ZF beamformers, the common beamformer $\boldsymbol{w}_C$ and its power $\|\boldsymbol{w}_C\|^2$, as well as the splitting factors α_i, for $i = 1, 2$.

For the constraints, we have a Multiple Access Channel (MAC) region at each SBSi, involving the rates R_{Pi}, R_{Ci} and their sum. Formally, this is a 3-user MAC channel with a three-dimensional achievable region. However, x_i is sent at a rate equal to the single-user capacity, i.e. $R_{Ui} = C(\gamma_{Ui})$, which determines a specific two-dimensional sub-region of the three-dimensional MAC region. Then the constraints not involving R_{Ui} can be dropped, since they will be fulfilled if the corresponding constraints with R_{Ui} are fulfilled. The UL message is treated as noise when decoding x_i and x_C. Writing $\overline{\gamma_{Pi}} = \frac{P_i|\boldsymbol{h}_i^H\boldsymbol{w}_i|^2}{\sigma^2(1+\gamma_{Ui})}$, $\overline{\gamma_{Ci}} = \frac{|\boldsymbol{h}_i^H\boldsymbol{w}_C|^2}{\sigma^2(1+\gamma_{Ui})}$ and $\overline{\alpha_i} = 1 - \alpha_i$, and recalling $R_{Pi} = \alpha_i R_{Di}$ and $R_{Ci} = \overline{\alpha_i} R_{Di}$, the optimization problem is:

$$
\begin{aligned}
\underset{P_i, \boldsymbol{w}_C, \alpha_i}{\text{minimize}} \quad & P_1 + P_2 + \|\boldsymbol{w}_C\|^2 \\
\text{subject to} \quad & \alpha_i R_{Di} \leq C\left(\overline{\gamma_{Pi}}\right) \\
& \overline{\alpha_1} R_{D1} + \overline{\alpha_2} R_{D2} \leq C\left(\overline{\gamma_{Ci}}\right) \\
& \alpha_i R_{Di} + \overline{\alpha_1} R_{D1} + \overline{\alpha_2} R_{D2} \leq C\left(\overline{\gamma_{Pi}} + \overline{\gamma_{Ci}}\right) \\
& P_i \geq 0, \;\; 0 \leq \alpha_i \leq 1, i = 1, 2.
\end{aligned}
$$

Let us define $\beta_{1i} = \sigma^2\left(2^{R_{Pi}} - 1\right)(1 + \gamma_{Mi})$, $\beta_{2i} = \sigma^2\left(2^{R_C} - 1\right)(1 + \gamma_{Mi})$, and $\beta_{3i} = \sigma^2\left(2^{R_{Pi}+R_C} - 1\right)(1 + \gamma_{Mi})$. The problem then becomes

$$
\begin{aligned}
\underset{P_i, \boldsymbol{w}_C, \alpha_i}{\text{minimize}} \quad & P_1 + P_2 + \|\boldsymbol{w}_C\|^2 \\
\text{subject to} \quad & \beta_{1i} \leq P_i|\boldsymbol{h}_i^H\boldsymbol{w}_i|^2 \\
& \beta_{2i} \leq |\boldsymbol{h}_i^H\boldsymbol{w}_C|^2 \\
& \beta_{3i} \leq P_i|\boldsymbol{h}_i^H\boldsymbol{w}_i|^2 + |\boldsymbol{h}_i^H\boldsymbol{w}_C|^2 \\
& P_i \geq 0, \;\; 0 \leq \alpha_i \leq 1, i = 1, 2
\end{aligned}
$$

The second and third constraints are not convex and we rewrite the problem using Semidefinite Programming (SDP) [12]. Let $\boldsymbol{H}_i = \boldsymbol{h}_i\boldsymbol{h}_i^H$ and $\boldsymbol{W}_C = \boldsymbol{w}_C\boldsymbol{w}_C^H$. We can write $\|\boldsymbol{w}_C\|^2 = \mathsf{Tr}\left(\boldsymbol{w}_C\boldsymbol{w}_C^H\right) = \mathsf{Tr}\left(\boldsymbol{W}_C\right)$, where Tr is the trace of a matrix. Also, $|\boldsymbol{h}_i^H\boldsymbol{w}_C|^2 = \mathsf{Tr}\left(\boldsymbol{h}_i\boldsymbol{h}_i^H\boldsymbol{w}_C\boldsymbol{w}_C^H\right) = \mathsf{Tr}\left(\boldsymbol{H}_i\boldsymbol{W}_C\right)$. The problem is

then rewritten to

$$\begin{aligned}
\underset{P_i, \boldsymbol{W}_C, \alpha_i}{\text{minimize}} \quad & P_1 + P_2 + \mathsf{Tr}\left(\boldsymbol{W}_C\right) \\
\text{subject to} \quad & \beta_{1i} \leq P_i |\boldsymbol{h}_i^H \boldsymbol{w}_i|^2 \\
& \beta_{2i} \leq \mathsf{Tr}\left(\boldsymbol{H}_i \boldsymbol{W}_C\right) \\
& \beta_{3i} \leq P_i |\boldsymbol{h}_i^H \boldsymbol{w}_i|^2 + \mathsf{Tr}\left(\boldsymbol{H}_i \boldsymbol{W}_C\right) \\
& \boldsymbol{W}_C \succeq 0, \ \mathsf{Rank}\left(\boldsymbol{W}_C\right) = 1 \\
& P_i \geq 0, \ \ 0 \leq \alpha_i \leq 1, i = 1, 2.
\end{aligned}$$

The constraint $\boldsymbol{W}_C \succeq 0$ means that $\boldsymbol{W}_C$ is positive semidefinite. This problem is not convex because of the rank one constraint [12]. By dropping this constraint, we obtain a lower bound on the objective, since the feasible set is enlargened. This problem can then be solved using SDP. Given the solution $\boldsymbol{W}_C$, we write it as $\boldsymbol{W}_C = \lambda_1 \boldsymbol{v}_1 \boldsymbol{v}_1^H + \lambda_2 \boldsymbol{v}_2 \boldsymbol{v}_2^H$, where $\lambda_1 \geq \lambda_2 \geq 0$ are the eigenvalues of $\boldsymbol{W}_C$, with corresponding eigenvectors $\boldsymbol{v}_1, \boldsymbol{v}_2$. When the solution $\boldsymbol{W}_C$ is rank 1 ($\lambda_2 = 0$), the solution is then $\boldsymbol{w}_C = \sqrt{\lambda_1}\boldsymbol{v}_1$. Otherwise ($\lambda_2 \neq 0$), we approximate the solution by $\sqrt{\lambda_1}\boldsymbol{v}_1$, provided it is feasible. If it is not, $\sqrt{\lambda_1}\boldsymbol{v}_1$ is scaled to make it feasible.

We now look at the minimal transmission power of SBS. The total transmission power of the SBSs is $P_{S1} + P_{S2}$ in the wired case. For simplicity, assume that for the wired backhaul, $P_{S1} = P_{S2} = P_S$, while for the wireless backhaul the power of SBSi is $\eta_i P_S$, where $\eta_i \geq 1$, such that the extra power compared to the wired case is $(\eta_1 - 1)P_S + (\eta_2 - 1)P_S$. When both SBSs transmit to the BS, the rate region at the BS is a two-sender Single-Input Multiple-Output MAC. The problem is then

$$\begin{aligned}
\underset{\eta_1, \eta_2}{\text{minimize}} \quad & \eta_1 + \eta_2 \\
\text{subject to} \quad & R_{D1} \leq \log_2 \left| I_{2M} + \eta_1 P_{S1} \boldsymbol{H}_1 / \sigma^2 \right| \\
& R_{D2} \leq \log_2 \left| I_{2M} + \eta_2 P_{S2} \boldsymbol{H}_2 / \sigma^2 \right| \\
& R_{D1} + R_{D2} \\
& \qquad \leq \log_2 \left| I_{2M} + (\eta_1 P_{S1} \boldsymbol{H}_1 + \eta_2 P_{S2} \boldsymbol{H}_2) / \sigma^2 \right| \\
& \eta_1 \geq 1, \ \eta_2 \geq 1.
\end{aligned}$$

where $|\boldsymbol{X}| = \det\left(\boldsymbol{X}\right)$ and with extra power $P_S(\eta_1 + \eta_2 - 2)$.

4 Numerical Results

The performance of WEW is demonstrated in this section. We assume that $\boldsymbol{h}_1, \boldsymbol{h}_2$ are Rayleigh faded. We set $M = 1$, so the BS has two antennas. The op-

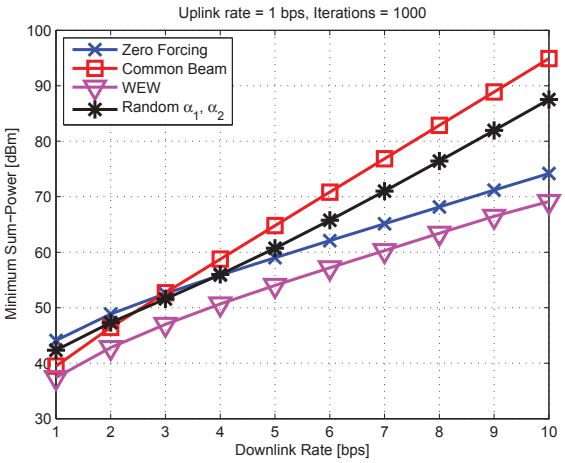

Fig. D.4: Comparison of minimum transmission power at BS, for the methods considered in this work.

timization problems in Sec. 3 are solved using the optimization software CVX. R_{Ui} and R_{Di} are set as simulation parameters and we assume $R_{U1} = R_{U2}$ and $R_{D1} = R_{D2}$. The results are averaged over 1000 channel realisations. The bandwidth is normalized to 1 Hz. In the simulations, the common beamformer is obtained using the approximation described in Sec. 3. In practically all cases, $\boldsymbol{W}_C$ is rank 1, so we can extract the solution $\sqrt{\lambda_1}\boldsymbol{v}_1$ directly.

In Fig. D.4, we compare WEW to using only ZF, only common beam, and random selection of the splitting factors. We set $R_{Ui} = 1$ bps, and vary R_{Di} between 1 and 10 bps. It is observed that WEW has an advantage of about 6 dBm over the other methods, in a large part of the range. Also, the optimization of α_1 and α_2 results in a gain over random selection. It can be noted that there is a crossing point when $R_{Di} = 4$ bps. For lower rates, the common beamformer has better performance, while ZF is better for higher rates. This is because ZF beamforming has an advantage at high SNRs, since low rate requirements translate into low SNR requirements. In Fig. D.5, the results of the power optimization of SBS is shown. We assume that the SBS-BS channels are statistically equal to the MS-SBS channels. As expected, the required extra power increases with the rate of the XORed packet, as it now needs also to be sent to the BS.

5 Conclusion

In this paper, we have proposed Wireless-Emulated Wire (WEW), a concept that enables efficient wireless backhaul for two-way traffic. At the Base Station (BS), our scheme leverages on transmitting data to the Mobile Stations

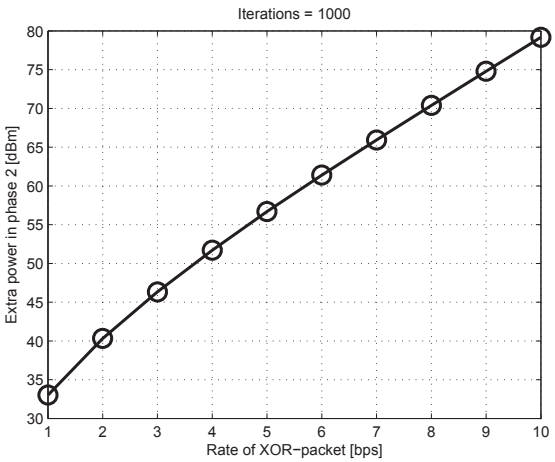

Fig. D.5: Total additional power required at the SBSs in phase 2.

(MSs) by partitioning it into a private and common part, that should be decoded by the respective Small BS (SBS). We formulated an optimization problem to find the minimal transmission power at the BS, given the rates of the wired backhaul. Due to nonconvexity, the problem was relaxed and a lower bound on the required power was found. We have also investigated the additional power required at each SBS to support wireless backhaul. The WEW concept opens up further challenges in resource allocation when more than two MSs are considered.

Acknowledgement

Part of this work has been performed in the framework of the FP7 project ICT-317669 METIS, which is partly funded by the European Union. The authors would like to acknowledge the contributions of their colleagues in METIS, although the views expressed are those of the authors and do not necessarily represent the project.

References

[1] N. Bhushan, J. Li, D. Malladi, R. Gilmore, D. Brenner, A. Damnjanovic, R. Sukhavasi, C. Patel, and S. Geirhofer, "Network densification: the dominant theme for wireless evolution into 5g," *Communications Magazine, IEEE*, vol. 52, no. 2, pp. 82–89, February 2014.

[2] J. G. Andrews, "Seven ways that HetNets are a cellular paradigm shift," *Communications Magazine, IEEE*, vol. 51, no. 3, pp. 136–144, 2013.

[3] Z. Ren, S. Stanczak, P. Fertl, and F. Penna, "Energy-aware activation of nomadic relays for performance enhancement in cellular networks," in *International Conference on Communications (ICC), IEEE*, 2014.

[4] R. Pabst, B. H. Walke, D. Schultz, P. Herhold, H. Yanikomeroglu, S. Mukherjee, H. Viswanathan, M. Lott, W. Zirwas, M. Dohler, H. Aghvami, D. Falconer, and G. Fettweis, "Relay-based deployment concepts for wireless and mobile broadband radio," *Communications Magazine, IEEE*, vol. 42, no. 9, pp. 80–89, Sept 2004.

[5] P. Popovski and H. Yomo, "Bi-directional amplification of throughput in a wireless multi-hop network," in *Vehicular Technology Conference, 2006. VTC 2006-Spring. IEEE 63rd*, vol. 2. IEEE, 2006, pp. 588–593.

[6] ——, "Physical Network Coding in Two-Way Wireless Relay Channels," in *IEEE Int. Conf. Communications*. IEEE, Jun. 2007, pp. 707–712.

[7] S. Zhang, S. C. Liew, and P. P. Lam, "Hot topic: physical-layer network coding," in *Proceedings of the 12th annual international conference on Mobile computing and networking*. ACM, 2006, pp. 358–365.

[8] C. D. T. Thai, P. Popovski, M. Kaneko, and E. de Carvalho, "Multi-Flow Scheduling for Coordinated Direct and Relayed Users in Cellular Systems," *IEEE Trans. Commun.*, vol. 61, no. 2, pp. 669–678, Feb. 2013.

[9] J. Du, M. Xiao, and M. Skoglund, "Cooperative network coding strategies for wireless relay networks with backhaul," *IEEE Trans. Commun.*, vol. 59, no. 9, pp. 2502–2514, Sept. 2011.

[10] H. Te Sun and K. Kobayashi, "A new achievable rate region for the interference channel," *Information Theory, IEEE Transactions on*, vol. 27, no. 1, pp. 49–60, 1981.

[11] T. Brown, E. de Carvalho, and P. Kyritsi, *Practical Guide to MIMO Radio Channel: with MATLAB Examples*. John Wiley & Sons, 2012.

[12] A. B. Gershman, N. D. Sidiropoulos, S. Shahbazpanahi, M. Bengtsson, and B. Ottersten, "Convex optimization-based beamforming: From receive to transmit and network designs," *Signal Processing Magazine, IEEE*, vol. 27, no. 3, pp. 62–75, 2010.

Paper E

CoMPflex: CoMP for In-Band Wireless Full Duplex

Henning Thomsen, Petar Popovski, Elisabeth de Carvalho,
Nuno K. Pratas, Dong Min Kim and Federico Boccardi

The paper has been accepted for publication in the
IEEE Wireless Communication Letters, 2015.

The layout has been revised.

Abstract

In this letter we consider emulation of a Full Duplex (FD) cellular base statiosubn (BS) by using two spatially separated and coordinated half duplex (HD) BSs. The proposed system is termed CoMPflex (CoMP for In-Band Wireless Full Duplex) *and at a given instant it serves two HD mobile stations (MSs), one in the uplink and one in the downlink, respectively. We evaluate the performance of our scheme by using a geometric extension of the one-dimensional Wyner model, which takes into account the distances between the devices. The results show that CoMPflex leads to gains in terms of sum-rate and energy efficiency with respect to the ordinary FD, as well as with respect to a baseline scheme based on unidirectional traffic.*

1 Introduction

5G wireless systems are expected to have a large number of Base Stations (BSs) per unit area [1]. The inter-BS connections lay the ground to use cooperative techniques, commonly referred to as *Coordinated Multi-Point (CoMP)* [2]. Another important wireless trend is the use of in-band full-duplex (FD) wireless transceivers [3], expected to lead to a two-fold spectral efficiency gain [4]. The key challenge in FD is the high transceiver complexity, required to cope with the strong self-interference induced by the *downlink (DL)* transmission path into the *uplink (UL)* receiving path [3]. The high transceiver complexity will likely make the FD feasible only for the BS, while a Mobile Station (MS) will remain half-duplex (HD), but the system can still harvest the FD gain by scheduling at least two different MSs, as shown in Fig. E.1(c).

Traditionally, UL and DL are treated in isolation, i.e. all MSs have only DL or only UL traffic, see Fig. E.1(a). The advent of FD has shifted the focus towards two-way optimization of wireless networks [5]. This leads to two transmission modes, as the one depicted on Fig. E.1(b), while in the second mode the roles are reversed (MS1 transmits and MS2 receives). In Fig. E.1(b) HD-BS1 sends the signal x_{D1} in the DL to MS1, while HD-BS2 receives x_{U2} in the UL from MS2. HD-BS2 receives interference from HD-BS1, while MS1 receives interference from MS2. However, HD-BS1 can use the high-bandwidth wired connection to HD-BS2 to send the data of x_{D1} to HD-BS2, such that HD-BS2 can recreate x_{D1} and perfectly cancel the interference from HD-BS1. Note that x_{U2} remains as interference to MS1, but it could be mitigated via e.g. scheduling. The setting on Fig. E.1(b) operates equivalently as a single FD-BS, see Fig. E.1(c). With Time Division Duplexing (TDD), the roles of MS1 and MS2 are reversed in the next transmission slot, thus serving both MSs two-way.

The previous example constitutes the main proposal of this letter: use the CoMP infrastructure, with interconnected HD-BSs, in order to obtain a distributed FD implementation, termed *CoMPflex (CoMP for in-band full duplex)*.

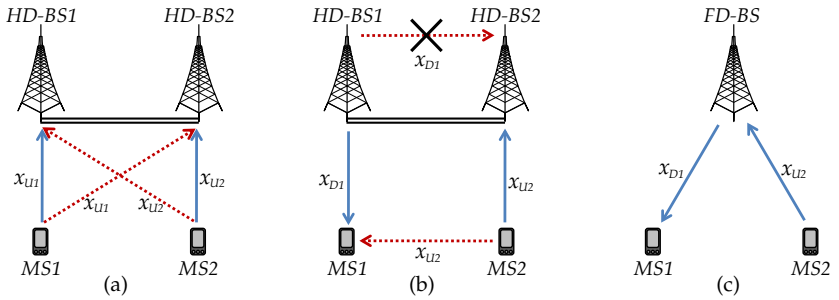

Fig. E.1: (a) Baseline scheme for UL; (b) The proposed CoMPflex scheme; (c) FD transmission. Solid arrows denote signals, dashed arrows denote interference, the double line is a wired connection.

In traditional CoMP, the BSs cooperate to serve the MSs either in DL or in UL, but not both simultaneously. The price of the performance gains of traditional CoMP over the non-cooperative schemes is the complex processing of interference using, e.g. dirty paper coding. Different from that, CoMPflex is a way to get performance gains over non-cooperative schemes, without complicated processing at the BSs. Note that the channel between two different BS is static, such that it can be easily estimated. Assuming a sufficient wired bandwidth between the HD-BSs, CoMPflex serves simultaneously two terminals that have opposite (UL/DL) connections. The ordinary FD is a special case of CoMPflex where the HD-BSs are at a distance zero. CoMPflex brings four advantages: (i) the coupling losses between the antennas associated with each path are mitigated; (ii) the self-interference coming from the DL transmission is now within the same order of magnitude as the UL signal, reducing the need for a high dynamic range receiver; and (iii) the reduction of the distance between the cellular devices and HD-BS, which leads to potential energy savings [6] both at the device and network side, and (iv) the separated transmitter and receiver of the HD-BSs can bring the infrastructure closer to the MSs, resulting in rate gains and decrease in interference. We will show that such a separation is *also* beneficial for a traditional setting with unidirectional traffic. In this way, CoMPflex brings a two-part gain over traditional non-cooperative schemes: (1) by an optimal spatial separation between the HD-BSs; and (2) serving the MSs with bidirectional traffic jointly instead of unidirectional traffic. Our analysis is based on the classical Wyner model [7], enriched to capture the geometric setting of CoMPflex and allow for studying the effect of varying the distance between the connected BSs.

A scheme similar to CoMPflex has been considered in [8]. In that work, the authors only consider the UL-DL traffic pattern, while the distances between the devices are not studied. Different from [8], we analyze the effect

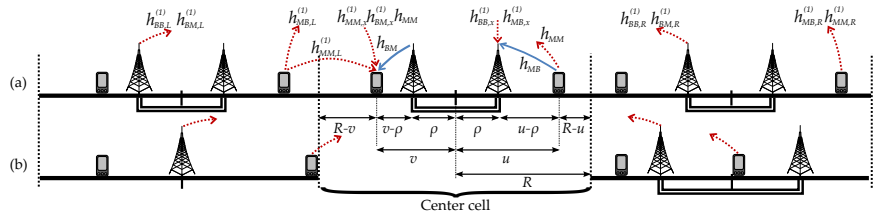

Fig. E.2: System model for CoMPflex, (a): The center cell and two adjacent cells, one to the left (L) and one to the right (R), with $x \in \{L, R\}$; (b): The worst case situation of transmitting BSs and MSs from neighboring cells.

of varying the BS-BS distance, and compare to a scheme using a FD-BS.

2 System Model

Our system model is perhaps the simplest one where the gain of CoMPflex can be demonstrated. It is based on an one-dimensional Wyner model, as shown in Fig. E.2a, where the cells have radius R.[1] The figure shows a 1-tier interference model, but it can be extended to several interfering tiers. In the center cell, there is either one FD-BS placed at the cell center (corresponding to $\rho = 0$), or two HD-BSs, one for DL placed in the left half of the cell, and one UL placed in the right half (corresponding to $\rho > 0$). Both HD-BSs have the same distance ρ to the cell center. We assume a sufficient number of active users in the cell, so that one DL-MS in the left half and one UL-MS in the right half can always be scheduled. The DL-MS is placed uniformly at random at position v in the left half of the cell, and the UL-MS is placed uniformly at random at position u in the right half of the cell.

In the baseline scheme, the BSs and MSs are deployed as in CoMPflex, except that the traffic is bidirectional in CoMPflex and unidirectional in the baseline. In the baseline scheme the BSs are not cooperating, which is sufficient to show the effect of using bidirectional versus unidirectional traffic. In both schemes, the positions of the nodes in the interfering cells depend on the interference model, see Sec. 2.2.

2.1 Signal Model

We explain the signal model for CoMPflex only; the one for the baseline scheme can be derived from it. In Fig. E.2a, wireless channels are indicated as arrows showing the transmission direction: a solid line for signal and a dashed line for interference. For clarity, only the links relevant to the center cell are shown. All channels are Rayleigh faded with unit mean power. The

[1] Here we treat the 1-D scenario. Obviously, the analysis can be extended to 2-D and 3-D models, but this is out of the scope for this introductory article.

pathloss[2] is modeled as $\ell(d) = (1 + |d|)^{-\alpha}$, where d is the distance from the transmitter to the receiver and α is the path loss exponent. The system bandwidth is normalized to 1 Hz. All nodes use the same frequency. We assume Additive White Gaussian Noise (AWGN), with power σ^2. Finally, we assume full channel state information at all nodes.

The distance between BS and UL-MS is $|u - \rho|$, and between DL-MS and BS, $|v - \rho|$. We restrict ρ to $[0, R/2]$, since $\rho > R/2$ would allow the MS to be closer to an interfering BS. In the UL, the signal received at the BS, y_B, is

$$y_B = h_{MB}\ell(\rho - u)^{\frac{1}{2}}x_M + I_B + z_B$$

where x_M is the symbol sent from MS and z_B is the AWGN at the BS. The term h_{MB} denotes the channel from the MS to the BS. $I_B = I_{BB} + I_{MB}$ is the interference from BSs (I_{BB}) and MSs (I_{MB}) in the neighboring cells (see Appendix). Then

$$\gamma_U(\rho, u) = \frac{P_M(\rho)g_{MB}\ell(\rho - u)}{\sigma^2 + \bar{I}_B} \tag{E.1}$$

is the UL SINR, where $P_M = |x_M|^2$, $g_{MB} = |h_{MB}|^2$ and $\bar{I}_B = |I_B|^2$ is the received interference power at the BS.

The DL-MS receives the signal y_M,

$$y_M = h_{BM}\ell(\rho - v)^{\frac{1}{2}}x_B + h_{MM}\ell(u + v)^{\frac{1}{2}}x_M + I_M + z_M$$

where x_B is the signal sent from BS, h_{BM} and h_{MM} denote respectively the channels between BS and MS, and the intra-cell channel between the MSs. $I_M = I_{BM} + I_{MM}$ is the interference from the BSs (I_{BM}) and the users (I_{MM}) in neighboring cells given in the Appendix, and z_M is the AWGN at the MS. The DL SINR is

$$\gamma_D(\rho, u, v) = \frac{P_B(\rho)g_{BM}\ell(\rho - v)}{P_M(\rho)g_{MM}\ell(u + v) + \bar{I}_M + \sigma^2} \tag{E.2}$$

where $P_B = |x_B|^2$, $g_{BM} = |h_{BM}|^2$, $g_{MM} = |h_{MM}|^2$ and $\bar{I}_M = |I_M|^2$ is the received interference power at the MS.

2.2 Power Adjustment and Inter-Cell Interference Models

The core of CoMPflex is in bringing the MSs and BSs closer to each other, therefore it is natural to allow them to adjust their transmission power accordingly. This transmission power is computed based on the required power received at either the BS, P_B^{req}, and the MS, P_M^{req}, when the MS is placed at the

[2] An offset equal to 1 is added to avoid a singularity when $d = 0$.

cell edge. The required powers are defined in Sec. 4. We denote the adjusted power as $P_B(\rho)$ and $P_M(\rho)$, for the BS and MS respectively, which is computed as:

$$P_y^{req} \leq P_x(\rho)\ell(R-\rho) \Leftrightarrow P_x(\rho) \geq P_y^{req}\ell(R-\rho)^{-1},$$

given a required cell edge rate R_{x_0} and a corresponding outage probability ε, where $x, y \in \{B, M\}$. It can be shown that the required power received at y, is $P_y^{req} = -\frac{(2^{R_{x_0}}-1)\sigma^2}{\log(1-\varepsilon)\ell(R)}$. Finally, in Sec. 4 we will also evaluate the *constant power* case, where $P_B = P_B(\rho = 0)$ and $P_M = P_M(\rho = 0)$.

We consider two inter-cell interference models when assessing the performance of CoMPflex and the baseline. In the first model, for both CoMPflex and the baseline, nodes in the interfering cells follow the same deployment pattern as the center cell, with one FD-BS or two HD-BSs placed at distance ρ from the center of the cell. The setup is shown in Fig. E.2a, and the expression of the interference is shown in the Appendix.

The second model is the worst-case interference, see Fig. E.2b, where the transmitting BSs and MSs are indicated by dashed arrows. In each cell, the interfering BSs and MSs are placed as close to the center cell as possible, since we want maximum interference at the center cell. For the cell to the left, the worst-case position of the interfering BS is at $\rho = 0$ (the center of its cell) and the MS at the cell edge. For the cell to the right, the worst-case position of the interfering BS is when $\rho = R/2$ (maximal) and the MS is at the cell center. These worst-case scenarios are not formally proved due to lack of space.

3 Analysis

In this section we show that a nonzero ρ will benefit the performance in terms of sum-rate and energy efficiency.

The sum-rate $R_{sum}(\rho)$ is given by

$$\begin{aligned} R_{sum}(\rho) &= \log_2\left(1+\gamma_U(\rho)\right) + \log_2\left(1+\gamma_D(\rho)\right) \\ &= \log_2\left(1+\gamma_U(\rho)+\gamma_D(\rho)+\gamma_U(\rho)\cdot\gamma_D(\rho)\right). \end{aligned}$$

For analytical tractability we consider *stationary* conditions: (i) the channel gains of all links are unitary, i.e. $g_x = 1$; (ii) the inter-cell interference comes from the nearest cell tier; (iii) the interfering MSs are at their average positions; and (iv) we fix the MSs in the center cell at the positions u and v.

Proposition 1. *In stationary conditions the following two statements hold:*

- $\forall \rho \in [0, v]$ *in the DL, we have* $\gamma_D(u, v, 0) \leq \gamma_D(u, v, \rho)$;
- $\forall \rho \in [0, u]$ *in the UL, we have* $\gamma_U(u, 0) \leq \gamma_U(u, \rho)$.

Proof. We only sketch the proof of the first statement; the second one is similar. The proof is done by analyzing the derivative of the DL SINR, which is denoted $\gamma_D(u,v,\rho) = \frac{S(v,\rho)}{I(u,v,\rho)+z_M}$, with respect to ρ. Here the DL signal is $S(v,\rho)$ and the DL interference is $I(u,v,\rho)$. Then from the rule of differentiating a quotient, we only look at the numerator of this derivative, since the denominator is squared. The DL signal is $S(v,\rho) = P_B(\rho)\ell(R-\rho)$ and the DL interference is

$$\begin{aligned} I(u,v,\rho) = (1+R-\rho)^{\alpha} \cdot \Big[& P_M^{req}\ell(2R+\rho-v) \\ & + P_M^{req}\ell(2R+\rho-v) + P_B^{req}\ell(1+3R/2-v) \\ & + P_B^{req}\ell(1+5R/2+v) + P_B^{req}\ell(u+v)\Big]. \end{aligned}$$

The numerator of $\frac{\partial}{\partial\rho}\gamma(\rho)$ equals

$$\frac{\partial}{\partial\rho}S(v,\rho)(I(u,v,\rho)+z_M) - \frac{\partial}{\partial\rho}(I(u,v,\rho)+z_M)S(v,\rho).$$

For $\rho \in [0,v]$, the derivative of $S(v,\rho)$ is

$$\begin{aligned} \frac{\partial}{\partial\rho}S(v,\rho) = & P_M^{req}\alpha(1+R-\rho)^{\alpha-1}(1+v-\rho)^{-\alpha} \\ & \cdot\Big(-1+(1+R-\rho)(1+v-\rho)^{-1}\Big), \end{aligned}$$

which is positive since $-1+(1+R-\rho)(1+v-\rho)^{-1} > 0$. The derivative $\frac{\partial}{\partial\rho}I(u,v,\rho)$ equals

$$\begin{aligned} & \frac{\partial}{\partial\rho}(1+R-\rho)^{\alpha}I(u,v,\rho) + (1+R-\rho)^{\alpha}\frac{\partial}{\partial\rho}I(u,v,\rho) \\ & -\alpha(1+R-\rho)^{\alpha-1}I(u,v,\rho) + (1+R-\rho)^{\alpha}\frac{\partial}{\partial\rho}I(u,v,\rho). \end{aligned}$$

It can be shown that $\frac{\partial}{\partial\rho}I(u,v,\rho) < 0$. Using the fact that $S(v,\rho) > 0$, $\frac{\partial}{\partial\rho}S(v,\rho) > 0$ and $I(u,v,\rho)+z_{MS} > 0$, we can conclude that $\frac{\partial}{\partial\rho}\gamma_D(\rho) > 0, \forall\rho \in [0,v]$ □

Corollary 1. *In stationary conditions,* $\forall\rho \in [0,\min\{u,v\}]$,

$$\gamma_U(0)\cdot\gamma_D(0) \leq \gamma_U(\rho)\cdot\gamma_D(\rho).$$

From Prop. 1 and Cor. 1, we can conclude that the sum-rate $R_{sum}(\rho)$, increases for $\rho \in [0,\min\{u,v\}]$.

The energy efficiency EE is defined as the amount of bits transmitted per unit of energy [9]. It is given by

$$EE(\rho) = \frac{R_{sum}(\rho)}{P_B(\rho) + P_M(\rho)}. \tag{E.3}$$

CoMPflex improves the EE, both due to increased sum-rate and lower transmission power as functions of ρ.

4 Performance Results

We evaluate the sum-rate and EE of CoMPflex via numerical simulations. The main simulation settings are listed in Tab. E.1. The positions of the MSs are random and uniform over their half-cell, all links have fading and we include N interfering cell tiers both to the left and right.

Table E.1: Simulation parameters.

Parameter	Description	Simulation Setting
R	Cell radius	100 m
σ^2	Noise power at MS and BS	-174 dBm
α	Path loss exponent	$3, 4, 5$
N	Number of interfering cells	10
R_{U_0}	Required UL rate	0.03 bps [10, Ch.11]
R_{D_0}	Required DL rate	0.06 bps [10, Ch.11]
ε	Cell edge outage probability	0.1

The sum-rate performance results are shown in Fig. E.3. We compare the proposed CoMPflex scheme with the baseline, using both deployments depicted in Figs.E.2a and E.2b, the latter denoted as the worst-case interference. Since the baseline serves unidirectional traffic over the entire transmission phase, we need two such phases to serve two-way traffic to the MSs. Therefore, the sum-rate is $\frac{R_U+R_D}{2}$, where R_U is the total UL rate and R_D is the total DL rate. We also depict the results for $\rho = 0$ (no splitting) for CoMPflex (ordinary FD) and the baseline. The performance of CoMPflex is almost always better than the baseline. Also, in both interference deployments, there is a benefit in increasing ρ. This confirms the conclusions from Sec. 3, but now with more realistic conditions. We also see that the difference between the sum-rate when using constant power versus power adjustment is negligible, such that power adjustment is chiefly beneficial for higher EE. It is also interesting that there is a gain in sum-rate *both* from splitting the BSs, as well as using the CoMPflex scheme instead of the baseline, even in the worst case.

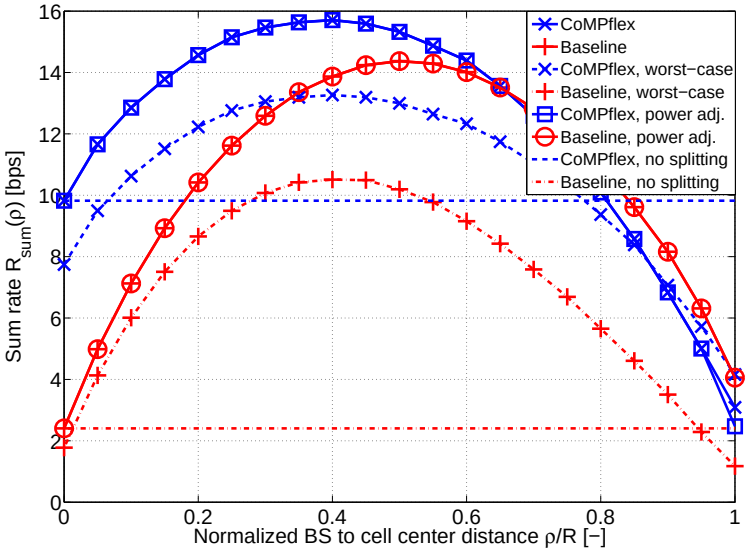

Fig. E.3: Sum-rate comparison of CoMPflex and baseline, comparing worst-case with simulation, where $\alpha = 4$.

To evaluate the EE gains of CoMPflex, we normalize the achieved EE at a certain ρ with the EE when $\rho = 0$ (Fig.E.1c). The normalized EE is:

$$\eta(\rho) = \frac{EE(\rho)}{EE(\rho = 0)}. \tag{E.4}$$

We also look at the total transmission power $P_{sum}(\rho) = P_B(\rho) + P_M(\rho)$, and study how it depends on ρ. These curves, along with the normalized EE, are shown in Fig. E.4, where we see that the total transmission power decreases as ρ increases. This is to be expected since the distance between a MS and its serving BS is decreased, requiring less power is used to maintain the same performance. The combination of a lower required transmission power with a higher sum-rate results in the observed dramatic increase in EE, especially when ρ tends to $R/2$. This increase is further accentuated in propagation environments with higher α values.

5 Conclusion

We have shown that the proposed CoMPflex scheme allows emulation of in-band FD operation by spatially dislocating the UL and DL traffic into two HD-BSs. Our results show that this splitting leads to a substantial increase in sum-rate as well as an EE increase ranging from $15\times$ to $45\times$ for high BSs splitting distance and increasing path-loss exponents. This initial study uses

a simple model, but the gains and the insights obtained warrant further analysis that relies on more complex models, such as the ones based on stochastic geometry.

6 Appendix

Using Fig. E.2, the distances between the MS in the nth cell and the receiving BS are

$$d^{(n)}_{MB,L} = 2nR - u_{n,L} + \rho, \qquad d^{(n)}_{MB,R} = 2nR + u_{n,R} - \rho,$$

for the left (L) and right (R) cell respectively. $u_{n,L}$ and $u_{n,R}$ describe the same distances as u and v in the left and right interfering cells. The BS-MS, BS-BS and MS-MS distances are, respectively,

$$\begin{aligned} d^{(n)}_{BM,L} &= 2nR + \rho - v, & d^{(n)}_{BM,R} &= 2nR - \rho + v, \\ d^{(n)}_{BB,L} &= 2nR + 2\rho, & d^{(n)}_{BB,R} &= 2nR - 2\rho, \\ d^{(n)}_{MM,L} &= 2nR - u_{n,L} - v, & d^{(n)}_{MM,R} &= 2nR + u_{n,R} + v, \end{aligned}$$

where the random variables u, v, $u_{n,L}$ and $u_{n,R}$ are independent. In the worst-case scenario (Fig. E.2b), the MS-BS, BS-MS, BS-BS and MS-MS distances are, respectively,

$$\begin{aligned} d^{(n),wc}_{MB,L} &= 2nR - R + \rho, & d^{(n),wc}_{MB,R} &= 2nR - \rho, \\ d^{(n),wc}_{BM,L} &= 2nR - v, & d^{(n),wc}_{BM,R} &= 2nR - R/2 + v, \\ d^{(n),wc}_{BB,L} &= 2nR + \rho, & d^{(n),wc}_{BB,R} &= 2nR - R/2 - \rho, \\ d^{(n),wc}_{MM,L} &= 2nR - R - v, & d^{(n),wc}_{MM,R} &= 2nR + v. \end{aligned}$$

Letting $\psi \in \{MB, BM, BB, MM\}$, and $h^{(n)}_{\psi,\varphi}$, $\varphi \in \{L, R\}$ the channel between a node in the nth cell and the receiver, the interference terms are then

$$I_\psi = \sum_{n=1}^{\infty} \left[h^{(n)}_{\psi,L} \sqrt{\ell(d^{(n)}_{\psi,L})} x^{(n)}_L + h^{(n)}_{\psi,R} \sqrt{\ell(d^{(n)}_{\psi,R})} x^{(n)}_R \right], \tag{E.5}$$

where $x^{(n)}_L$ and $x^{(n)}_R$ are symbols sent from appropriate nodes.

References

[1] F. Boccardi, R. W. Heath Jr, A. Lozano, T. L. Marzetta, and P. Popovski, "Five disruptive technology directions for 5G," *IEEE Commun. Mag.*, vol. 52, no. 2, pp. 74–80, Feb. 2014.

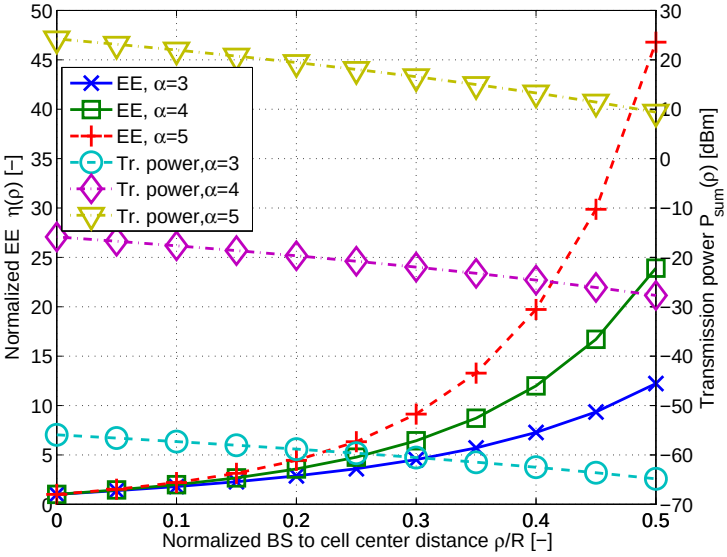

Fig. E.4: Power usage and EE of CoMPflex.

[2] D. Lee, H. Seo, B. Clerckx, E. Hardouin, D. Mazzarese, S. Nagata, and K. Sayana, "Coordinated multipoint transmission and reception in LTE-advanced: deployment scenarios and operational challenges," *Communications Magazine, IEEE*, vol. 50, no. 2, pp. 148–155, 2012.

[3] A. Sabharwal, P. Schniter, D. Guo, D. Bliss, S. Rangarajan, and R. Wichman, "In-Band Full-Duplex Wireless: Challenges and Opportunities," *IEEE J. Select. Areas Commun.*, vol. 32, no. 9, pp. 1637–1652, Sept. 2014.

[4] S. Goyal, P. Liu, S. Hua, and S. Panwar, "Analyzing a full-duplex cellular system," in *Proc. of the IEEE Conference on Information Sciences and Systems (CISS 2013)*, Mar. 2013.

[5] P. Popovski, O. Simeone, J. J. Nielsen, and Č. Stefanović, "Interference spins: Scheduling of multiple interfering two-way wireless links," *IEEE Commun. Lett.*, vol. 19, no. 3, pp. 387–390, Mar. 2015.

[6] I. Chih-Lin, C. Rowell, S. Han, Z. Xu, G. Li, and Z. Pan, "Toward green and soft: a 5G perspective." *IEEE Commun. Mag.*, vol. 52, no. 2, pp. 66–73, Feb. 2014.

[7] A. D. Wyner, "Shannon-theoretic approach to a Gaussian cellular multiple-access channel," *IEEE Trans. Inf. Theory*, vol. 40, no. 6, pp. 1713–1727, Nov. 1994.

[8] P. Larsson and N. Johansson, "Method and apparatus for interference reduction," Feb. 2013, uS Patent 8,369,261.

[9] G. Y. Li, Z. Xu, C. Xiong, C. Yang, S. Zhang, Y. Chen, and S. Xu, "Energy-efficient wireless communications: tutorial, survey, and open issues," *IEEE Wireless Commun.*, vol. 18, no. 6, pp. 28–35, Dec. 2011.

[10] H. Holma and A. Toskala, *LTE advanced: 3GPP solution for IMT-Advanced*. John Wiley & Sons, 2012.

Paper F

Full Duplex Emulation via Spatial Separation of Half Duplex Nodes in a Planar Cellular Network

Henning Thomsen, Dong Min Kim, Petar Popovski, Nuno K. Pratas and Elisabeth de Carvalho

The paper has been submitted to the
17th IEEE International workshop on Signal Processing Advances in Wireless Communications (SPAWC), 2016.

The layout has been revised.

Abstract

A Full Duplex Base Station (FD-BS) can be used to serve simultaneously two Half-Duplex (HD) Mobile Stations (MSs), one working in the uplink and one in the downlink, respectively. The same functionality can be realized by having two interconnected and spatially separated Half Duplex Base Stations (HD-BSs), which is a scheme termed CoMPflex *(CoMP for In-Band Wireless Full Duplex). A FD-BS can be seen as a special case of CoMPflex with separation distance zero. In this paper we study the performance of CoMPflex in a two-dimensional cellular scenario using stochastic geometry and compare it to the one achieved by FD-BSs. By deriving the Cumulative Distribution Functions, we show that CoMPflex brings BSs closer to the MSs they are serving, while increasing the distance between a MS and interfering MSs. Furthermore, the results show that CoMPflex brings benefits over FD-BS in terms of communication reliability. Following the trend of wireless network densification, CoMPflex can be regarded as a method with a great potential to effectively use the dense HD deployments.*

1 Introduction

As the wireless cellular networks evolve towards the 5G generation, it is expected that the number of Base Stations (BSs) per area will noticeably increase [1], leading to *network densification*. The availability of multiple proximate and interconnected BSs leads to the usage cooperative transmission/reception techniques, commonly referred to as *Coordinated Multi-Point (CoMP)* [2]. Motivated by these recent trends, a transmission scheme for serving bidirectional traffic simultaneously via spatially separated HD-BSs was investigated in [3]. The scheme emulates Full Duplex (FD) operation using two interconnected HD-BSs, and is termed *CoMPflex*: CoMP for In-Band Wireless Full-Duplex. In the initial work, the performance was analyzed through a simplified one-dimensional Wyner-type deployment model. CoMPflex can be seen as a generalization of FD, where a FD BS corresponds to CoMPflex with interconnection distance zero. We show that the nonzero separation distance in CoMPflex brings two benefits: (i) The distance between a BS and its associated Mobile Stations (MSs) decreases; and (ii) the distance between two interfering MSs increases. This translates into improved transmission success probability in uplink (UL) and downlink (DL).

The use of in-band FD wireless transceivers [4] has recently received significant attention. However, due to the high transceiver complexity, FD is currently only feasible at the network infrastructure side [5] and the MSs keep the HD transceiver mode. An in-band FD BS can serve one UL and one DL MSs simultaneously, on the same frequency. Other approaches to FD emulation by HD devices have been studied in the literature, such as hav-

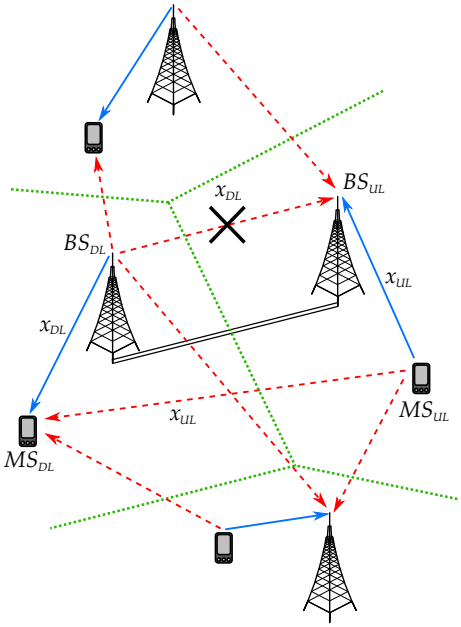

Fig. F.1: CoMPflex system model.

ing the transmissions in UL and DL (partially) overlap in time. That is, the UL and DL time slots, which conventionally should take place at separate time intervals, are now overlapping, an approach used by the Rapid On-Off Division Duplexing (RODD) in [6]. The authors of [7] consider the physical UL and DL channels themselves, and have them overlap. Compared to these approaches, CoMPflex takes advantage of the spatial dimensions in a cellular network.

In this paper, we treat CoMPflex in a two-dimensional scenario, with planar deployment of interconnected HD-BSs. Following the trend in the literature for modeling spatial randomness of network nodes, we analyze the performance using the tools of stochastic geometry. Stochastic geometry has been used in many papers in the literature to model the placement of network nodes, including FD capable ones as in [8]. The setup of CoMPflex is shown in Fig. F.1, where one HD-BS working in the UL cooperates via a wired connection (double dashed line) with another HD-BS that operates in the DL. The solid arrows indicate signals; the dashed arrows interference. Two interfering cells are also shown, and the boundaries between them are indicated by dotted lines. Using the interconnection link, the interference from the DL-BS to the UL-BS is perfectly canceled. Note that, for the sake of clarity, not all interference from neighboring cells is shown.

2 System Model

We consider a scenario where HD-BSs serve HD-MSs with bidirectional traffic. We assume Rayleigh fading with unit mean power. The power of the channel between nodes i and j is written g_{ij}, and from the assumption of Rayleigh fading we have $g_{ij} \sim \text{Exp}(1)$.[1] The distance between nodes i and j is written as r_{ij}. We use the pathloss model $\ell(r) = r^{-\alpha}$, where α is the path loss exponent. We assume Additive White Gaussian Noise (AWGN) with power σ^2. Full channel state information is assumed at all nodes. The default transmission power of a BS and MS is P_B and P_M, respectively.

2.1 Deployment Assumptions

We assume that the BSs are deployed according to a Poisson Point Process (PPP) Φ_C with intensity λ_C. The $i-$th BS located at $\mathbf{x}_i \in \mathbb{R}^2$, defines a *Voronoi region* $\mathcal{V}(\mathbf{x}_i)$,

$$\mathcal{V}(\mathbf{x}_i) = \left\{ \mathbf{x} \in \mathbb{R}^2 \mid \|\mathbf{x} - \mathbf{x}_i\| \leq \|\mathbf{x} - \mathbf{x}_j\|, j \neq i \right\}, \tag{F.1}$$

where $\|\cdot\|$ is the Euclidean distance. This region consists of those points $\mathbf{x}$ in $\mathbb{R}^2$ that are closer to the BS at $\mathbf{x}_i$ than any other BS. From this definition, the intersection of any two Voronoi regions $\mathcal{V}(\mathbf{x}_i)$ and $\mathcal{V}(\mathbf{x}_j)$ is empty, when $i \neq j$. This concept will be important when we consider the MS association in Subsec. 2.3. We assume that the Voronoi tessellation determines the rule by which the MS associates with the BS, both for DL and UL, and further that, at a specific time, only one MS randomly located in a Voronoi cell is active.

2.2 BS Pairing

As stated previously, in CoMPflex we assume that all nodes are HD. We define a *CoMPflex pair* as two adjacent and connected HD-BSs, one serving UL and the other DL traffic. The algorithm for pairing the BSs works as follows:

Given a deployment Φ_C, we consider a finite observation window with dimensions s km (i.e. of size s^2 km^2), and choose a BS at random in this window. We then list all the *unpaired* neighbors of this BS, and choose one of those randomly. These two BSs are then considered to be a CoMPflex pair. The algorithm then proceeds to the other unpaired BSs, and pairs the adjacent ones that are unpaired. The BS closest to the origin is called the *typical* BS. Fig. F.2(a) shows one instance of the algorithm, where the CoMPflex pairs are indicated by bold lines between the corresponding BSs (shown as triangles in the figure). In each CoMPflex pair, one BS is assigned either UL or DL

[1] The notation $g \sim \text{Exp}(\mu)$, means that g is exponentially distributed with parameter μ.

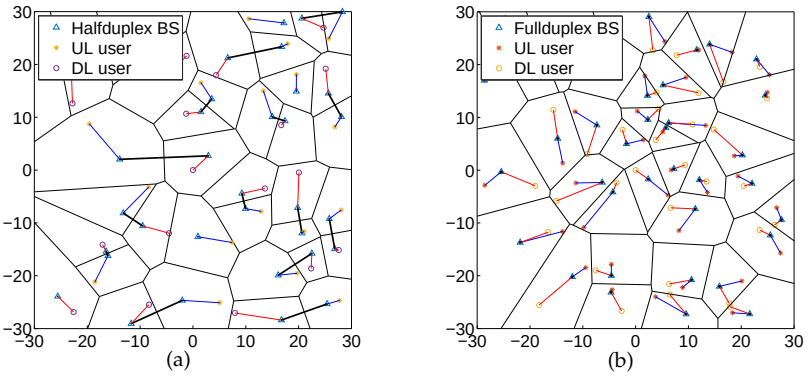

Fig. F.2: Snapshot of network deployments. In the CoMPflex deployment, each bold line indicates a CoMPflex pair.

randomly with probability 0.5 for each. The other BS is assigned the opposite traffic direction. Given a MS i, the BS serving that MS is denoted by $B(i)$. The algorithm terminates when it is no longer possible to pair any BSs. By the rule of pairing, in any CoMPflex pair the two BSs must have adjacent Voronoi regions. Therefore, any BS whose Voronoi region is surrounded by Voronoi regions that belong to paired BSs remains unpaired. We assign the unpaired BSs either as UL or DL at random, with probability 0.5 for each.

After the BS pairing, all BSs have been assigned either UL or DL. Since BSs are assigned either UL or DL at random, on average half of the BSs are UL, the other half, DL. We have $\lambda_C = \lambda_{C,U} + \lambda_{C,D}$, where $\lambda_{C,U}$ is the density of the CoMPflex UL-BSs, and $\lambda_{C,D}$ the density of the CoMPflex DL-BSs.

We recall that given a PPP Φ with intensity λ, we can define a new process by independently selecting each point in Φ with probability p, resulting in a *thinned* PPP Φ' with intensity $p\lambda$. We approximate the point processes of UL-BSs and DL-BSs as independent thinned PPPs. This is only an approximation, as from the algorithm it follows that the selection of DL/UL is not independent, since a DL-BS must be adjacent to a UL-BS.

2.3 User Association and Scheduling

Given the Voronoi regions defined by the BS deployment, the MS in a given region is scheduled to be served by the BS corresponding to that region. By the definition of a Voronoi region, a MS is associated to one unique BS. More specifically, for every Voronoi region $\mathcal{V}(\mathbf{x}_i)$ one MS is attached to this BS. The position of the MS is chosen uniformly at random in the region. The traffic direction of the MS is matched to the corresponding BS, i.e. if the BS is UL,

then the MS has UL traffic, similarly for DL.

A snapshot of the deployment and pairing of BSs, along with the associated UL and DL MSs, is shown in Fig. F.2(a).

2.4 Full Duplex Baseline Scheme

In the FD baseline scheme, the BSs are deployed according to a PPP Φ_F with intensity $\lambda_F = 0.5\lambda_C$. In each Voronoi region, one UL MS and one DL MS is served. The location of the two MSs attached to BS i at location $\mathbf{x}_i$ is chosen uniformly at random inside the Voronoi region $\mathcal{V}(\mathbf{x}_i)$ of the BS. The two MSs are assumed to be HD devices. Note that in this setting, the number of MSs is the same as that of CoMPflex, since each FD BS serves two MSs.

3 Signal Model

The UL signal to interference plus noise ratio (SINR) at BS $B(i)$ is

$$\gamma_{B(i)} = \frac{g_{i,B(i)}\ell(r_{i,B(i)})P_M}{I^{\psi}_{B(i)} + I^{\varphi}_{B(i)} + \sigma^2}. \tag{F.2}$$

In the above, the numerator represents the UL signal. In the denominator, the term $I^{\psi}_{B(i)}$ is the interference from other DL BSs, $I^{\varphi}_{B(i)}$ is the interference from other UL MSs, and σ^2 is the AWGN. The interference can be written as:

$$I^{\psi}_{B(i)} = \sum_{u \in \psi_{B(i)}} g_{u,B(i)}\ell(r_{u,B(i)})P_B, \tag{F.3}$$

$$I^{\varphi}_{B(i)} = \sum_{v \in \varphi_{B(i)}} g_{v,B(i)}\ell(r_{v,B(i)})P_M, \tag{F.4}$$

where $\psi_{B(i)}$ and $\varphi_{B(i)}$ are the sets of interfering BSs and MSs respectively. The DL SINR at MS j is given as

$$\gamma_j = \frac{g_{B(j),j}\ell(r_{B(j),j})P_B}{I^{\psi}_j + I^{\varphi}_j + \sigma^2}. \tag{F.5}$$

In the above, the numerator represents the DL signal. The first term in the denominator, I^{ψ}_j, is the aggregate interference from other DL BSs to DL MS j, and I^{φ}_j is the interference from the other UL MSs. The interference terms equal

$$I^{\psi}_j = \sum_{u \in \psi_j} g_{u,j}\ell(r_{u,j})P_B, \tag{F.6}$$

$$I^{\varphi}_j = \sum_{v \in \varphi_j} g_{v,j}\ell(r_{v,j})P_M, \tag{F.7}$$

where ψ_j and φ_j are the sets of interfering BSs and MSs.

4 Reliability Analysis

We analyze the performance of CoMPflex using the transmission success probability. This metric and its complement, the outage probability, are often used in works that analyze cellular networks through stochastic geometry. In the analysis, we consider a pair of typical BSs and their associated MSs. The typical UL-BS is denoted $B(U)$ and the DL-MS $B(D)$, while the UL-MS and DL-MS are denoted U and D respectively. These BSs and MSs represent the performance of the entire network. We write the SINR at this BS as γ_U (for UL). Similarly, the DL SINR at a typical MS is written as γ_D. A transmission is successful if the SINR is not lower that the target threshold SINR at the receiver.

4.1 UL and DL Distance Distributions

Recall that the BSs are deployed according to a PPP with density λ_C. The distribution of the distance between a DL-BS $B(i)$ and its associated MS i is denoted $f_{r_{B(i),i}}(r)$. In deriving this distribution, we assume that the BS is located at the origin, i.e. we consider a typical BS. The distance is then denoted $f_{r_{U,B(U)}}(r)$. Similarly, the density of the distance between a MS i and its UL-BS $B(j)$ is written $f_{r_{B(U),U}}(r)$.

As stated from the assumptions, the location of the scheduled MS is uniform at random inside the Voronoi region of the BS. For analytical tractability, we assume that the location of the MS can be any point in $\mathbb{R}^2$. Under this assumption, the distance from the typical BS to its MS then has the Cumulative Distribution Function (CDF):

$$F_{r_{B(U),U}}(r) = \Pr\{r_{B(i),i} \leq r\} = 1 - \exp\left(-\lambda_C \pi r^2\right), \tag{F.8}$$

This simplification is routinely made in the literature (see e.g. [9]) for analytical tractability. We assume that the UL distance CDF $F_{r_{U,B(U)}}(r)$ is the same as the DL. The numerical results confirm that this approximation is reasonable.

4.2 Transmission Success Probability of CoMPflex

In this section, we approximate the success probabilities in UL and DL for CoMPflex. In the derivations, we assume that BSs and MSs are deployed according to independent PPPs with density λ_C. Note that we approximate the locations of the MSs as a PPP, even though they are constrained to be inside the Voronoi cell of their serving BS. Also recall that the interference

from the paired DL-BS to the UL-BS is cancelled, and this is reflected in the interference expressions in the proof.

Theorem 2. *Assuming independent PPP deployment of MSs and BSs, the success probability in UL in CoMPflex is*

$$P_U^C = 2\pi\lambda_C \int_0^\infty r \exp\left(-\pi\lambda_C r^2 - s\sigma^2\right) \mathcal{L}_\psi(s)\mathcal{L}_\varphi(s)\mathrm{d}r, \tag{F.9}$$

where $s = \frac{\mu\beta_U r^\alpha}{P_M}$ *and the Laplace transforms of the interference from BSs* $\mathcal{L}_\psi(s)$ *and MSs* $\mathcal{L}_\varphi(s)$ *are*

$$\begin{aligned}\mathcal{L}_\psi(s) = &\int_0^\infty 2\pi\lambda_{C,D} t \exp\left(-\pi\lambda_{C,D}t^2\right) \cdot \\ &\exp\left(-2\pi\lambda_{C,D}\int_t^\infty \frac{\beta_U \frac{P_B}{P_M}\left(\frac{r}{x}\right)^\alpha}{1+\beta_U\frac{P_B}{P_M}\left(\frac{r}{x}\right)^\alpha} x\,\mathrm{d}x\right)\mathrm{d}t,\end{aligned} \tag{F.10}$$

$$\mathcal{L}_\varphi(s) = \exp\left(-2\pi\lambda_{C,U}\int_r^\infty \frac{\beta_U\left(\frac{r}{y}\right)^\alpha}{1+\beta_U\left(\frac{r}{y}\right)^\alpha} y\,\mathrm{d}y\right). \tag{F.11}$$

Proof. We consider the UL SINR γ_U, and choose a typical BS. Then we condition on the distance from the BS to the nearest UL-MS being r. The success probability is

$$P_U^C = \Pr\{\gamma_U \geq \beta_U\} = \int_0^\infty \Pr\{\gamma_U \geq \beta_U \,|\, r\} f_{U,B(U)}(r)\mathrm{d}r.$$

The conditioned CDF of the SINR equals (note that we drop the explicit notation of the conditioning for readability)

$$\begin{aligned}\Pr\{\gamma_U \geq \beta_U \mid r\} &= \Pr\left\{\frac{g_{U,B(U)} r^{-\alpha} P_M}{I^\psi_{B(U)} + I^\varphi_{B(U)} + \sigma^2} \geq \beta_U\right\} \\ &\overset{(a)}{=} \mathbb{E}\left[\exp\left(-s(I^\psi_{B(U)} + I^\varphi_{B(U)} + \sigma^2)\right)\right] \\ &= \exp\left(-s\sigma^2\right)\mathcal{L}_\psi(s)\mathcal{L}_\varphi(s),\end{aligned}$$

where in (a) we have used that $g_{U,B(U)} \sim \mathrm{Exp}(\mu)$, and we set $s = \frac{\mu\beta_U r^\alpha}{P_M}$. We now derive the interference from the other DL-BSs. In the derivation, we condition on the distance to the nearest interfering DL-BS to be t because this distance is independent from r. The distance t represents the approximation of the distance to the paired DL-BS, whose transmission is perfectly cancelled

and this gives an upper bound. The density of interfering DL-BSs is $\lambda_{C,D}$. Then

$$\begin{aligned}\mathcal{L}_{\psi}(s) &= \mathbb{E}_{I^{\psi}}\left[\exp\left(-s\sum_{i\in\psi_{B(i)}} P_B g_{i,B(i)} r_{i,B(i)}^{-\alpha}\right)\right] \\ &\overset{(a)}{=} \mathbb{E}_{I^{\psi}}\left[\prod_{i\in\psi_{B(i)}} \mathbb{E}_g\left[\exp\left(-sP_B g_{i,B(i)} r_{i,B(i)}^{-\alpha}\right)\right]\right] \\ &\overset{(b)}{=} \exp\left(-2\pi\lambda_{C,D}\int_t^{\infty}\left(1-\mathbb{E}_g\left[\exp\left(-sP_B g_{i,B(i)} x^{-\alpha}\right)\right]\right) x\mathrm{d}x\right) \\ &\overset{(c)}{=} \exp\left(-2\pi\lambda_{C,D}\int_t^{\infty}\left(\frac{sP_B x^{-\alpha}}{1+sP_B x^{-\alpha}}\right) x\mathrm{d}x\right),\end{aligned}$$

where in (a) we have used that the channels $g_{i,B(i)}$ are independent, (b) is from the Probability Generating Functional (PGFL) of a PPP with density $\lambda_{C,D}$ and $x = r_{i,B(i)}$, and in (c) we rewrite using the Moment Generating Function (MGF) of an exponential random variable. Combining this with the pdf of the distance t and using $s = \frac{\mu\beta_U r^{\alpha}}{P_M}$, we get Eq. (F.10). Using similar arguments, Eq. (F.11) also can be derived. Note however, that in Eq. (F.11), the distance to the nearest interfering UL-MS follows the same distribution as the distance to the served UL-MS. □

For DL, recall that we approximate the interfering MSs as a PPP, and this approximation implies that an interfering UL-MS could be inside the Voronoi cell of the DL-MS. However, in CoMPflex there is exactly one MS in each cell. Therefore, the interference is overestimated.

Theorem 3. *Assuming independent PPP deployment of MSs and BSs, the success probability in DL for CoMPflex is*

$$P_D^C = 2\pi\lambda_C\int_0^{\infty} r\exp\left(-\pi\lambda_C r^2 - s\sigma^2\right)\mathcal{L}_{\psi}(s)\mathcal{L}_{\varphi}(s)\mathrm{d}r, \tag{F.12}$$

where $s = \frac{\mu\beta_D r^{\alpha}}{P_B}$ *and the Laplace transforms of the interference from BSs* $\mathcal{L}_{\psi}(s)$ *and MSs* $\mathcal{L}_{\varphi}(s)$ *are*

$$\mathcal{L}_{\psi}(s) = \exp\left(-2\pi\lambda_{C,D}\int_r^{\infty}\frac{\beta_D\left(\frac{r}{x}\right)^{\alpha}}{1+\beta_D\left(\frac{r}{x}\right)^{\alpha}} x\,\mathrm{d}x\right), \tag{F.13}$$

$$\mathcal{L}_{\varphi}(s) = \exp\left(-2\pi\lambda_{C,U}\int_0^{\infty}\frac{\beta_D\frac{P_M}{P_B}\left(\frac{r}{y}\right)^{\alpha}}{1+\beta_D\frac{P_M}{P_B}\left(\frac{r}{y}\right)^{\alpha}} y\,\mathrm{d}y\right). \tag{F.14}$$

Proof. The proof follows similar steps as the one for UL, and so is omitted due to space limitations. □

Note that the integration range of Eq. (F.14) starts at 0, since there is no interference cancellation in DL, contrary to UL. From this, we obtain a lower bound on the success probability.

4.3 Transmission Success Probability of Full Duplex

In the FD baseline, for DL, Eq. (9) in [10] gives the outage probability of a scenario similar to our FD baseline. The success probability can be directly derived from that equation.

In deriving the UL success probability, we can use a strategy similar to the one used for DL in [10]. Then, the UL success probability in the FD baseline is

$$P_U^F = 2\pi\lambda_F \int_0^\infty r \exp\left(-\pi\lambda_F r^2 - s\sigma^2\right) \mathcal{L}_\psi(s)\mathcal{L}_\varphi(s)\, \mathrm{d}r, \tag{F.15}$$

where $s = \frac{\mu\beta_U r^\alpha}{P_M}$ and the Laplace transforms of the interference from BSs $\mathcal{L}_\psi(s)$ and MSs $\mathcal{L}_\varphi(s)$ are

$$\mathcal{L}_\psi(s) = \exp\left(-2\pi\lambda_F \int_r^\infty \frac{\beta_U \frac{P_B}{P_M}\left(\frac{r}{x}\right)^\alpha}{1+\beta_U \frac{P_B}{P_M}\left(\frac{r}{x}\right)^\alpha} x\, \mathrm{d}x\right), \tag{F.16}$$

$$\mathcal{L}_\varphi(s) = \exp\left(-2\pi\lambda_F \int_r^\infty \frac{\beta_U \left(\frac{r}{y}\right)^\alpha}{1+\beta_U \left(\frac{r}{y}\right)^\alpha} y\, \mathrm{d}y\right). \tag{F.17}$$

5 Numerical Results

We show the performance of CoMPflex, and the comparison with the FD baseline schemes, using both numerical simulations and the analytical model given in the previous section. The simulation assumptions are shown in Table F.1, where the densities are chosen comparable with [10].

We study the success probability in both UL and DL for CoMPflex, in terms of varying the SINR threshold, and compare with FD. The BS and MS transmission powers are held constant according to the values in Tab. F.1. The UL success probability for CoMPflex and FD, both simulation and analytical, is shown in Fig. F.3. Here, the analytical curve approximates the simulated values quite closely. However, the success probability in UL is lower than DL, which can be partially explained by the MS power being lower than the BS power.

Table F.1: Simulation parameters.

Parameter	Description	Simulation Setting
s	Size of observation window	200 km
λ_C	BS density (CoMPflex)	0.02 BS/km^2
λ_F	BS density (FD)	0.01 BS/km^2
σ^2	Noise power at MS and BS	-174 dBm
α	Path loss exponent	4
β	SINR thresholds	$-20, -15, -10, \ldots, 20$ dB
P_B	BS transmission power	40 dBm
P_M	MS transmission power	20 dBm

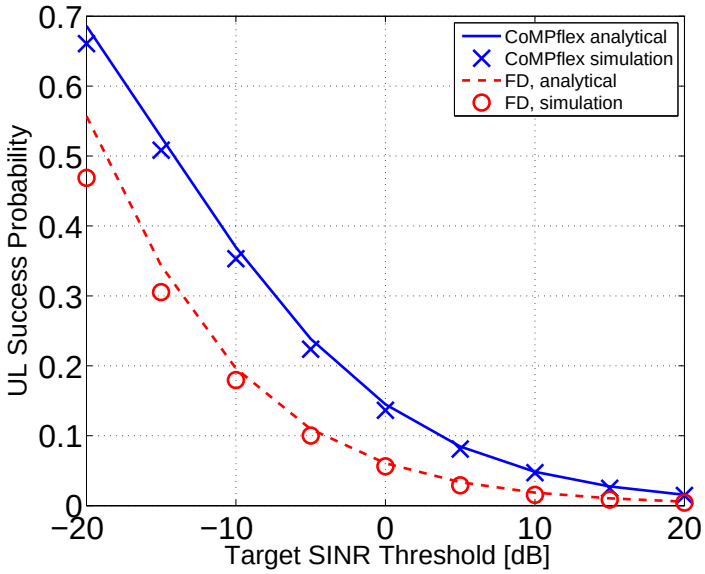

Fig. F.3: Success Probability in UL vs. SINR threshold.

The resulting success probability for DL is shown in Fig. F.4. In this figure, we can observe that the analytical derivations result in a lower bound on the success probability. This was to be expected, since the point processes in CoMPflex are not truly PPP. However, as the figure shows, the PPP approximation is quite close and serves well as an indicator of the expected performance of CoMPflex. We also observe that the success probability in CoMPflex is about 30% higher than FD, for most of the range of SINR thresholds. The explanation of this can be attributed to how CoMPflex affects the distances of the signal and interference links.

Since one of the main features in CoMPflex is that it brings the MSs closer

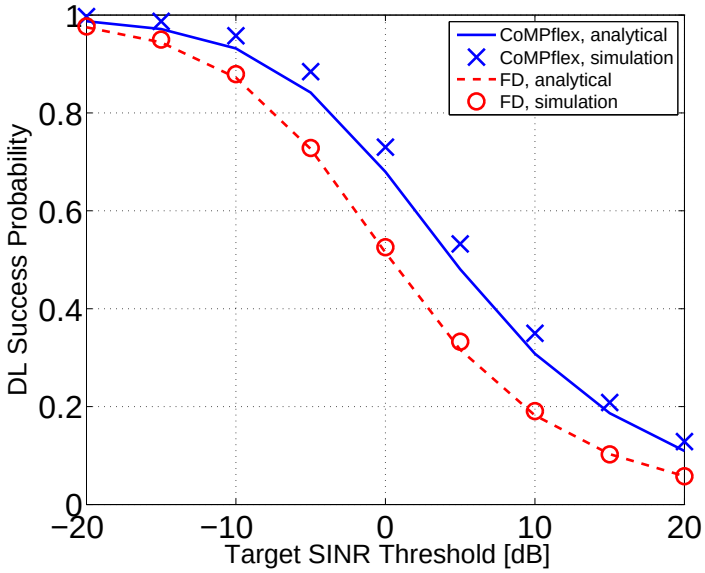

Fig. F.4: Success Probability in DL vs. SINR threshold.

to the serving BSs, we analyze and compare the CDFs of the various distances for signal and intra-cell interference links in CoMPflex and FD. This comparison is shown in Fig. F.5. The simulated CDF are shown as lines, while the analytical CDF using Eq. (F.8) are shown as markers[2]. From this figure, we can observe two important points:

First, we compare the CDFs of the distances between an UL-MS and BS, and between a BS and DL-MS. We see that for both CoMPflex and FD, the UL and DL distance curves overlap. This implies that the distances of UL and DL follow the same distribution. What is also interesting is that the CDFs of the distances in CoMPflex are shifted to the *left*, compared to FD. This means that the lower MS to BS distances have higher probability in CoMPflex compared to FD.

Second, the CDF curve of the intra-cell interference distance in CoMPflex is shifted to the *right* compared to FD. This means that higher interference distances have higher probability in CoMPflex compared to FD. Taken together, these two points can explain the performance advantages of CoMPflex over FD, which come from having a lower signal distance and a higher interference distance *simultaneously*.

[2]Note that the analytical CDF of CoMPflex is shifted to the left, compared to FD, since $\lambda_F = 0.5\lambda_C$

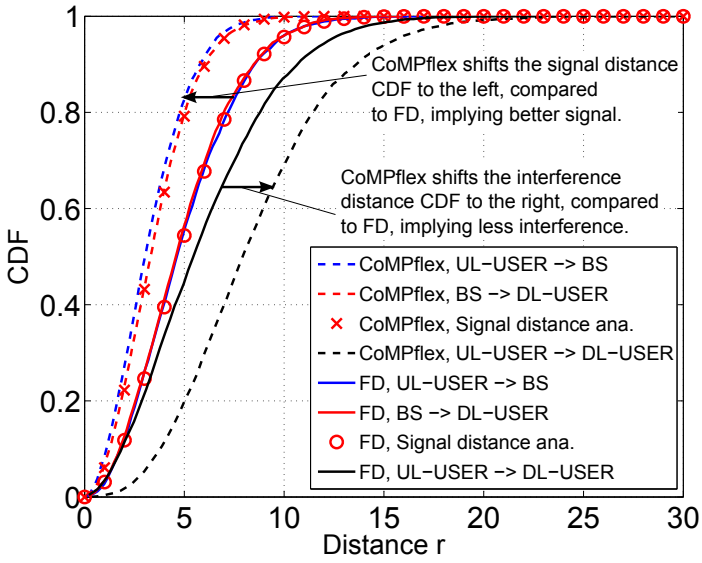

Fig. F.5: Comparison of the CDFs of the node distances in the CoMPflex and FD scenarios.

6 Conclusion

In this work, we have analyzed the performance of CoMPflex in a planar network setting, and compared it with a FD baseline scheme. We have derived the success probability for UL and DL, and validated the results via simulations. It was observed that the success probability of both UL and DL was higher for CoMPflex than in FD, an effect which can be attributed to the effects of CoMPflex on the node distances. Thus it is beneficial to consider the usage of HD devices instead of FD, which is also useful for using already existing technology and avoiding the signal complexities of FD.

One promising research direction is to consider more than two connected BSs, and more general clustering criteria. Also, it would be interesting to compare CoMPflex with other interference mitigation techniques such as CoMP.

Acknowledgment

This work has been supported by the Danish High Technology Foundation via the Virtuoso project.

References

[1] F. Boccardi, R. W. Heath Jr, A. Lozano, T. L. Marzetta, and P. Popovski, "Five disruptive technology directions for 5G," *IEEE Commun. Mag.*, vol. 52, no. 2, pp. 74–80, Feb. 2014.

[2] D. Lee, H. Seo, B. Clerckx, E. Hardouin, D. Mazzarese, S. Nagata, and K. Sayana, "Coordinated multipoint transmission and reception in LTE-advanced: deployment scenarios and operational challenges," *Communications Magazine, IEEE*, vol. 50, no. 2, pp. 148–155, 2012.

[3] H. Thomsen, P. Popovski, E. de Carvalho, N. Pratas, D. Kim, and F. Boccardi, "Compflex: Comp for in-band wireless full duplex," *IEEE Wireless Communication Letters*, vol. PP, no. 99, pp. 1–4, 2015.

[4] A. Sabharwal, P. Schniter, D. Guo, D. Bliss, S. Rangarajan, and R. Wichman, "In-band full-duplex wireless: Challenges and opportunities," *IEEE J. Select. Areas Commun.*, vol. 32, no. 9, pp. 1637–1652, Sept. 2014.

[5] E. Dahlman, G. Mildh, S. Parkvall, J. Peisa, J. Sachs, Y. Selen, and J. Skold, "5G wireless access: requirements and realization," *IEEE Communications Magazine*, vol. 12, no. 52, pp. 42–47, 2014.

[6] D. Guo and L. Zhang, "Virtual full-duplex wireless communication via rapid on-off-division duplex," in *Proc. of the Allerton Conference on Communication, Control, and Computing (Allerton 2010)*, Sept. 2010.

[7] A. AlAmmouri, H. ElSawy, and M.-S. Alouini, "Harvesting full-duplex rate gains in cellular networks with half-duplex user terminals," in *Proc. IEEE ICC*, May 2016.

[8] Z. Tong and M. Haenggi, "Throughput analysis for full-duplex wireless networks with imperfect self-interference cancellation," *Communications, IEEE Transactions on*, vol. 63, no. 11, pp. 4490–4500, 2015.

[9] T. D. Novlan, H. S. Dhillon, and J. G. Andrews, "Analytical modeling of uplink cellular networks," *IEEE Trans. Wireless Commun.*, vol. 12, no. 6, pp. 2669–2679, Jun. 2013.

[10] C. Psomas and I. Krikidis, "Outage Analysis of Full-Duplex Architectures in Cellular Networks networks," in *Vehicular Technology Conference (VTC Spring), 2015 IEEE 81st*. IEEE, 2015, pp. 1–5.

ISSN (online): 2246-1248
ISBN (online): 978-87-7112-528-3

AALBORG UNIVERSITY PRESS